สมบัติและการประยุกต์ใช้โครงพรุนแบคทีเรียเซลลูโลส-อัลจิเนตคอมโพสิต

นางสาวสุชาตา เกิดผลภัทระ

วิทยานิพนธ์นี้เป็นส่วนหนึ่งของการศึกษาตามหลักสูตรปริญญาวิศวกรรมศาสตรดุษฎีบัณฑิต
สาขาวิชาวิศวกรรมเคมี ภาควิชาวิศวกรรมเคมี
คณะวิศวกรรมศาสตร์ จุฬาลงกรณ์มหาวิทยาลัย
ปีการศึกษา 2555

PROPERTIES AND APPLICATIONS OF BACTERIAL CELLULOSE-ALGINATE COMPOSITE SPONGES

Miss Suchata Kirdponpattara

A Dissertation Submitted in Partial Fulfillment of the Requirements
for the Degree of Doctoral of Engineering Program in Chemical Engineering
Department of Chemical Engineering
Faculty of Engineering
Chulalongkorn University
Academic Year 2012

Thesis Title	PROPERTIES AND APPLICATIONS OF BACTERIAL CELLULOSE-ALGINATE COMPOSITE SPONGES
By	Miss Suchata Kirdponpattara
Field of Study	Chemical Engineering
Thesis Advisor	Associate Professor Muenduen Phisalaphong, Ph.D.

Accepted by the Faculty of Engineering, Chulalongkorn University in Partial Fulfillment of the Requirements for the Doctoral Degree

……Dean of the Faculty of Engineering
(Associate Professor Boonsom Lerdhirunwong, Dr.Ing.)

THESIS COMMITTEE

……Chairman
(Associate Professor Sarawut Rimdusit, Ph.D.)

……Thesis Advisor
(Associate Professor Muenduen Phisalaphong, Ph.D.)

……Examiner
(Associate Professor Bunjerd Jongsomjit, Ph.D.)

……Examiner
(Associate Professor Artiwan Shotipruk, Ph.D.)

……External Examiner
(Sopee Sa-Nguandekul, Ph.D.)

สุชาตา เกิดผลภัทระ: สมบัติและการประยุกต์ใช้โครงพรุนแบคทีเรียเซลลูโลส-อัลจิเนตคอมโพสิต. (PROPERTIES AND APPLICATIONS OF BACTERIAL CELLULOSE-ALGINATE COMPOSITE SPONGES) อ.ที่ปรึกษาวิทยานิพนธ์หลัก: รศ.ดร.เหมือนเดือน พิศาลพงศ์, 121 หน้า.

วัสดุที่สามารถย่อยสลายได้ทางชีวภาพได้ถูกนำมาประยุกต์ใช้อย่างแพร่หลาย เนื่องจากความเป็นมิตรและไม่เป็นพิษต่อสิ่งแวดล้อม ในอีกด้านหนึ่ง การหาพลังงานทางเลือกใหม่มาทดแทนเชื้อเพลิงฟอสซิลและการปลูกถ่ายเนื้อเยื่อในมนุษย์กำลังได้รับความสนใจเป็นอย่างมากในปัจจุบัน แบคทีเรียเซลลูโลสและอัลจิเนตเป็นโพลิเมอร์จากธรรมชาติที่มีศักยภาพสูงในการนำไปใช้เป็นวัสดุตรึงเซลล์จุลินทรีย์ และเป็นโครงเลี้ยงเซลล์ในวิศวกรรมเนื้อเยื่อ อย่างไรก็ตาม ไบโอโพลิเมอร์ทั้งสองชนิดนี้ก็ยังมีข้อจำกัดอยู่ ตัวอย่างเช่น แบคทีเรียเซลลูโลสและอัลจิเนตเจลที่ยังไม่ได้ผ่านการปรับปรุงโครงสร้างจะมีปัญหาความต้านทานในการถ่ายโอนมวลของสารตั้งต้นและผลิตภัณฑ์สูง, อัลจิเนตเจลมีความแข็งแรงที่ต่ำและไม่มีความเสถียรเมื่อนำไปประยุกต์ใช้ในระยะเวลานาน และในอีกด้านหนึ่ง พันธะไฮโดรเจนที่เกิดขึ้นระหว่างสายโซ่ของเซลลูโลส ทำให้เซลลูโลสมีความแข็งแรงและความเสถียร ซึ่งความแข็งแรงและความเสถียรนี้ทำให้เซลลูโลสยากที่จะละลายในน้ำหรือตัวทำละลายอินทรีย์ทั่วไป ดังนั้น การที่จะปรับปรุงโครงสร้างของแบคทีเรียเซลลูโลสจึงเป็นเรื่องที่ทำได้ยาก

เพื่อนำคุณสมบัติที่ดีของทั้งสองไบโอโพลิเมอร์มาส่งเสริมซึ่งกันและกัน และเพื่อลบล้างข้อจำกัดของไบโอพอลิเมอร์แต่ละตัว โครงพรุนแบคทีเรียเซลลูโลส-อัลจิเนตคอมโพสิตจึงได้ถูกพัฒนาขึ้น โดยโครงพรุนนี้ได้ถูกขึ้นรูปโดยการเชื่อมต่อระหว่างสายโซ่และการทำแห้งแบบเยือกแข็ง เพื่อเพิ่มการถ่ายโอนมวลของสารตั้งต้นหรือผลิตภัณฑ์ และเพิ่มความแข็งแรงให้กับโครงพรุน

โครงพรุนแบคทีเรียเซลลูโลส-อัลจิเนตคอมโพสิตได้ถูกนำมาประยุกต์ใช้เป็นวัสดุตรึงเซลล์ยีสต์ในการหมักเอทานอล โครงพรุนนี้มีโครงสร้างที่ไม่เป็นแบบเดียวกัน ซึ่งประกอบด้วย ชั้นบางๆภายนอกและโครงสร้างที่เป็นรูพรุนเชื่อมต่อกันภายใน โครงพรุนนี้แสดงถึงคุณสมบัติที่ดีหลายประการ เช่น ความพรุนสูง, ขนาดรูพรุนที่เหมาะสม, ความชอบน้ำสูง และความแข็งแรงทางกล ทางเคมีและความเสถียรต่ออุณหภูมิที่สูง จากผลการทดลองพิสูจน์ให้เห็นว่า โครงพรุนแบคทีเรียเซลลูโลส-อัลจิเนตคอมโพสิตเป็นโครงตรึงเซลล์มีประสิทธิภาพและความเสถียรที่สูงสำหรับการนำไปใช้ในการหมักเอทานอลในระยะเวลานาน (อย่างน้อยหนึ่งเดือน)

โครงพรุนแบคทีเรียเซลลูโลส-อัลจิเนตคอมโพสิตได้ถูกปรับปรุงความชอบน้ำด้วยการบำบัดด้วยยูวี/โอโซนเพื่อเพิ่มผลผลิตของเอทานอล ค่ามุมสัมผัสของโครงพรุนที่ผ่านและไม่ผ่านการบำบัดได้ถูกวัด ความชอบน้ำของโครงพรุนได้ถูกวิเคราะห์ด้วยเทคนิค Washburn capillary rise ซึ่งพบว่าการวิเคราะห์ด้วยวิธีนี้สามารถนำมาใช้ประเมินอิทธิพลของการปรับปรุงวัสดุได้ โดยจะแสดงค่าความแตกต่างของมุมสัมผัสของวัสดุก่อนและหลังการปรับปรุง และพบว่าเนื่องจากอิทธิพลของการเกิดรอยแตกในการปรับปรุงวัสดุด้วยออกซิเจนพลาสมา ทำให้ผิวของโครงพรุนมีความหยาบมากขึ้น ส่งผลให้ค่ามุมสัมผัสของน้ำมีค่าลดลง อย่างไรก็ตาม เทคนิคออกซิเจนพลาสมาไม่สามารถสร้างหมู่ฟังก์ชันที่ชอบน้ำบนพื้นผิวของโครงพรุนได้ ดังนั้น จึงไม่เห็นความแตกต่างอย่างเป็นนัยสำคัญของผลผลิตเอทานอลในการหมักแบบกะที่ได้จากระบบการตรึงเซลล์บนโครงพรุนที่ผ่านและยังไม่ผ่านการปรับปรุง

นอกจากนี้สำหรับการประยุกต์ใช้ในวิศวกรรมเนื้อเยื่อ โครงพรุนแบคทีเรียเซลลูโลส-อัลจิเนตคอมโพสิตได้นำมาขึ้นรูปด้วยวิธีที่ถูกพัฒนาแล้ว ซึ่งเป็นวิธีที่ทำสลับขั้นตอนกับวิธีการขึ้นรูปแบบเดิม โครงพรุนที่ผ่านการปรับปรุง (N-BCA) แล้วมีลักษณะเป็นรูเปิดและรูพรุนเชื่อมต่อกันทั่วทั้งโครงสร้าง จากการวิเคราะห์คุณสมบัติต่างๆของ N-BCA พบว่า N-BCA อาจจะเหมาะแก่การนำไปประยุกต์ใช้เป็นโครงเลี้ยงเซลล์ในวิศวกรรมเนื้อเยื่อ

ภาควิชา.....วิศวกรรมเคมี..... ลายมือชื่อนิสิต.....

สาขาวิชา.....วิศวกรรมเคมี..... ลายมือชื่อ อ. ที่ปรึกษาวิทยานิพนธ์หลัก.....

ปีการศึกษา.....2555.....

5171857721: MAJOR CHEMICAL ENGINEERING
KEYWORDS : BACTERIAL CELLULOSE / ALGINATE / COMPOSITE / ETHANOL FERMENTATION / CONTACT ANGLE / OXYGEN PLASMA/ TISSUE ENGINEERING

SUCHATA KIRDPONPATTARA: PROPERTIES AND APPLICATIONS OF BACTERIAL CELLULOSE-ALGINATE COMPOSITE SPONGES. ADVISOR: ASSOC. PROF. MUENDUEN PHISALAPHONG, Ph.D., 121 pp.

Biodegradable materials have been utilized in many applications because of its environmental friendly and non-toxicity. On the other side, the replacement of fossil fuel by alternative energies and the implantation of culture cells in vivo have been widely concentrated in recent years. Bacterial cellulose (BC) and alginate are natural polymers, which have high potential to be used as support materials for microbial cell immobilization and as a scaffold for tissue engineering. However, there are still some limitations of both biopolymers. For example, without modification of the structure, hydrophilic gels of BC and gelatin have high mass transfer resistance of substrate and product transport. Alginate gel has rather low mechanical strength and it is not stable to be used over a long periods of time. On the other hand, the hydrogen bonds that occur between cellulose chains of BC are very strong and stable, which make BC very hard to dissolve in water or in general organic solvents. Consequently, modification of the structure of pure cellulose is not simple.

To gain their beneficial properties and break through the limitations of both biopolymers, the composite sponge of bacterial cellulose-alginate (BCA) was developed. The BCA sponge was fabricated by cross-linking and freeze drying method in order to increase the substrate/product mass transfer and to enhance mechanical properties of the sponge.

BCA sponge was applied in ethanol fermentation as a yeast cell carrier. It presented the heterogeneous structure which consisted of the thin layer on the outer and the interconnected porous structure in the interior. The BCA sponge exhibited several advantageous properties, such as high porosity, appropriate pore size, strong hydrophilicity and high mechanical, chemical and thermal stabilities. The results demonstrated that BCA sponge represented a highly effective and stable cell carrier for use in long-term (at least one month) ethanol fermentations.

BCA sponge was enhanced its hydrophilicity by UV/ozone treatment to improve ethanol production. The advancing water contact angles of BCA sponge with and without UV/ozone treatment were measured. The hydrophilicity of BCA sponge was assessed using Washburn capillary rise (WCR) method. It was shown that WCR method could be used to estimate the treatment effect on the material by providing the advancing contact angle of the material before and after the treatment. It was shown that due to the etching effect in oxygen plasma application; the roughness of treated BCA was increased, resulting in a decrease of advancing water contact angle. However, oxygen plasma was unable to create hydrophilic functional groups on the surface of BCA. Thus, under batch fermentation, there was no significant difference in ethanol production obtained from the immobilized cell (IC) systems using carriers of treated BCA compared to the untreated one.

Furthermore, for tissue engineering application, BCA sponge was fabricated with the adapted method, which was the reversal of the previous one. The highly open and interconnected porous structure throughout the modified BCA (N-BCA) sponge was obtained. The characterizations of N-BCA revealed that N-BCA should be suitable to be used as a scaffold for tissue engineering.

Department :……Chemical Engineering. Student's Signature……..……
Field of Study :…Chemical Engineering. Advisor's Signature…..…….……...
Academic Year :..2012……..

ACKNOWLEDGEMENTS

I would like to express my sincere gratitude to all who gave me the possibility to complete this thesis. I am particularly grateful for my advisor, Associate professor Dr. Muenduen Phisalaphong for her valuable guidance, useful discussions and warm encouragement. I also would like to express my sincere thank to Associate professor Dr. Bi-min Zhang Newby who kindly hosted my research visit at The University of Akron, Ohio, United State of America for her valuable suggestions and guidance. I would like to thank Associate professor Dr. Neeracha Sanchavankit for providing valuable suggestion about the tissue engineering study. Moreover, I also grateful for the members of thesis examination committee, Associate Professor Dr. Sarawut Rimdusit, Associate Professor Dr. Artiwan Shotipruk, Associate Professor Dr. Bunjerd Jongsomjit, and Dr. Sopee Sa-Nguandekul, who gave helpful suggestions for this thesis.

This thesis would not have been possible without the financial supports provided by the Thailand Research Fund (TRF) through the Royal Golden Jubilee Ph.D program and Chulalongkorn University.

Finally, I would like to express my heartfelt thanks to my parents and my family for their blessing, support and encouragement as well as my friends in the Department of Chemical Engineering, Chulalongkorn University for the completion of my study.

CONTENTS

PAGE

CHAPTER PAGE

CHAPTER PAGE

CHAPTER PAGE

LIST OF TABLES

TABLE PAGE

LIST OF FIGURES

FIGURE PAGE

CHAPTER I
INTRODUCTION

1.1 Introduction

Currently, global warming is the major problem of our world. One of the most severe ever-growing courses has been related to garbage and waste. The use of biodegradable materials instead of non-degradable and non-disintegrate substances has positive effects on the environment. Consequently, researches on developing new biomaterials for various purposes have become increasingly important.

Bacterial cellulose (BC) is cellulose produced by bacteria, however, only the *Acetobacter* species produce enough cellulose for considerable commercial interest. BC is an outstanding biomaterial with unique properties including high water holding capacity, high crystallinity, high tensile strength and a highly pure and ultra- fine fiber network structure. In addition, BC is biocompatibility, non-toxicity and biodegradability. BC has been studied in a wide range of applications. BC has potential to be used as an immobilization matrix of protein or chromatography (Jonas and Farah, 1998), a cells carrier of ethanol production (Nguyen et al., 2009), a scaffold in tissue engineering of skin, vessel or cartilage (Szot et al., 2009), a carrier of controlled-drug release (Guzun et al., 2007), a membrane for separation (Pandey et al., 2005) or fuel cell application (Brown et al., 1996), a mixing agent in food industries (Jonas and Farah, 1998), fibers in paper industries (Jonas and Farah, 1998) and etc.

Alginate isolated from algae and seaweed is another important natural products. Alginate forms well-characterized hydrogel by adding divalent cations under physiological conditions. In the immobilization technology, alginate has been extensively used as hydrogel for cell or enzyme entrapment. For example, it has been used for cell immobilization for ethanol fermentation (Najafpour et al., 2004) and lactic acid fermentation (Idris and Suzana, 2006) or for micro-algae entrapment to produce carotenoid-rich biomass (Leach et al., 1998). Furthermore, alginate is one of

the most studied and applied natural polymers in tissue engineering. Alginate or alginate composite is fabricated to apply for tissue engineering such as cardiac (Shachar et al., 2011), bone (Li et al., 2005) and cartilage tissue (Stevans et al., 2004).

A blend of one or more biopolymers with another one to improve properties has been applied extensively in recent years. In medical application, alginate is introduced into chitosan (Shao and Hunter, 2007) and collagen (Sun et al., 2008) for improved structure, mechanical strength, and biological properties of the biopolymers. With an appropriate addition of alginate into a polyvinyl alcohol (PVA)-based biopolymer, an increased rate of wound healing was observed when it was applied as a dressing (Kim et al., 2008). Modification of separation membranes of polyvinyl pyrrolidone (PVP) (Solak et al., 2008) and cellulose cuoxam (Yang et al., 2000) with alginate was shown to enhance permeability flux, separation factor and mechanical strength. In the similar way, polymer blends with BC have been extensively investigated due to its unique properties. An addition of BC was shown to improve tensile strength of PVA-BC polymer closely porcine aorta for cardiovascular graft replacement (Millon et al., 2008). BC supplement in chitosan-based membranes was shown to increase pervaporative separation index (PSI) (Dubey et al., 2005).

The aim of this research was to fabricate a composite biomaterial from BC and alginate (BCA). BCA was investigated as a cell carrier for immobilization of *Saccharomyces cerevisiae* for ethanol fermentation. BCA was further improved its hydrophilicity by oxygen plasma treatment and then was reexamined as a cell carrier for ethanol fermentation. The technique of contact angle measurement for BCA was studied to assess its hydrophilicity. Moreover, the potential use of BCA as a scaffold in tissue engineering was evaluated.

1.2 Objectives

1. To fabricate bacterial cellulose/alginate composite sponges (BCA) and characterize for its physical, mechanical and biological properties.
2. To apply BCA as a cell carrier for immobilized yeast cells in ethanol fermentation.
3. To assess contact angle (hydrophilic property) of BCA

4. To investigate the effect of hydrophilicity of BCA as a cell carrier on ethanol production
5. To apply BCA as a scaffold in tissue engineering.

1.3 Research scopes

1. Bacterial cellulose/alginate composite sponges (BCA) is fabricated by gelation and freeze drying technique.
   1.2 Characterization of BCA:
      1.2.1 Scanning Electron Micrographs (SEM) for investigating morphology
      1.2.2 Fourier Transform Infrared (FT-IR) spectrometer for identifying the chemical structure
      1.2.3 Universal testing machine for determining stress-strain curve
      1.2.4 Equilibrium water content for examining the water uptake ability
   1.3 Application of BCA for immobilization of *Saccharomyces cerevisiae* M30 for ethanol fermentation.
      1.3.1 Batch ethanol fermentation
         a. Effect of the proportion of BC and alginate content (0:100, 50:50, 60:40, 70:30 and 100:0)
         b. Effect of alginate concentration (1.5, 2, 3, 4, 5 and 6% by wt.) in BCA formulation
         c. Effect of the immobilization methods (adsorption and entrapment)
      1.3.2 Repeated batch ethanol fermentation
         a. The efficiency comparison of immobilized culture in BCA, immobilized cultures entrapped in alginate gel and suspended cell culture
         b. The stability of BCA

2. The study of Washburn capillary rise method (WCR) for determining BCA.
   2.1 Comparison of advancing contact angles obtained from WCR and sessile drop method by using four common polymers (polystyrene, polymethymethacrate, nylon 6 and nylon 6/6)
   2.2 Effect of powder size (0-250, 250-500, 500-2000 and 0-2000 μm of nylon 6/6) and packing
   2.3 Effect of advancing rate on contact angle
   2.4 Analysis of liquid penetrating profile to obtain suitable contact angle by Washburn capillary rise method (WCR)
   2.5 Water contact angle on BCA
3. Investigation effect of BCA hydrophilicity on ethanol fermentation
   3.1 Treatment of BCA with oxygen plasma
   3.2 Characterizations of treated BCA
      3.2.1 Scanning Electron Micrographs (SEM) for investigating morphology
      3.2.2 Fourier Transform Infrared (FT-IR) spectrometer for identifying the chemical structure
      3.2.3 Washburn capillary rise (WCR) for assessing the advancing water contact angle
      3.2.4 Equilibrium water content for examining the water uptake ability
   3.3 Batch ethanol fermentation
      3.3.1 Ethanol production comparison of immobilized cell culture in treated BCA and un-treated BCA, and suspended cell culture
4. Fabrication of BCA sponge with an adepted method
   4.1 Characterization of a new BCA sponge
      4.1.1 Scanning Electron Micrographs (SEM) for investigating morphology
      4.1.2 Universal testing machine for determining stress-strain curve
      4.1.3 Equilibrium water content for examining the water uptake ability
      4.1.4 Stability of structure

CHAPTER II
BACKGROUND AND LITERATURE REVIEWS

2.1 Bacterial cellulose

Cellulose is the most abundant biopolymer found in plants as a structural component of the main cell wall. It is also formed by some algae, fungi and bacteria. Cellulose is an organic compound of the formula $(C_6 H_{10}O_5)_n$ with the repeating unit of D-glucose joined by β-1,4-glycosidic linkages as polysaccharides (Figure 2.1).

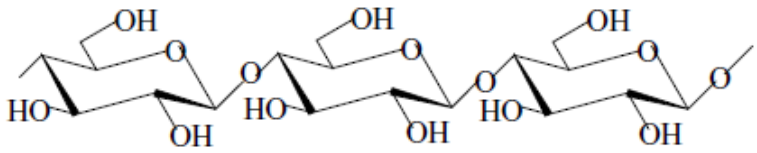

Figure 2.1 Structure of Cellulose (Krajewska et al., 2004)

Bacterial cellulose (BC) is a form of cellulose which is synthesized by bacteria. BC belongs to specific products of primary metabolism. There are many genera producing BC such as *Acetobacter*, *Rhizobium*, *Agrobacterium*, and *Sarcina*. An overview of BC producers is presented in Table 2.1 (Jonas and Farah, 1998).The most efficient BC producers is *Acetobacter xylinum* (reclassified as *Gluconacetobacter xylinus*), which has been applied as a model bacterium for basic and applied studies on cellulose (Rezaee et al., 2005). *Acetobacter xylinum* is a simple gram-negative, rod shaped, and strickly aerobic bacterium, which has an ability to synthesize a large quantity of high-quality cellulose organized as twisting ribbons of microfibrillar bundles.

Table.2.1 Microbe producing BC (Jonas and Farah, 1998)

Genus	Cellulose structure
Acetobacter	extracellular pellicle composed of ribbons fibrils
Achromobacter	fibrils
Aerobacter	short fibrils
Agrobacterium	fibrils
Alcaligenes	no distinct
Pseudomonas	fibrils
Rhizobium	short fibrils
Sarcina	amorphous cellulose
Zoogloea	not well defined

2.1.1 Synthesis of bacterial cellulose

The synthesis of BC in *Acetobacter xylinum* occurs between the outer membrane and cytoplasma membrane by a cellulose-synthesizing comp1ex, which is in association with pores at the surface of the bacterium (Figure 2.2) (Jonas and Farah, 1998) .

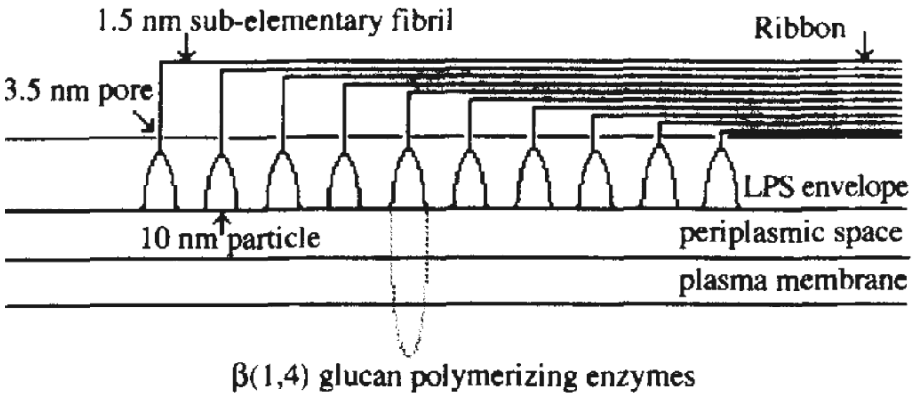

Figure 2.2 Scheme for the formation of BC (Jonas and Farah, 1998)

The cellulose synthese is considered to be the most important enzyme in this process. The enzyme was partially purified and cloned. Cyclic diguanylmonophosphate (c-di-GMP) was identified as activator of cellulose synthase. A principal biochemical pathway from glucose to cellulose (Figure 2.3) was proposed, which should be linked to cell growth as well as to cellulose formation. The produced cellulose leaves the pores as fibrils and forms together with many synthesized fibrils a ribbon of crystalline cellulose. A self-assembly process should be responsable for the crystallization after the polymerization of the fibrils was completed. Factors which influenced on BC production were carbon source, nitrogen source, pH and temperature (Jonas and Farah, 1998) .

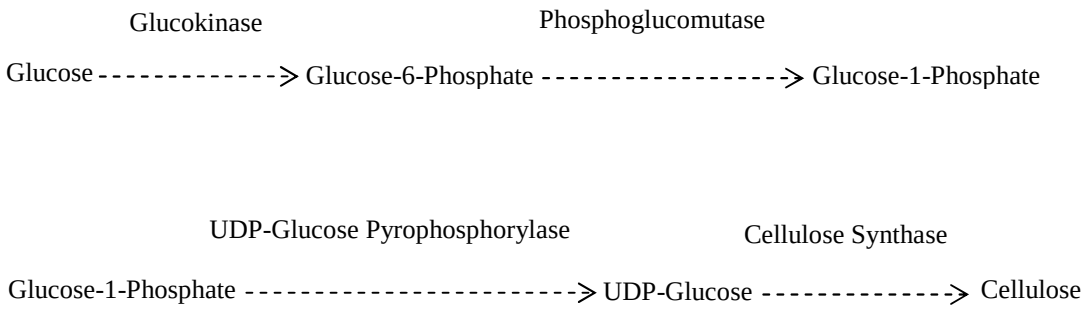

Figure 2.3 Biochemical pathway for BC synthesis in *Acetobacter xylinum* (Jonas and Farah, 1998)

2.1.2 Structure of bacterial cellulose

Nascent chains of BC aggregate to form subfibrils, which have a width of approximately 1.5 nm and belong to the thinnest naturally occurring fibers, comparable only to subelemental fibers of cellulose detected in the cambium of some plants. BC subfibrils are crystallized into microfibrils, these into bundles, and the latter into ribbons. Dimensions of the ribbons are 3 - 4 (thickness), 70 - 80 nm (width), whereas the width of cellulose fibers produced by pulping of birch or pine wood is two - three orders of magnitude larger (1.4 - 4.0×10^{-2} and 3.0 - 7.5×10^{-2} mm, respectively). The length of the ultrafine ribbons of microbial cellulose ranges from 1

to 9 µm. BC is also distinguished from its plant counterpart by degrees of crystallinity (above 60% for BC) and polymerization (DP) (usually between 2000 and 6000 for BC whereas the average DP of plant polymer varies from 13,000 to 14,000 (Rezaee et al., 2005)). Summarily, some advantages of BC over plant cellulose include:

- BC has finer and more complex structure.
- BC does not need to removed hemicellulose or lignin.
- BC has longer fiber length so it is much stronger.
- BC can be grown to virtually any shape.
- BC can be produced on a variety of substrates.

Macroscopic morphology of BC strictly depends on culture conditions. In static conditions, bacteria accumulate cellulose mats on the surface of nutrient broth, at the oxygen-rich air-liquid interface. The subfibrils of cellulose are continuously extruded from linearly ordered pores at the surface of the bacterial cell, crystallized into microfibrils, and forced bonds, forming parallel but disorganized planes. The adjacent BC produced in static condition strands branch and interconnect less frequently than these in BC produced in agitated culture, in a form of irregular granules, stellate and fibrous strands, well-dispersed in culture broth. The strands of reticulated BC produced in agitated condition interconnect to form a grid-like pattern, and have both roughly perpendicular and roughly parallel orientations (Rezaee et al., 2005).

Based on the properties of BC, e.g. high purity, high water adsorption capacity, high mechanical strength or molding capabilities during the biosynthesis, there is an increasing interest on the development of large number of applications. BC also displays unique physical, chemical and mechanical properties including high crystallinity, large surface area, elasticity and biocompatibility.

2.1.3 Applications of BC

2.1.3.1 Ethanol fermentation

In recent years, BC has been attracted attention as a carrier for cell immobilization because of its unique properties which differ from those of plant cellulose. Nguyen et al. (2006) immobilized lactic acid bacteria in BC. The experimental results showed that the biocatalyst could be reused for many batches without significant change in metabolic activity. Afterwards, they investigated BC as a support for yeast immobilization in wine production. From the experiments, the concentration of immobilized yeast cell could reach 1.4×10^9 cells/g BC. The metabolic activities of the immobilized yeast in BC were much higher than those of the suspended cell (SC) culture. The fermentation time of the system using the immobilized cell (IC) culture was decreased by 28.4% in comparison with that of the SC culture. The sugar uptake rate of the immobilized yeast was always higher than that of the free yeast. In addition, the immobilization of glucoamylase on BC could enhance its stability against changes in the pH and temperature (Wu and Lia, 2008).

2.1.3.1 Tissue engineering

BC is also potentially suitable for applications as scaffolds in tissue engineering due to its unique properties, including a high water retention capability (hydrophilic), a fine fibrous network, which allows cell growth and proliferation, high tensile strength, in situ moldability and low production cost. In medicine, non-porous cellulose membranes are used as stent coatings for dura-mater substitution in tumor or trauma cases or as skin protection in cases of burn and deep wounds. In odontology, cellulose films are applied for periodontal tissue recovering (Rambo et al., 2008).

Svensson et al. (2005) reported the response of primary bovine chondrocytes on native and chemically modified BC. Phophorylation and sulfation of matrices were explored in order to add surface charges to mimic the glucosaminoglycans in cartilage tissue in vivo. The results were indicated that the

unmodified BC supported chondrocyte proliferation at levels of approximately 50% of the native tissue substrate. However, compared to tissue culture plastic and alginate, unmodified BC showed significantly higher levels of chondrocyte growth at similar levels of in vitro immune response. Phosphorylation and sulfation did not enhance chondrocyte growth on BC. It was also confirmed that chondrocytes maintain their differentiated form when growing on BC and that the scaffold supports cell ingrowth. The Young's modulus of unmodified BC was in the same range as articular cartilage while the tensile strength of BC was higher than the tensile strength of highly crosslinked collagen.

Magdalena et al. (2010) investigated microporous BC scaffolds prepared by incorporating 300-500µm paraffin wax microspheres into the fermentation process for bone application. The paraffin wax microspheres were subsequently removed, and SEM confirmed a microporous surface of the scaffolds. Tensile measurements showed a Young's modulus of approximately 1.6 MPa. MC3T3-E1 osteoprogenitor cells seeded on microporous BC and nanoporous (control) BC scaffolds were observed by confocal microscopy and histology for cell distribution and mineral deposition. Cells clustered within the pores of microporous BC, and formed denser mineral deposits than cells grown on control BC surfaces.

Recouvreux et al. (2010) synthesized large three-dimensional hydrogels of BC by agitated culture conditions. The mechanical properties and biocompatibility were investigated. The optimal agitation frequency of hydrogels shaped as cocoons was 3.3 Hz. The average density of 3D hydrogels was 0.96g/cm^3. In average, the water content of the hydrogels remained constant (99.1%wt.). The three dimensional fibrous network structure was well identified. The quasi-hexagonal cells exhibit equivalent diameters of approximately 10µm, and fibres dispersed in a relative density of 0.65. The mean elastic modulus determined for the BC hydrogels is lower compared to a bovine kidney. Therefore, the cocoons exhibit enough mechanical resistance for handling and for organ replacement. From the result of biocompatibility, cell attachment may be a result of adhesion of proteins from the medium to the BC surface. In this case cells would attach to the BC bonded proteins.

However, BC has problems in some cases when it is used in its natural state. For instance, BC is not enzymatically degradable in vivo and this has become an essential limiting factor in its potential applications (Li et al., 2009). To improve its properties, BC is usually coated with another polymer such as gelatin or modified by adding some substances into the flask cultures of *Acetobacter xylinum.* Another strategy is hybridizing BC with another polymer by mechanically mixing BC solution with the solution of another polymer such as PVA (Luo et al., 2008).

Luo et al. (2008) described the biosynthesis of a novel collagen-BC (COL/BC) composite by adding collagen to the culture medium. The morphology and characterization of COL/BC composite were observed. It is found that the structure of BC network changes when collagen is present in the nutrient medium. The former was being more rugged and porous. However, in the formation process of COL/BC, the well-aligned planes of cellulose and *d*-spacing remain unchanged.

Kristen et al. (2009) studied the design and synthesis of BC/hydroxyapatite nanocomposites for bonehealing applications using a biomimetic approach. BC with various surface morphologies (pellicles and tubes) was negatively charged by the adsorption of carboxymethyl cellulose (CMC) to initiate nucleation of calcium-deficient hydroxyapatite (cdHAp). Field Emission Scanning Electron Microscopy (FESEM) images showed that the cdHAp crystal size increased with increasing nanocellulose fibril density. According to the fluorescence microscopy results, pure BC scaffolds alone would not be a feasible material for a bone healing scaffold. Biomineralized scaffolds yielded a better cellular response. Rather than forming colonies on the surface, the cells formed a confluent layer and the F-actin spread over the entire surface.

Li et al. (2009) modified BC by periodate oxidation to give rise to a biodegradable 2,3-dialdehyde bacterial cellulose (DABC). The morphology, chemical and physical properties of DABC were observed. The results demonstrated that the modified DABC nano-network was able to degrade into porous scaffold with micro-sized pores in water, phosphate buffered saline (PBS) and the simulated body fluid (SBF). The degradation process began from the oxidized amorphous part of the network and concurrently hydroxyapatite formed on the scaffold surface during the

process in SBF. The data also demonstrated that the tensile mechanical properties of the DABC nano-network were suitable for its use in tissue engineering scaffolds

2.2 Alginate

Alginate or alginic acid is a linear polysaccharide, normally isolated from the cell walls of many strains of marine brown seaweed and algae. Its color ranges from white to yellowish-brown. Alginate is intensively used in food, pharmaceutical, textile and paper applica

2.2.1 Production of alginate

Alginate is the term usually used for the salts of alginic acid. Since alginic acid is insoluble, to convert a water- soluble form, alginic acid is transformed into commercial alginate through the incorporation of different salts. The most widely used alginic acid is sodium alginate which promptly dissolved in water. The rationale behind the extraction of alginate from the seaweed is to convert all the alginate salts to the sodium salt. This procedure is illustrated in the flow diagram in Figure 2.4 (McHugh, 1987).

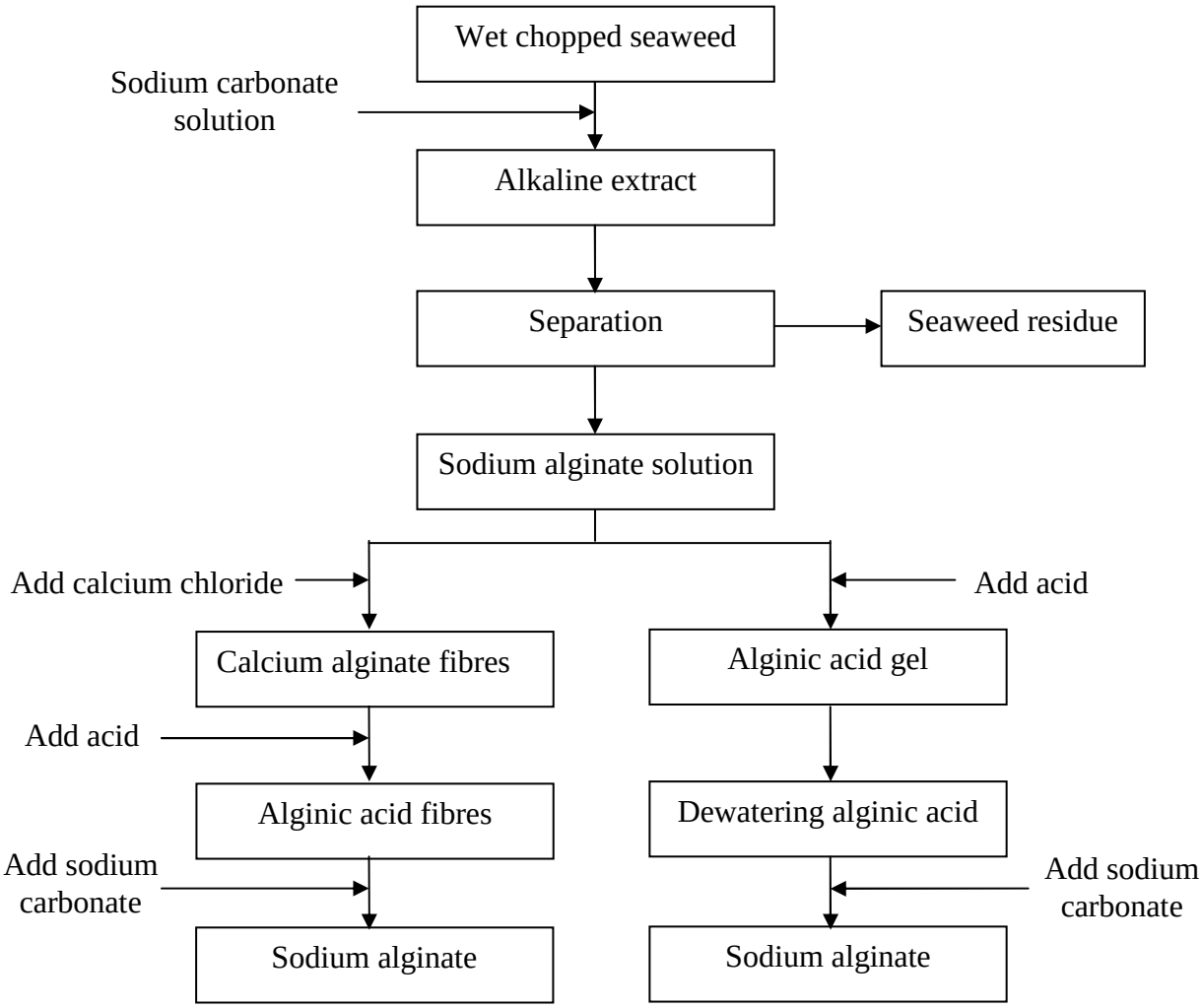

Figure 2.4 The flow diagram of sodium alginate production (McHugh, 1987)

2.2.2 Structure of alginate

Alginate belongs to a family of linear copolymer of (1-4)-linked β-D mannuronic acid (M) and α-L-guluronic acid (G) residues. Within the alginate polymer, the M and G monomers are sequentially assembled in either repeating (MM or GG) or alternating (MG) blocks. The amount and distribution of each monomer depend on the species, section and age of seaweed or algae which the alginate is isolated. The chemical structure of alginate is shown in Figure 2.5.

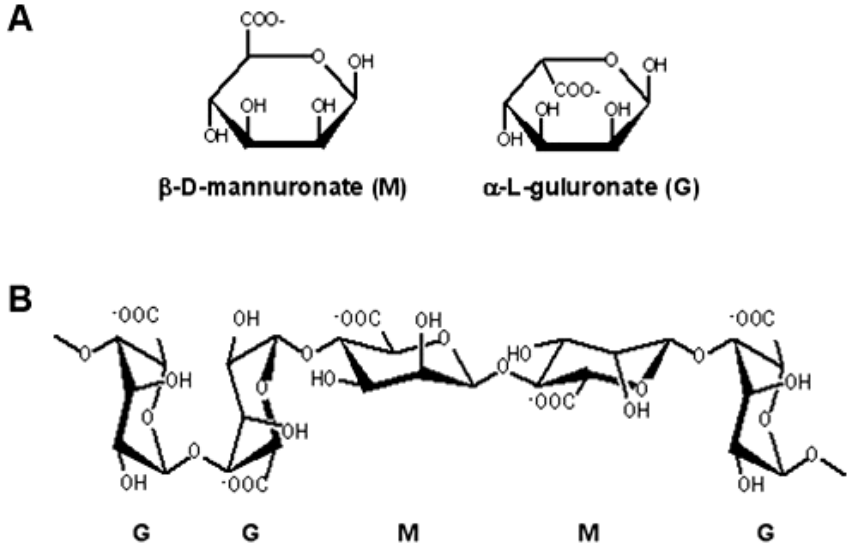

Figure 2.5 The chemical structures of M and G monomers (A) and alginate (B) (Sriamornsak and Sungthongjeen, 2007)

Although the M/G ratio can be obtained relatively easily, the detailed molecular compositions of alginates in terms of block lengths and block distributions are much more difficult to determine. As a result, alginates are usually referred to as high M or high G, depending on the proportions of M and G they contain. Most commercial products are of the high-M type. The best alginate is obtained from giant kelp. In general terms, high-G alginates produce strong, brittle gels that are heat-stable, while high-M alginates provide weaker, more elastic gels that have less heat stability but more freeze/thaw stability. Specifically, the G blocks are buckled while the M blocks have a shape referred to as an extended ribbon (Sriamornsak and Sungthongjeen, 2007) .

2.2.3 Applications of alginate

2.2.3.2 Ethanol fermentation

In ethanol fermentation, entrapment in alginate gel has been one of the most used methods for whole cell entrapment due to its simplicity and non-

toxic character. There are several studied on the component of alginate and suitability for cell immobilization (Ghorbani et al., 2011).

Zorlu et al. (2000) investigated the continuous production of ethanol from beet molasses by Ca-alginate immobilized yeast in a packed-bed bioreactor. The effects of bead diameter, alginate concentration, pH, substrate concentration and recirculation of the substrate on the process variables were determined. The highest ethanol production was obtained with cells entrapped in 2.0-2.4 mm Ca-alginate beads. Increasing in bead diameter decreased ethanol production. Smaller beads yielded more ethanol, probably due to an increase in surface-volume ratio for mass transfer of substrate into and through the beads. The optimal Na-alginate concentration was 2%w/v. Although similar ethanol production and yield values were obtained in beads obtained from 1.0% and 1.5% Na-alginate, these beads were highly susceptible to compaction and disintegration during the operation of packed-bed bioreactor. Above 2%w/v Na-alginate concentration, ethanol production decreased probably due to the lower diffusion efficiency of the beads.

Melzoch et al. (1993) examined the activity and behavior of *Saccharomyces cerevisiae* SL 100 cells entrapped for a long-term period in calcium alginate gel beads. After such a long period (up to 5 years) the entrapped cells were in a viable state confirmed that the process of immobilization significantly increases and supports stability of living yeast cells. The metabolic activity was found in cells immobilized in calcium alginate beads and having been stored for the entire time in 4°C water as non-growing and starveling IC culture. The behavior of yeast cells entrapped in Ca-alginate was described that the cells totally occupied all accessible free spaces in a gel matrix. It is possible to assume that cell growth within a calcium alginate matrix nearly stopped, the entrapped cell ability to bud is suppressed and these cells are held in the gel matrix practically without possibility to their turnover. Finally, the bead size did not suffer any significant change during activation and cultivation and practically remained stable for the entire cultivation time.

Lee et al. (1982) studied the use of immobilized whole yeast cells in Ca-alginate of 2%w/v for ethanol fermentation. A packed column reactor was used in a continuous operation to test the operational stability and ethanol productivity.

Microscopic examination of the gel particles revealed that the cell concentration was higher near the gel surface, where the availability of substrate and oxygen is relatively higher. Some decrease in effluent ethanol concentration was seen after 20 days because some deactivation of cells was observed. The performance of a packed column reactor in terms of ethanol productivity was considerably better than that of a stirred tank reactor. This difference was due partly to attrition of active yeast cells and distintegration of gel particles in the stirred tank reactor.

Najafpour et al. (2004) succeeded to improve the performance of ethanol fermentation in an immobilized cell reactor (ICR). The fixed cell loaded ICR was carried out at initial stage and cell was entrapped by Ca-alginate. From the evaluation of immobilized cells, the suitable alginate concentration based on activity of the beads for ethanol production was 2%w/v and 4.9-5mm in diameter. SEM micrographs showed yeast growth on the surface of the bead and no apparent leakage of cells from the bead. The results indicated that yeast cell entrapped in alginate possesses the capacity not only to utilize high concentration of sugar but also to yield higher ethanol productivities during the course of continuous fermentation.

Nikolic et al. (2010) studied the ethanol fermentation of enzymatically obtained corn meal hydrolyzates by suspended and immobilized *Saccharomyces ceresiae* var. *ellipsoideus* yeast in a batch system. The yeast cells were immobilized in 2%w/v Ca-alginate of 0.8mm average diameter. The results demonstrated that immobilized cells exhibited an elevated tolerance to higher substrate and product concentration compared with the free cells. During the fermentation with immobilized cells, substrate inhibition occurred at an initial sugar concentration of 200g/L, whereas free cells were inhibited with a lower initial substrate concentration of 176g/L. Moreover the same optimal inoculums concentration was found for both free and immobilized yeast. They concluded that this immobilization method was appropriate and thus no substrate diffusion restrictions were noticed.

The particular application of alginate bead, on the other hand, has been limited by the problems of gel degradation, low physical strength and severe mass transfer limitation. Furthermore, large-scale production of these carriers often

requires complex and sophisticated equipment leading to high cost of production (Phisalaphong et al., 2007). Elimination of these disadvantages and development of alginate gel have been studied. Some materials were combined with alginate gel such as inorganic, cellulosic materials for solving these problems.

Phisalaphong et al. (2007) focused on developing a new carrier by combining alginate gel and loofa sponge namely, the alginate-loofa matrix (ALM). Ethanol production by repeat batch fermentation using yeast cells immobilized within the ALM was examined and compared with that using SC and cell immobilized in 3%w/v Ca-alginate beads. From the SEM images, ALM carriers were composed of stacked layers of thin alginate films, high porosity and better cell distribution whereas the structure of alginate beads was dense and less porous. Due to mass transfer limitation, many cells near the surface other than in the middle of alginate bead were observed. In term of ethanol concentration, ALM carrier exhibited a slightly higher than alginate beads. An ALM with a size of $9\times9\times3mm^3$ was effective for cell immobilization, which is comparable to a 2-mm-diameter alginate bead.

Mongkolkajit et al. (2011) evaluated the performance of [gramma]- alumina doped alginate gel (AEC) as a cell carrier for ethanol production. The feasibility of the carrier for cell immobilization was examined and compared with SC culture and immobilized cell on [gramma]- alumina (AC). In repeated batch modes, AEC culture demonstrated a good potential of reusability. Its ethanol production and conversion yield of the first, second and third repeated batch were comparable to those of SC and AC cultures. In addition, its ethanol production was more stable than that of SC culture. The yeast cell immobilization yield of ACE was approximately 85.6 %.

Liu et al. (2008) reported ethanol fermentation in a magnetically fluidized bed reactor with immobilized yeast cells in magnetic particles. Sodium alginate of 3%w/v and Mn-Zn ferrite powder of 0.5%w/v were used in magnetically stabilized fluidized bed bioreactor as a carrier. The effects of $CaCl_2$ concentration, particle loading rate and dilution rate were examined. The experimental results revealed that $CaCl_2$ at a concentration of 2%w/v was suitable where these particles were flexible and enough strong to hold their weight of packing in the

reactor. The ethanol fermentation efficiency was highest at 41%v/v of particle loading rate and 0.4h^{-1} of dilution rate, respectively.

2.2.3.1 Tissue engineering

Suitable biomaterials for tissue engineering applications potentially include alginate. Alginate is considered biocompatible and forms hydrogels in the presence of multivalent cations through the ionic interaction between the carboxylic acid groups located on the polymer backbone and the chelating cation. Calcium cross-linked alginate hydrogels have been used in many biomedical applications, including cell transplantation and drug delivery (Eiselt et al., 2000).

Wang et al. (2003) investigated the ability of rat bone marrow cells to proliferate and differentiate on alginates of differing composition and purity. The tensile strength and water content of three types of alginate gels, including high G content (MVG), high M content (LVM) and reagent grade alginate, were measured in culture medium. Water content of alginate gels was found to show similar patterns among the three alginate gels. The patterns of water content were affected by a slight shrinkage of the substrates and gel swelling. MVG gels have more strength for longer than the LVM gels but reagent grade alginate was the weakest with a tensile failure stress of 50 kPa. The strength of these materials was affected by gel swelling. The mechanism of degradation in vivo is by means of substitution of cross-linking divalent ions by monovalent ions such as sodium. There was a greater rate of rat bone marrow cell proliferation on the MVG gels than the other alginates. It is possible that M-block fractions are anti-adhesive preventing proliferation and colonization whilst G-block fractions promote adhesion and subsequent colonization.

Alginate is typically used in the physical form of a hydrogel with small pores (nm size scale) that do not allow for cell movement in or out of the material. Processing approaches previously used to achieve a macroporous alginate structure involve lyophilization of the hydrogel matrix (Eiselt et al., 2000).

Zmora et al. (2002) investigated the effect of freezing regime on the internal structure of alginate scaffolds, in order to gain a better control over pore microstructure by freezing in a -20^{o}C freezer, submerging into a -35^{o}C oil bath or -196^{o}C liquid nitrogen. The scaffolds were characterized for albumin release profiles from the different alginate scaffolds and the effect of pore microstructure on hepatocyte morphology. The SEM microphages indicated that the scaffolds that were prepared by freezing in the -20^{o}C freezer displayed round, isotropic pores throughout the scaffold volume. The pores had spherical shape and were interconnected. The range of average pore size was 131-170µm which was close to the synthetic polymeric matrices prepared via thermally induced solid–liquid phase separation. Moreover, the scaffolds were capable of resisting larger compressive loads of 1163 kPa. In the albumin release characterization, the albumin molecule moves in the water filled pores without being affected by the torturous path, because of the large size of the scaffold pores as compared to the effective molecular size of albumin. The images of hepatocytes seeded within the scaffold revealed that the cells aggregated in the elongated pore shape, and were lined along the pores. The relative simplicity of this methodology as well as the promising properties of alginate scaffolds was suitable for the cultivation of various mammalian cells.

Shapiro et al. (1997) examined the preparation and characterization of 3D porous sponge made from alginate for creating a cell-matrix scaffold. The scaffold was prepared by a three-step procedure: gelation, freezing and lyophilization. The concentration and type of alginate, the type and concentration of the cross-linkers and freezing regime influenced the pattern and the extent of scaffold porosity. By controlling these variables, macroporous scaffolds (pore size of 70-300µm) that were suitable for cell culture were obtained. The alginate sponges conserved their initial volume for at least 3 months.

Eiselt et al. (2000) developed a method to form macroporous beads with an interconnected pore structure from alginate for tissue engineering application. A mixture comprised of 7%w/w alginate, 0.54%w/w F108, and 0.9%w/w $NaHCO_3$ yielded stable foam. The interior of the beads showed a more interconnected, open pore structure than the surface. The total pore volume was calculated to be 54% and the interconnected, surface accessible porosity was

determined to be 74%. Seeding fibroblasts into the beads and visualizing the cells utilizing the MTT assay was used to verify the porous beads. The experimental result was found that a uniform cell distribution was again noted throughout the entire bead volume, confirming the interconnected pore structure of the beads. Therefore, these structures may provide ideal matrices for tissue engineering applications.

Dar et al. (2002) investigated the characteristic of cardiomyocytes seeded within an alginate scaffold. The porous alginate scaffolds in an attempt to achieve 3D high-density cardiac constructs with a uniform cell distribution. Cell seeding onto the scaffold was efficient because of its high porosity (>90%) and interconnected pore structure. Cell seeding resulted in a uniform cell distribution throughout the scaffolds and high percent cell yield (60-90%). SEM revealed that the cells aggregated within the scaffold pores. Some of the aggregated were contracting spontaneously within the matrix pores.

Sang et al. (2001) examined the fabrication of collagen-alginate composite scaffolds with different collagen/alginate ratios by lyophilizing the respective composite gels formed via collagen fibrillogenesis in vitro and then chemically crosslinking. The effects of alginate amount and cross-linking treatment on pore architecture, swelling behavior, enzymatic degradation and tensile property of composite scaffolds were systematically investigated. The relevant results indicated that the present strategy was simple but efficient to fabricate highly interconnected strong biomimetic 3D scaffolds with nanofibrous surface. Compared with the mechanically weakest crosslinked collagen sponges, the cell-cultured composite scaffolds presented a good porous architecture, thus permitting cell proliferation on the top surface as well as infiltration into the inner part of 3D composite scaffolds. These composite scaffolds with pore size ranging from 150~300 mm, over 90% porosity, biodegradability and water uptake capability are promising for tissue engineering applications.

Li et al. (2004) studied a biodegradable porous scaffold made from chitosan and alginate. The modification by addition of alginate significantly improved mechanical and biological properties of the scaffold as compared to its chitosan counterpart. Enhanced mechanical properties were attributable to the formation of a complex structure of chitosan and alginate. Bone-forming osteoblasts

readily attached to the chitosan–alginate scaffold, proliferated well, and deposited calcified matrix. The in vivo study showed that the hybrid scaffold had a high degree of tissue compatibility. Coacervation of chitosan and alginate combined with liquid–solid separation provides a scaffold with high porosity, and mechanical and biological properties suitable for rapid advancement into clinical trials.

Shachar et al. (2010) explored the beneficial effects of immobilizing RGD peptide into macroporous alginate scaffolds on cardiac tissue engineering. The behavior of cardiac cells subpopulations in the peptide sequence arginine-glycine–aspartate (RGD)-immobilized and unmodified alginate scaffolds were investigated. Both scaffolds exhibited over 90% porosity, with pore diameters in the range of 50–100 μm. From cardiac cells investigation, the unmodified alginate matrix provided an excellent surrounding for elucidating the effects of specific cell–matrix interactions due to its inertness and notable lack of cell adherence. In addition, the presence of immobilized RGD peptide in the scaffold promoted the regeneration of cardiac tissue, as well as its preservation in culture.

CHAPTER III
BACTERIAL CELLULOSE-ALGINATE BLEND AS A YEAST CELL CARRIER FOR ETHANOL PRODUCTION

3.1 Introduction

The disadvantages of alginate such as its poor mechanical properties and its dense structure have limited the application as immobilization support material in industrial fermentation processes (Verbelen et al., 2006). Chemical and physical properties of alginate could be improved by blending with some special polymers. BC developed by *Acetobacter xylinum* has been reported for many unique properties including high crystallinity, high water holding capacity, high tensile strength and high purity. Recently, it has been applied in paper and food industries. In addition, it has been used as a biomaterial in cosmetics and medicine (Cheng et al., 2009). In this work, the blend polymer of BC and alginate was developed as immobilization support material of *Saccharomyces cerevisiae* for ethanol fermentation. The performance comparison between the IC culture by the entrapment within bacterial cellulose/alginate blend (BCA) and pure alginate gel (AL) was examined by batch fermentation.

3.2 Material and methods

3.2.1 Microorganism and culture media

The yeast strain studied in this research was *Saccharomyces cerevisiae* M30. Cell preparation was begun with transferring cell from PDA slant to 150mL sterilized culture media which consisted of palm sugar 15g, 0.015g KH_2PO_4, 0.00525g $MgSO_4.7H_2O$ and 0.075g $(NH_4)_2SO_4$. The initial pH of the culture media

was adjusted to 5.0 by adding 0.1M NaOH or HCl solution. The cell culture flasks were incubated at 33^{o}C, 150rpm for 24h. After that, the obtained cell suspension was concentrated by precipitation.

3.2.2 Cell immobilization

Sodium alginate of 2%w/v was formulated by dissolving Na-alginate powder in deionized water (DI). BC was homogenized in a blender and then was mixed with alginate solution by the weight ratio of 6:4, which was the optimal ratio obtained from our preliminary study. Afterward, the concentrated cell suspension was added into the mixture by the weight ratio of 1:10. The mixture of the blend polymers and cells was cross-linked by 0.12M $CaCl_2$ solution in a tray to form cell carrier and was cut in rectangular shape of 2.0×2.0×0.2cm^3. Finally, the carriers were rinsed 3 times with DI water for removing excess Ca^{2+}. Carriers were prepared under aseptic condition.

3.2.3 Batch fermentation

Molasses was used as a carbon source in batch fermentation. The medium contained 220g/L initial sugar concentration and 0.05%w/v $(NH_4)_2SO_4$. The initial pH was adjusted to 5.0 with 0.1M NaOH and HCl solution and the medium was sterilized at 121^{o}C for 15min. To begin the experiment, the SC culture and the IC cultures in AL carriers or BCA carriers were transferred into 250mL of the medium in 500mL Erlenmeyer flasks. The experiments were carried out in the shake flask incubator at 150rpm, 33^{o}C for 72h. The samples were taken every 8h for sugar, ethanol and cell analyses. The experiments were conducted in duplicate.

3.2.4 Analytical methods

To measure total sugar concentration, the sample solution was hydrolyzed in 37% HCl at 100°C for 10min and neutralized with 20% NaOH solution. The sugar content was then determined by YSI (Model 2700), SELECT Biochemistry Analyzer, Yellow Springs, Ohio. The ethanol concentration was analyzed by gas chromatograph using Shimadzu Model GC7 AG equipped with a flame ionization detector. Determination of free cell concentration was measured with a UV-2450 UV-visible spectrophotometer at 660nm absorbance.

3.3 Results and discussion

The result of ethanol fermentation for 72h is shown in Fig. 3.1. The maximum ethanol concentration of the IC culture using the BCA carrier was 78.4g/L, which was relatively higher than that of the system using AL as support material (68.0g/L). Because of the dense structure of alginate gel after the crosslink method, there was a considerable limitation for substrate diffusion into the gel matrix resulting in a decrease in the cell growth rate and the ethanol productivity (Seki et al., 1990). The addition of BC in alginate gel could reduce the mass transfer problem. As a result, the ethanol concentration obtained from the system using BCA as cell carrier was about 15% higher than that using AL. Furthermore, the addition of BC also enhanced mechanical strength of the cell carrier owing to the hydrogen-bonding formation between the hydroxyl groups of cellulose and the carboxyl group of alginate (Phisalaphong et al., 2008).

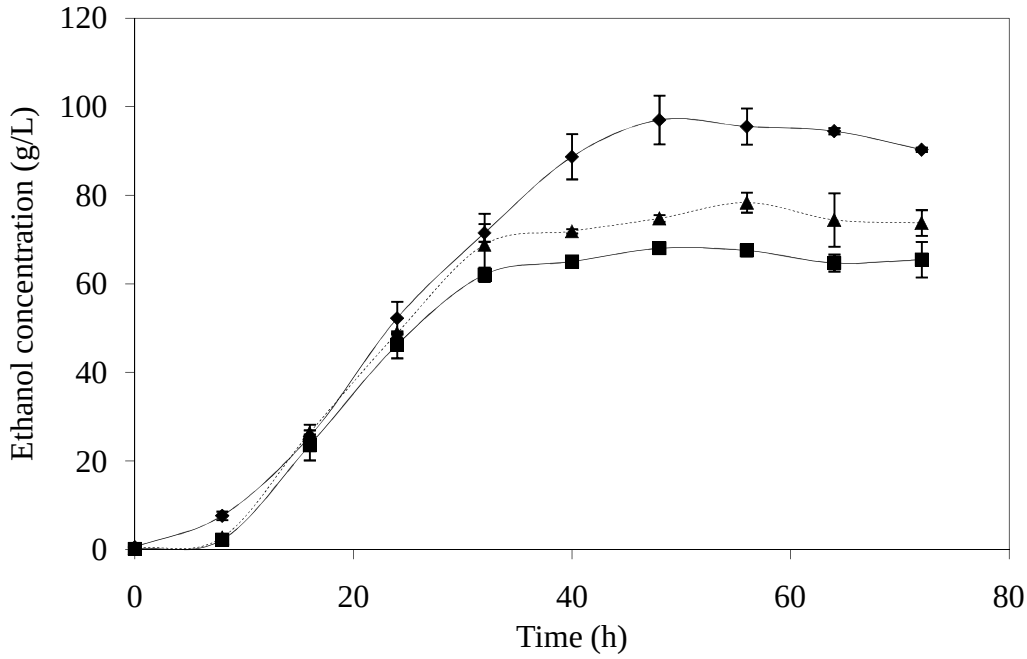

Figure 3.1 Ethanol concentrations during the fermentation by the suspended cell culture (solid line) and immobilized cell culture (AL (dot-dashed line), BCA (dashed line))

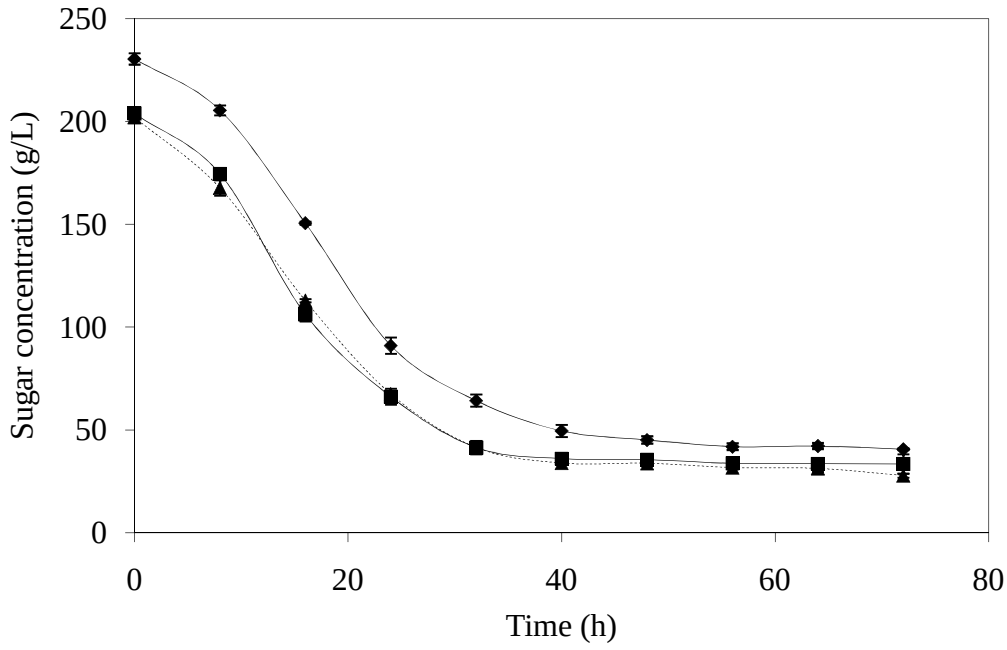

Figure 3.2 Sugar concentrations during the fermentation by the suspended cell culture (solid line) and immobilized cell culture (AL (dot-dashed line), BCA (dashed line))

The comparison of ethanol production between the immobilized cell cultures and the SC culture revealed the consequence of mass transfer limitation in both of BCA and AL carriers. The result in the batch fermentation showed that the ethanol productivity by the SC culture was higher than that of the IC culture. However, in order to improve ethanol productivity in industrial processes, continuous fermentation system using IC culture should be employed (Vasconcelos et al., 2004). The existence of substrate or product inhibition in the continuous fermentation system increases death rate of yeast cells; therefore, the ethanol production efficiency is lower. In this case, the protection of the cells by immobilization in a suitable support material can lead to a significant tolerance to inhibitors or unsuitable condition better than that of the SC culture and the efficiency of ethanol productivity by the IC culture becomes higher (Phisalaphong et al., 2007).

3.4 Conclusion

The results in this research demonstrated that the system using the immobilized yeast cells in the BCA carriers yielded higher ethanol fermentation efficiency than that in the AL carriers. The mass transfer within the carrier material could be improved by the addition of BC into alginate gel, since the BCA matrix might have higher porosity than that of AL. Moreover, the mechanical strength of the carrier was enhanced. However, ethanol concentration obtained from the immobilized yeast cell in BCA was significantly lower than that obtained from SC culture which meant that the diffusion limitation still occurred in BCA matrix. Consequently, the BCA carrier was improved the structure to improve the mass transfer limitation in the next study.

CHAPTER IV
BACTERIAL CELLULOSE-ALGINATE COMPOSITE SPONGE AS A YEAST CELL CARRIER FOR ETHANOL PRODUCTION

4.1 Introduction

IC technology has been applied to both repeated batch and continuous ethanol fermentations to improve ethanol productivity, increase cell density, retain the stability of the cells' activities and protect cells from inhibitors (Wang and Hettwer, 1982; Mojovic et al. 2010). The inhibition effect of the substrate and ethanol on the cell activities, lowering both cell and ethanol yields has been extensively studied (Phisalaphong et al., 2006; Zafar and Owais, 2005). During ethanol fermentation, the existence of either substrate or product inhibition in a long-term operation reduce the activity of yeast cells, resulting in lower ethanol production. In this case, IC culture with proper carriers could help yeast cells tolerate inhibitors or unsuitable conditions better than SC culture, resulting in higher and more stable ethanol productivity (Phisalaphong et al., 2007). Many immobilization techniques have been applied in ethanol fermentation systems such as entrapment (Akacha et al., 2008; Zhao and Xia, 2010), adsorption (Guenette and Duvnjak, 1996; Serpil and Fikret, 2008) and self-aggregation (Xu et al., 2005). The entrapment of cells within beads of calcium alginate is a commonly used technique for immobilizing living cells, especially in smaller scale laboratory settings, because it is simple and maintains high cell viability and activity (Verbelen et al. 2006). However, the drawbacks of alginate gel beads, including its poor mechanical properties, its rapid degradation and its dense structure, have limited its applications in larger scale production in industrial fermentation processes (Mongkolkajit et al., 2011; Yu et al., 2007; Nguyen et al., 2009). During fermentation, the evolution of carbon dioxide influences AL by expanding and causing rapid disruption. Consequently, AL is not a stable cell carrier for use in long-

term ethanol fermentation (Nguyen et al., 2009). The chemical and physical properties of AL could be improved by blending it with some special polymers such as polyvinyl alcohol (Caykara and Demirci, 2006; Tarun and Gobi, 2012) and polyethylene oxide (Moon et al., 2009; Caykara et al. 2005). Sodium alginate-graft-poly (N-vinyl-2-pyrrolidone (NaAlg-g-PVP) beads was developed and applied for ethanol fermentation (Inal and Yigitoglu, 2011). Due to the hydrophilic property of N-vinyl-2-pyrrolidone, this polymeric bead showed better mass transfer characteristics compared with conventional alginate beads. The incorporation of alumina into AL improved the porous structure of the carrier and had a positive influence on yeast cell activity during ethanol fermentation Mongkolkajit et al., 2011). In addition, improved mechanical and biological properties could be obtained from a composite of BC and alginate (Phisalaphong et al., 2008; Kanjanamosit et al., 2010). Our novel composite sponge made of BC and AL was fabricated by a freeze-drying process, and it has been successfully developed for use as mucosal flaps in oral tissue regeneration (Chiaoprakobkij et al., 2011). The freeze-dried sponge with a blending composition of 70/30 BC/AL was stable in both water and PBS and retained its overall size after being used as a cell scaffold. BC was synthesized by *Acetobacter xylinum* in the form of a pellicle, a fine web-like network of cellulose fibers. BC has been reported to have many unique properties, including a high crystallinity, high water retention, high tensile strength and high purity. It has also been reported to have high biocompatibility and low toxicity (Svensson et al., 2005; Zaborowska et al., 2010).

To obtain suitable immobilization carriers, characteristics of the carrier such as pore structure, water content, hydrophilicity and electrical charge should be considered (Sakuria et al., 2000; Fujii et al., 1999). Ethanol production from IC can be improved by a polymeric matrix carrier with high hydrophilicity (Inal and Yigitoglu, 2011). However, excessive hydrophilicity and excessively large pores could lead to the decrease of polymer strength and linkage of immobilized cells Zhaoxin and Fujimura, 2000). Yu et al., 2007 also reported that a larger number of pores in sorghum bagasse facilitated the mass transfer of substrates and products in IC. In addition, the higher electrical conductivity of the modified sorghum bagasse promoted ethanol production and cell adhesion (Yu et al.2010).

In the present study, a bacterial cellulose-alginate composite sponge (BCA) was fabricated via freeze-drying to carry yeast cells for ethanol fermentation. The BCA sponges had an asymmetric structure, consisting of a top dense skin layer and a sponge-like porous layer. The optimal ratio of BC to alginate and the suitable concentration of alginate were investigated. The ethanol productions by batch and repeated batch fermentation using BCA-IC culture were compared with those of SC as well as IC culture entrapped within AL. The stability of BCA in a long-term operation was also studied.

4.2 Material and methods

4.2.1 Microorganism and culture media

The yeast strain used throughout the experiments was *Saccharomyces cerevisiae* M30, which was provided by the laboratory of Dr. Savithree Limthong (Department of Microbiology, Kasetsart University, Bangkok). The stock culture was maintained on a Potato Dextrose Agar (PDA) slant at 4 °C. Starter cultures were prepared by transferring cells from stock PDA slants to 150 mL of sterilized culture medium in a 500 mL Erlenmeyer flask. The culture media was composed of 100 g/L reducing sugar in the form of palm sugar, 0.05% w/v $(NH_4)_2SO_4$, 0.01% w/v KH_2PO_4 and 0.0035% w/v $MgSO_4 \cdot 7H_2O$. The initial pH of the culture media was adjusted to 5.0 by the addition of either 0.1 M NaOH or 0.1 M HCl solution. The cell culture was then cultivated in an Innova 4330 Refrigerated Incubator Shaker from New Brunswick Scientific (NJ, USA) at 33 °C and 150 rpm for 24 h. The stock cell suspension was obtained by decantation of the cell culture at the late exponential phase.

4.2.2 BCA sponge preparation and cell immobilization

The BCA sponge was prepared using the following three-step method: (1) homogenizing the Na-alginate-BC solution, (2) cross-linking with a $CaCl_2$ solution to form a gel and (3) freeze-drying the BCA hydrogel. First, the sodium alginate solution was formulated by dissolving Na-alginate powder in deionized (DI) water. The purified BC pellicles (size 1 cm×1 cm×1 cm) were homogenized in a blender and were then mixed with the Na-alginate solution in a weight ratio of 50/50, 60/40 and 70/30. To form the cross-linked BCA hydrogel, the homogeneous slurry mixture was poured into a tray and was cross-linked by the addition of a 0.12 M $CaCl_2$ solution for 24 h. Next, the BCA hydrogel was rinsed with deionized (DI) water 3 times and was submerged in DI water overnight to removing any excess Ca^{2+}. The BCA hydrogel was then placed in a -40 °C freezer for 24 h and dried under vacuum pressure (<100 mTorr) for 48 h. The dried BCA sponges were cut into rectangular shapes of 2.0×2.0×0.2 cm^3 (≈0.116 g) and were sterilized in an autoclave for 15 min at 121 °C. Then, the 2.5 g sterile BCA sponges were mixed with 250 mL of sterile culture medium in a 500 mL Erlenmeyer flask. Finally, 10 mL of stock cell suspension was added to the culture medium and incubated at 150 rpm and 33 °C for 24 h to induce natural cell adsorption.

4.2.3 Batch and repeated batch fermentations

The IC in the BCA sponges were each transferred into a 500 mL Erlenmeyer flask, containing 250 mL of sterile main medium with 220 g/L of initial sugar from cane molasses and 0.05% w/v $(NH_4)_2SO_4$ at a pH of 5.0. All experiments were carried out at 33 °C and 150 rpm for 72 h and were performed in duplicate. The experiment was monitored by aseptically removing 2 mL of sample every 8 h for cell, sugar and ethanol analysis. For repeated batch fermentations, after 48 h of each initial batch, the fermentation broth was withdrawn, the ethanol and sugar concentrations were determined, and the BCA sponges were transferred to fresh medium to begin the next batch.

4.2.4 Analytical methods

A gas chromatograph (Model GC-7 AG) from the Shimadzu Co. (Shimadzu, Japan), equipped with a flame ionization detector, was used to analyze the ethanol concentration. To measure the total sugar concentration, the sample solution was hydrolyzed with 370 g/L HCl in a boiling water bath for 10 min. After hydrolysis, the sample was neutralized by 200 g/L NaOH. The total sugar content was then determined by a YSI (Model 2700) SELECT Biochemistry Analyzer from YSI Incorporated (OH, USA). To calculate the free cell concentration, the absorbance at 660 nm was measured by a UV-2450 UV–Visible spectrophotometer (Shimadzu Scientific Instruments, Inc., Japan) and then converted to the dry cell concentration using a corresponding standard curve (Rattanapan et al., 2011). To determine the IC concentration, the carrier sponge was cut into small pieces and stirred in DI water for 1 h. Then, the carrier was removed and the concentration of cells in the resulting suspension was determined similarly to the free cell calculation. Cell concentrations were reported in dry cell mass (g) per volume of fermentation broth (L). The immobilization yield (Y_I) was determined from a ratio of the immobilized cell concentration (X_I) to the total cell concentration (X_T). The ethanol yield ($Y_{P/S}$) was determined from a ratio of ethanol accumulation to sugar consumption.

4.2.5 Material Characterizations

4.2.5.1 Scanning Electron Microscope (SEM)

An examination of the structural properties of the carriers was performed by SEM. The carriers were frozen in liquid nitrogen, immediately snapped, and vacuum-dried. Then, the carriers were sputtered with gold and photographed. The coated specimens were examined under SEM using a JOEL JSM-5410LV microscope (Tokyo, Japan).

4.2.5.2 Equilibrium water content

The equilibrium water content (EWC) was determined by immersing the pre-weighed dry sample of BCA in DI water at room temperature until equilibration occurred. The BCA was then removed from the water. After excess water on the surface of the BCA was blotted off with Kimwipes paper, the weight of the swollen BCA was determined. This procedure was repeated until there was no further weight change. All tests were run five times, and the equilibrium water content was determined using the following equation:

$$\text{Water uptake ability} = (W_w - W_d)/W_d$$

where W_w and W_d represent the weight of wet and dry samples, respectively.

4.2.5.3 Mechanical properties measurement

The mechanical strength of the carriers was measured by a Universal Testing Machine-H 10 KM (Hounsfield, USA). The test conditions followed the standard procedure ASTM D882. The samples were cut into strip-shaped specimens of 10 mm in width and 10 cm in length (with 50 mm between the grips). The stretch rate was 2 mm/min. The tensile strength was averaged over five specimens.

4.3 Results and discussion

4.3.1 Batch fermentation

Batch fermentation using cane molasses as the main carbon source was carried out at 33 °C and 150 rpm for 72 h. In our preliminary study, it was found that the ethanol fermentation performance by using yeast cells immobilized in BC by adsorption method was relatively poor with the cell immobilization yield lower than 5% (data not shown). Therefore, BCA sponge was developed for improved yeast

fermentation performance. For a conventional alginate matrix, the optimal alginate concentration was ~2.0% by wt. (Mongkolkajit et al., 2011; Najafpour et al., 2004). Therefore, in this study, an alginate solution of 2% by wt. was used to formulate the AL and BCA carriers. As shown in Table 4.1, the ethanol concentration produced by the SC system was significantly higher than that from the system of IC in AL. A maximum ethanol concentration of 87.9 g/L was obtained at 48 h of the batch fermentation from the SC system, which was 28.5% higher than that of IC in the AL carriers. Besides, the productivity and production yield ($Y_{p/s}$) of SC system were 1.83 g/(Lh) and 0.48, respectively, which were higher than those of IC in AL carrier (1.42 g/(Lh) and 0.35, respectively). A diffusion limitation of the cells into the substrate has often been observed for IC in AL carriers because of AL's dense structure (Mongkolkajit et al., 2011). The preference of cells to grow near the surface instead of in the middle of a gel matrix has been previously reported (Phisalaphong et al., 2007; Verbelen et al., 2006; Bangrak et al., 2011). Growing yeast cells in an environment with insufficient nutrients causes a low sugar uptake rate and low ethanol production (Bai et al., 2008). Low mechanical strength and rapid degradation are other large drawbacks of an alginate gel (Bangrak et al., 2011). Some leakage of cells was also found on the surface of AL (Figure not shown). However, the ethanol fermentation by IC in BCA carriers showed comparable productivity to that of the SC system. This result indicates that BCA is a superior carrier of IC for ethanol production. The designed BCA structure, consisting of a thin film with micro pores on the outer surface and large pores distributed in the spongier interior, was found to be effective for yeast immobilization (Mongkolkajit et al., 2011; Chandel et al., 2009). Due to the high porosity of the BCA carrier, a higher mass transfer rate could be achieved, which allowed for the relatively higher ethanol concentration.

Table 4.1 Concentrations of products, yields of cell immobilization (Y_I), yields of ethanol ($Y_{P/S}$) and ethanol productivities (Q_P) at 48 h of batch fermentation using the SC and IC culture entrapped within AL and BCA fabricated with different BC/AL ratios

System		Ethanol (g/L)	Residue sugar (g/L)	Cells (g/L)		Y_I (%)	$Y_{P/S}$ (%)	Q_P (g/(Lh))
				Free cell	Immobilized cell			
SC		87.9±3.0	31.6±0.1	4.6±0.1	-	-	47.7±1.7	1.83±0.06
AL		68.4±2.9	37.9±1.3	1.6±0.1	3.6±0.5	69.9±0.9	34.6±4.1	1.42±0.18
BCA	50/50	90.7±0.1	22.5±1.7	1.5±0.1	3.5±0.3	70.7±2.1	46.2±0.4	1.89±0.01
	60/40	92.0±3.1	26.3±2.6	1.8±0.1	5.1±0.8	74.4±1.5	48.4±2.3	1.92±0.07
	70/30	89.8±1.2	25.7±2.2	1.9±0.0	5.0±0.3	73.7±1.9	45.8±1.2	1.87±0.03

Table 4.1 shows a comparison between the ethanol concentrations produced by SC, IC in AL carriers, and IC in BCA carriers at 48 h of the fermentation with different ratios of BC/AL (50/50, 60/40 and 70/30). The maximum ethanol concentrations of the system with IC in BCA were slightly higher (2.2-4.7%) than those obtained from the SC system. It has been previously reported that the immobilization of yeast with proper carriers leads to higher cell densities, protects cells from both inhibitors and toxins, and allows for high ethanol productivity (Phisalaphong et al., 2007; Mongkolkajit et al., 2011; Rattanapan et al., 2011; Bangrak et al., 2011; Sree et al., 2000). Y_I values of IC in BCA were slightly higher than that of IC in AL. Although cell entrapment technique is efficient for high initial cell loading into cell carriers, large numbers of yeast cells attached on the surface of AL were observed.

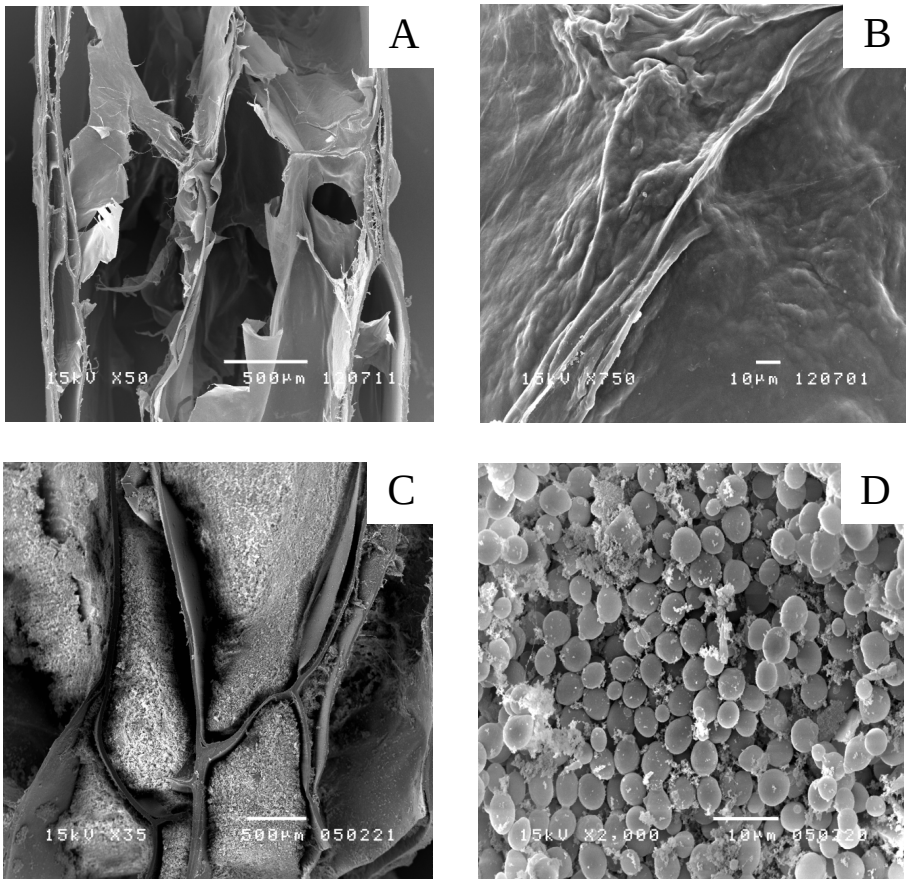

Figure 4.1 SEM images of fresh BCA carrier (0 h): (A) cross section and (B) surface and BCA carrier after 72 h of batch fermentation: (C) cross section and (D) a closer look of yeast cells in a hollow space

The SEM images of the fresh BCA (0 h) and the BCA carrier at the end of the batch fermentation are shown in Figure 4.1. The BCA had an asymmetric structure that consisted of a thin surface layer with interconnected hollow spaces in the interior, which facilitated the transmission of substrates and products between the carrier and the medium. After being used for 72 h in ethanol fermentation, large numbers of yeast cells adhered to the inner and outer surfaces of the BCA sponges; cell agglomeration in the hollow spaces of the carrier was also observed, indicating that the substrates were adequate for cell growth. In a previous study of cellulose carriers, the structure consisting of small pores distributed on the outer surface and large pores distributed in the interior was found to be effective for yeast immobilization (Sakuria et al., 2000).

The structural characteristics of the carrier, such as porosity and water uptake ability, are important factors that influence cell adhesion and ethanol productivity (Zhaoxin and Fujimura, 2000). The blending composition influences the structure and properties of composite materials. From SEM observation (cross-sectional view), the BCA carriers, with BC/AL ratios varying from 50/50 to 70/30 using 2% (by wt.) alginate solution, presented an interconnected porous structure with an average pore size of 500-1,000 μm. The water uptake ability of the BCA carriers varied from 6.0-12.2, depending on the AL content. The tensile strengths and elongations of the BCA carriers varied from 2.8-4.4 MPa and 10.7-13.0%, respectively. A decline in tensile strength was observed with increasing AL content. Alginate is very hydrophilic; as more alginate was incorporated into the BCA film, the film became more hydrophilic (Kanjanamosit et al., 2010). The presence of alginate in the BCA sponge could also enhance the molecular motion of cellulose in the blend and perturbed the strong hydrogen bond of pure cellulose resulting in the reduction in mechanical strengths. The increase in water uptake ability and the drop in mechanical strength in BC/AL composites with increasing AL content has been previously reported (Kanjanamosit et al., 2010; Chiaoprakobkit et al., 2011). In our experimental results, the highest ethanol concentration and ethanol conversion yield ($Y_{P/S}$) at 92.0 g/L and 0.48, respectively, were obtained from IC in a BCA carrier with a BC/AL weight ratio of 60/40. Ethanol production from IC in BCA carriers with BC/AL ratios of 50/50 and 70/30 were approximately 1.5% and 2.5% lower, respectively, than that of the optimal ratio (60/40). Therefore, the blending composition of 60/40 BC/AL was selected for the fabrication of our BCA sponge.

4.3.2 Effect of alginate concentration

A decrease in the mass transfer diffusivity of the gel matrix with increasing alginate concentrations has been reported (Phisalaphong et al., 2007; Mongkolkajit et al., 2011; Najafpour et al., 2007). However, a gel matrix formulated with a low concentration of alginate gel (≤1.5%) is too soft and easily degrades when it is used in a shaking incubator or a packed-bed reactor. The effects of the AL

concentration on the fabrication of BCA at the blending BC/AL ratio of 60/40 was examined by batch ethanol fermentation for 48 h as shown in Table 4.2.

Table 4.2 Concentrations of products and yields of cell immobilization (Y_I), yields of ethanol ($Y_{P/S}$) and ethanol productivities (Q_P) at 48 h of batch fermentation using the IC culture entrapped within BCA fabricated with different alginate concentrations [AL]

BCA (60/40)		Ethanol (g/L)	Residue sugar (g/L)	Cells (g/L)		Y_I (%)	$Y_{P/S}$ (%)	Q_p (g/(Lh))
				Free cell	Immobilized cell			
[AL] (% by wt.)	1.5	93.4±3.2	31.2±0.1	2.8±0.2	5.3±1.2	65.3±3.8	49.5±1.7	1.95±0.07
	2.0	93.8±1.2	31.7±0.6	2.5±0.0	4.8±0.5	65.8±2.8	49.8±0.5	1.95±0.03
	2.5	93.6±0.1	33.0±0.0	2.7±0.2	5.5±0.0	66.7±1.6	50.1±0.0	1.95±0.01
	3.0	99.6±1.7	32.6±0.6	2.2±0.4	12.2±2.1	84.3±2.7	53.1±0.7	2.08±0.03
	4.0	99.7±3.6	31.5±1.1	2.4±0.2	7.9±0.6	76.8±3.1	52.9±1.6	2.08±0.08
	5.0	99.0±2.2	33.6±0.8	2.1±0.2	6.4±0.7	75.7±0.1	53.1±1.4	2.06±0.05
	6.0	99.1±1.4	35.2±0.6	3.2±0.6	4.6±0.4	59.3±2.5	53.6±0.9	2.06±0.03

Table 4.3 Effect of alginate concentrations on physical properties and porous structure of BCA

Alginate concentration (% by wt.)	BCA						
	1.5	2.0	2.5	3.0	4.0	5.0	6.0
Thickness (mm)	0.1-0.2			0.2-0.3			
Porous structure	interconnected				multi-layer		
Tensile strength (MPa)	5.5± 1.4	5.5± 1.6	5.8± 1.3	7.3± 2.2	6.8± 1.7	7.9± 2.1	4.1± 0.9
Elongation (%)	10.7± 1.4	10.2± 3.0	10.4± 1.3	10.5± 1.9	10.1± 1.0	10.0± 0.5	10.7± 0.5
Water uptake ability	5.9± 0.3	7.1± 0.7	7.8± 0.6	8.6± 0.9	8.1± 0.3	7.9± 0.5	6.4± 0.1

The results of ethanol fermentation by IC in BCA with different concentrations of AL could be divided into 2 groups: (1) low-medium AL concentrations (1.5-2.5% by wt.) and (2) high-medium AL concentrations (3.0-6.0% by wt.). The maximum ethanol concentrations produced from the first group were approximately 6% higher than in the SC system, whereas the ethanol concentrations from the second group were approximately 13% higher than in the SC system. The observed physical properties and pore structure of the prepared BCA sponges with different concentrations of AL are summarized in Table 4.3. It was found that shrinkage in the BCA structure during the cross-linking step was influenced by the AL concentration. The sponges formulated with an AL solution at a low concentration (less than 3.0 %) were thin and lacked firmness; only slight shrinkage of their structure was observed during the cross-linking step. The main disadvantages of the thin BCA sponges were poor mechanical properties and instability. On the other hand, the sponges fabricated with an AL solution at a higher concentration (more than 3.0%) showed considerable shrinkage during the cross-linking step and formed a multilayer structure instead of an interconnected porous structure. Accordingly, at an AL concentration greater than 3.0%, the water uptake ability decreased. The interconnected porous structure and high water uptake ability were shown to promote cell growth, cell immobilization and ethanol productivity. The highest immobilized

cell density and ethanol concentration were obtained from IC in BCA formulated by AL at 3.0% by wt., where the immobilized cell concentration, immobilized yield (Y_I) and ethanol concentration were at 12.2 g/L, 84.3% and 99.6 g/L, respectively. Therefore, the suitable AL concentration for BCA sponge formation was found to be 3.0% by wt. In a previous study, the diffusion of substances was not only influenced by the structure of the carrier but also affected by the carrier's hydrophilicity (Zhaoxin and Fujimura, 2000). The hydrophilicity or hydrophobicity can affect the distribution and availability of substrates and products (Tischer and Wedekind, 1999).

4.3.3 Repeated batch fermentation

The BCA carrier fabricated by the 60/40 mixture of BC/AL (using a 3.0% by wt. AL solution) was used as a cell carrier for 5 repeated batch ethanol fermentations. Repeated batch fermentation was carried out under similar conditions as batch fermentation, with each batch lasting 48 h. Figure 4.2 A and B show a comparison of the ethanol concentration and residue sugar concentration profiles, respectively, between repeated batch systems with SC, IC in the AL carrier, and IC in the BCA carrier.

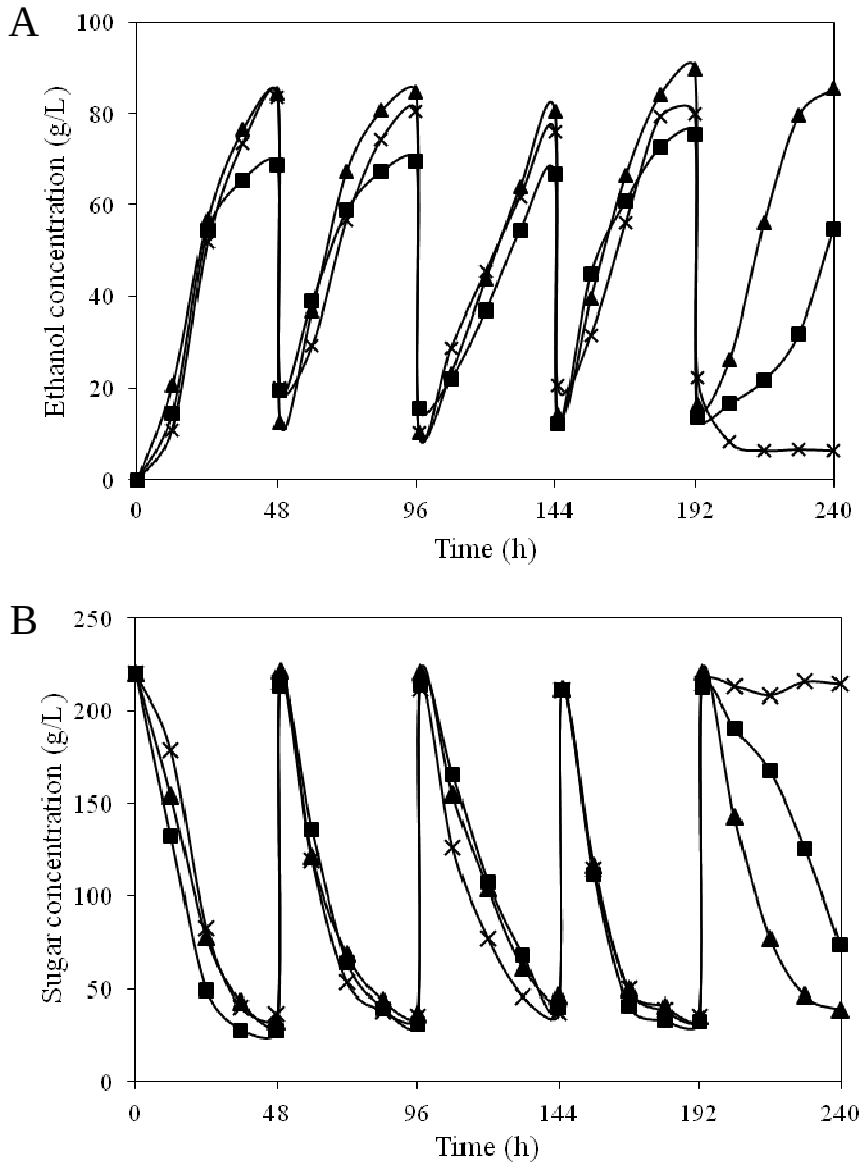

Figure 4.2 Profiles of ethanol (A) and residue sugar (B) of repeated batch fermentation (48 h for each batch) using the SC (cross) and IC culture entrapped within AL (square) and BCA (triangle)

The highest ethanol concentration and highest total cell concentration were obtained from the system of IC in BCA. Instabilities of the SC and the IC in AL systems were observed in the fifth batch. For long-term fermentation, the SC culture exhibited a poorer tolerance to higher sugar and ethanol concentrations than did IC (Nikolic et al., 2010). In the AL carrier, degradation and breakage of the carriers undergoing long-term operations resulted in the leakage of cells and a reduction of

ethanol production in the fifth batch. A degradation of the AL surface has been previously reported to cause a decrease in the immobilization yield after a four-cycle repeated batch (Phisalaphong et al., 2007). Previously, degradation of the AL gel after the second batch of ethanol fermentation was reported (Rakin et al., 2009). A comparison of our results showed that the BCA carrier was more stable, as it retained its overall carrier size and ethanol productivity at about 1.7-1.9 g/L h for the entire course of the examination. In addition, at the end of the fifth cycle of the repeated batch, the total cell concentration was 25.8 g/L, which was 69.0% and 24.4% higher than that of the SC and the IC in AL systems, respectively. The incorporation of BC enhanced the mechanical strength of the BCA carrier (Phisalaphong et al., 2008). The existence of substrate or product inhibition in long-term repeated batch fermentation or continuous fermentation can deactivate yeast cells; therefore, the ethanol production efficiency becomes lower. In this case, the protection of the cells by immobilization in a suitable support material can lead to a significantly improved tolerance to inhibitors and unsuitable conditions over the SC culture (Phisalaphong et al., 2007).

The difference in ethanol productivity in IC systems could mainly due to the difference in the internal structure and properties of polymer carrier, such as surface charge, hydrophilicity, and swelling ability of polymer carrier (Zhaoxin and Fujimura, 2000). Previously, BC hydrogel was applied as a yeast cell carrier (Nguyen et al., 2009). It was reported that *S. cerevisiae* adsorbed mostly on the surface of BC pieces and might diffuse partially to the inside structure. However, owing to the dense structure of BC hydrogel, after 2 days of the incubation, yeast cell number in the biocatalyst decreased as a result of the lack of substrates for yeast metabolism. It was found in this study that yeast cells could attach and grow from the surface to the inside of BCA. The growth and aggregation of yeast cells were observed throughout the entire space of the BCA carrier. Therefore, the diffusional resistance to substrates/ products (ethanol) transport was minor. Consequently, in the repeated batch fermentation using IC in BCA, the very high cell density was obtained. The cell density during repeated batch fermentation using IC in BCA was relatively high compared to that of our previous work using thin shell silk cocoon (Rattanapan et al., 2011) and alginate–loofa (Bangrak et al., 2011) as support materials, whereas the

ethanol productivity was comparable to that of IC on thin shell silk cocoon and relatively higher than that of IC in alginate–loofa.

4.3.4 Stability of BCA

A 15 cycle repeated batch system (30 days) was used to investigate the long term-stability of the BCA carrier for ethanol fermentation. The results are summarized in Fig. 4.3. The final ethanol concentrations of each batch are fluctuated between 87.4-96.8 g/L during the 30 days of the repeated batch fermentation. The average ethanol concentration produced by using the IC in the BCA carrier was at 92.1 g/L. Therefore, the IC and their BCA carrier could be reused for at least 30 days, retaining high activity. In a study of IC in sugarcane stalks, it was reported that after an 8 cycle repeated batch fermentation (over 12 days), ethanol fermentation gradually decreased (Chandel et al., 2009). The difference in the obtained results might also arise from differences in yeast strains and system conditions. The results of our repeated batch experiment demonstrated that the BCA carrier's mechanical properties could withstand the shear force applied during the shaking process and the evolution of carbon dioxide during ethanol fermentation. No significant degradation or breakage was observed. The BCA carrier also exhibited good porous structure and good water uptake ability. Therefore, it represented a highly effective and stable cell carrier for use in long-term repeated batch and continuous ethanol fermentations. Besides, the BCA sponge has a good potential to be applied as cell carrier for other microorganisms, animal cells and plant cells.

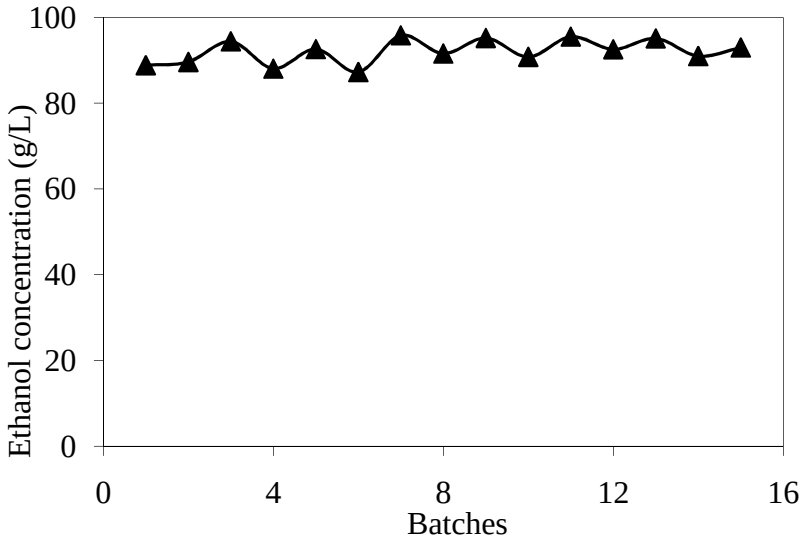

Figure 4.3 Ethanol concentrations at the end of each repeated batch for 15 cycles

4.4 Conclusion

Our biocompatible porous cell carrier, BCA, was fabricated from BC and AL via a freeze-drying process. BCA was effectively used as a yeast cell carrier for ethanol fermentation due to its advantageous porous structure, mechanical strengths, stability and hydrophilic character. The outer, thin layer covering the interior interconnected macroporous structure of the BCA sponge was found to be very effective for yeast immobilization while minimizing internal mass transfer limitations. The BCA carrier also showed good mechanical properties, withstanding the shear force in the mixing process and the evolution of carbon dioxide during ethanol fermentation. The IC in BCA carriers was more stable than SC and IC in AL carriers. An examination using 15 cycle repeated batch fermentation demonstrated that BCA was capably reused as a carrier for at least one month.

CHAPTER V
APPLICABILITY OF WASHBURN CAPILLARY RISE FOR DETERMINING CONTACT ANGLES OF POWDERS/POROUS MATERIALS

5.1 Introduction

Surface wettability, one of the most crucial surface properties of materials, is a key parameter for understanding the interactions of materials with their surrounding and for their applications. As a result, proper characterization techniques to obtain the accurate surface wettability of these materials are highly desired.

Surface wettability is generally characterized by contact angle of a liquid on a solid surface. For a flat solid surface, many common techniques, e.g. sessile drop and Wilhelmy plate (Shang et al., 2008), can be applied for measuring contact angles. For powders/porous materials, capillary rise, i.e. flowing of a liquid up a capillary by attractive forces between the liquid and the solid surface, is normally used to characterize their wettabillity. In particular, WCR, which is derived from the rate of capillary rise of liquid penetrating in a packed cylindrical tube, has been widely employed. To deduce the contact angle values, either the rate or the height of the capillary rise is measured. The equation is based on Poiseuille's law as expressed below:

$$dV = \frac{r^4 \pi \Delta P}{8 \eta h} dt \qquad (5.1)$$

where V is the volume of the liquid, r is the radius of the cylindrical tube, ΔP is the pressure drop, η is the vicosity of the liquid, h is the height of the liquid risen, and t is the time that the liquid flows to a certain height.

In this case, pressure drop (ΔP) is a pressure difference between the capillary pressure (P_c) and the hydrostatic pressure (P_h), i.e. $\Delta P = P_c - P_h$, which can be further espressed as:

$$\Delta P = \left(\frac{2\gamma \cos\theta}{r} \right) - \rho g h \qquad (5.2)$$

By comparison, the hydrostatic pressure (ρgh) is much smaller than the capillary pressure $\left(\frac{2\gamma \cos\theta}{r} \right)$, therefore, the liquid rising upward through the tube is primary contributed by the capillary pressure. For equation (5.1), the volume of liquid inside the cylindrical tube can be writen as $V = \pi r^2 h$, substitute this and equation (5.2) into equation (5.1) and intregate it with an initial condition (at $t=0$, $h=0$) and a particular time (i.e. at $t=t$, $h=h$) leads to

$$h^2 = \frac{r\gamma \cos\theta}{2\eta} t \qquad (5.3)$$

Equation (5.3) is Washburn's equation that presents the relation between a squared height of the penetrating liquid and the penetrating time. In the case of powders or porous materials packed in a tube, voids between materials could be described as many bundles of capillary tubes (Costanzo et al., 1995). Therefore, WCR can be applied to obtain contact angles for powders or porous materials and can also be expressed in term of a squared mass of the penetrating liquid ($m=\rho A h \varepsilon$) and the penetrating time as:

$$m^2 = \frac{C\rho^2 \gamma \cos\theta}{\eta} t \quad \text{with} \quad C = \frac{r_{eff} A^2 \varepsilon^2}{2} \qquad (5.4)$$

where, r_{eff} is the effective radius or the equivalent radius of voids in the packed powders or porous materials, A is the cross-section of the tube, and ε is the porosity of the packing in the tube. To determine contact angles of liquids on powders or porous materials using WCR, four conditions have to be satisfied for the process (i.e. Washburn's equation is derived based on these four assumptions): (1) steady state laminar flow, (2) no external pressure, (3) negligible gravitational force and (4) zero velocity of the liquid at the solid/liquid interface (no slip).

Washburn's equation based on the principle of capillary rise has been widely applied to determine the contact angle or surface free energy of powder materials (Siebold et al., 1997 ; Schoelkopf et al., 2002). However, a main concern for contact angles characterized by using WCR is how reasonable the determined values are. This concern is based on several facts regarding to applying WCR. First, the packing of materials is expected to affect liquid penetration, hence contact angle values, although some researchers have reported that packing with particles of different sizes and pore sizes had no effect on contact angles (Subrahmanyam and Prestidge, 1996 ; Troger et al., 1998 ; Dang-Vu and Hupka, 2005). Second, some unsucessful contact angle characterizations of porous materials by applying WCR have been documented (Jackson et al., 2004). One limitation of WCR is to find a suitable complete wetting liquid to be used for determining the geometric factor of the packing, i.e. the C value in equation (5.4).

Due to the concerns of applying WCR for contact angle characterization of powders and porous materials, some potential issues of contact angle detemination for materials that exhibit large contact angle hysteresis, which is the difference between the advancing contact angle and the receding contact angle, by using WCR are being addressed in this paper. The contact angles characterized by WCR and by the sessile drop method for four common polymers: polystyrene (PS), polymethymethacrate (PMMA), nylon 6 and nylon 6/6, were compared. Based on the results, nylon 6/6, which exhibited the largest water contact angle hysteresis based on sessile drops, was chosen as the model material to grind into powders of different sizes. The effects of powder size and packing on the water and ethanol advancing contact angles of nylon 6/6 powders determined using WCR were examined. It was found that larger powders whose packing contained larger voids slowed down the liquid penetration rate, leading to a smaller and more reasonable advancing contact angles for nylon 6/6. On the other hand, the penetration rate of the packed powders of PS, whose flat films showed a small water contact angle hysteresis, had little effect on the advancing contact angle obtained using WCR. Both cases indicated that larger powders were likely to result in smaller and more reasonable advancing contact angles, and the applicability of such approach was also assessed by using a bacterial cellulose-alginate sponge as a test material.

5.2 Material and methods

5.2.1 Materials and equipment

Polystyrene (PS, Mw = 50,000 g/mol, PDI = 1.06) was purchased from Polyscience, Inc. (Warrington, PA), and polymethyl methacrylate (PMMA, Mw = 120,000 g/mol, PDI = 1.8), nylon 6 and nylon 6/6 were purchased from Sigma – Aldrich Co. (Saint Louis, MO). Solvents used included ACS grade toluene (99.5%, Fisher Scientific International Inc., Fair Lawn, NJ), acetone (99.5%, Sigma –Aldrich Co.), formic acid (88%, J.T. Baker, Phillipsburg,NJ), octane (99%, Acros Organics, Morris Plains, NJ), decane (99%, Sigma –Aldrich Co.), hexadecane (99%, Acros Organics), ethanol (99.98%, Pharmco-Aaper and commercial alcohols, Brookfield, CT), and de-ionized (DI) water purified in house (with a conductivity of 77.5 μS/cm). BC was provided by the Institute of Research and Development of Food Products, Kasertsart University, Thailand. Sodium alginate (Na-alginate) was supplied by Carlo Erba, Italy. Other materials included heavy duty aluminum foils (Reynolds, Richmond, VA), sterilize cotton balls (CVS Phamarcy, Inc., Woonsocket, RI), and glass tubes (0.5 cm inside diameter and 9 cm in length, from Friedrich & Dimmock Inc.).

The equipment used include an analytical balance (E1RR80, Ohaus Explorer Pro., Parsippany, NJ, with an accuracy of 0.1 mg), a spin coater (p-6000, Specialty Coating Systems Inc., Indianapolis, IN), an ultrasonic bath (1510 MT, Branson Ultrasonic Corp., Danbury, CT), a grinder (IDS77, MR. COFFEE, Boca Raton, FL), a set of Metric Test Sieves (W. S. Tyler, Mentor, OH), an UV-ozone cleaner (Model 42, Jelight Company Inc., CA), a digital camera (DSC-W100, Sony Corp., Japan), a CCD camera (Sony), Diamond VC500 one-touch video capture software 176 (Diamond Multimedia, Chatsworth, CA) and the ImageJ software (National Institutes of Health, Bethesda, MD).

5.2.2 Preparation of polymer sheets

A 20% w/w of PS and nylon 6 solutions were prepared in toluene and formic acid, respectively. For PMMA and nylon 6/6, 10% w/w solutions were prepared in acetone and formic acid, respectively. To fabricate the polymer sheets to be ground into powders, these polymer solutions were poured, separately, in home-made cleaned aluminum foil trays (~ 8 inches x 9 inches) and then were placed in the fume hood until them were dry.

5.2.3 Preparation of bacterial cellulose-alginate composite sponge

To fabricate BCA, 3% w/w of Na-alginate was prepared by dissolving Na-alginate in DI water, and then the homogenized BC was mixed with the Na-alginate solution by a weight ratio of 6:4. After that, 160 g of the mixer was poured in a plastic tray (~ 7 inches x 12 inches) and then cross-linked with a 0.12 M $CaCl_2$ solution in water for 24 h to form a hydrogel. The hydrogel was rinsed by a copious amount of DI water 3 times and then was immersed in a DI water bath for 24 h to remove the excess Ca^{2+}. The hydrogel was frozen in a freezer at -20 ^{o}C. Afterward, the frozen hydrogel was immediately transferred to lyophilize under vacuum pressure (<100 mTorr) at the condenser temperature of -40 ^{o}C for 48 h. BCA was then kept in a desiccator prior to its use.

Oxidation of BCA was carried out by using the UV-ozone cleaner. BCA sheets were placed in the UV-ozone chamber at a distance ~2 mm away from the UV light source and were oxidized for 15 min.

5.2.4. Wettability characterization by using WCR

To characterize the wettability of the polymers using WCR, dried polymer sheets were ground and then sieved into three different size ranges: 0-250, 250-500, and 500-2000 μm. To obtain the fourth size, 0-2000 μm, powders from each sieved size were combined.

The glass tube used to pack the polymeric powders was cleaned sequentially with acetone, ethanol and deionized water by sonication (5 min for each solvent). For packing the ground polymers in the glass tube, the bottom of the tube was first plugged with 0.02 g cotton (to a height of ~ 5 mm) and then 0.2 g polymer powders were packed into the tube by tapping at least 100 times until the packed height reached a given value. The packed tube was then secured to a micro-manipulator, which was moved down slowly until the bottom of the tube just touched the test liquid that was inside a petri-dish placed on the analytical balance. During the experiment, mass loss of the liquid penetrating into the packed tube and penetrating time were recorded using the digital camera. The displays of a timer and the balance were inside the view of the digital camera. At least three sets of experiments were run for each liquid to make sure the data was reproducible.

5.2.5 Wettability characterized by the sessile drop method

In order to generate thin films of PS and PMMA, cleaned glass slides were coated with the polymer solutions by using a spin coater at 2000 rpm for 30 s. Spin coating was found to be challenging for generating uniform and smooth nylon 6 and nylon 6/6 films, as a result, the melts of nylon 6 and nylon 6/6 were pressed into thin layers. Specifically, a pellet of nylon 6 or nylon 6/6, was sandwiched in between two cleaned glass microscope slides and heated (e.g. ~ 200 and 250 ^{o}C, respectively for nylon 6 and nylon 6/6). As soon as the pellet started melting, a metal weight was pressed onto the top glass slide to spread the pellet out into a layer, and then the entire assembly was quickly removed from the heater and left in the fume hood to cool to room temperature. The advancing contact angles of water and ethanol on the polymer thin films were examined by using the sessile drop method. The liquid drop was firstly placed and formed on the surface of the thin film and then the liquid was slowly added into the drop. The images of the drop, at different liquid advancing rates, were captured by using a Sony CCD camera and the Diamond VC500 one-touch software. The contact angles at the three-phase contact line were measured by ImageJ software from the images.

5.3 Results and discussion

5.3.1 Wettability of polymeric powders by the Washburn capillary rise method

A typical advancing/penetrating rate profile of a liquid up a tube packed with different materials is shown in Fig. 5.1. Basically, different slopes are observed when the liquid flows through the tube packed with different materials. In these experiments, the liquid first penetrated up through cotton (t_0 to t_1), then the polymer powders (t_1 to t_2), and finally the open air (at t_2), thus the advancing rate profile can be seen to divide into three corresponding regions (Fig.5.1). Only the second region, associated with the penetration of liquid through the packed polymer powders, was utilized to estimate the advancing contact angle of the liquid on the material based on the Washburn's analysis.

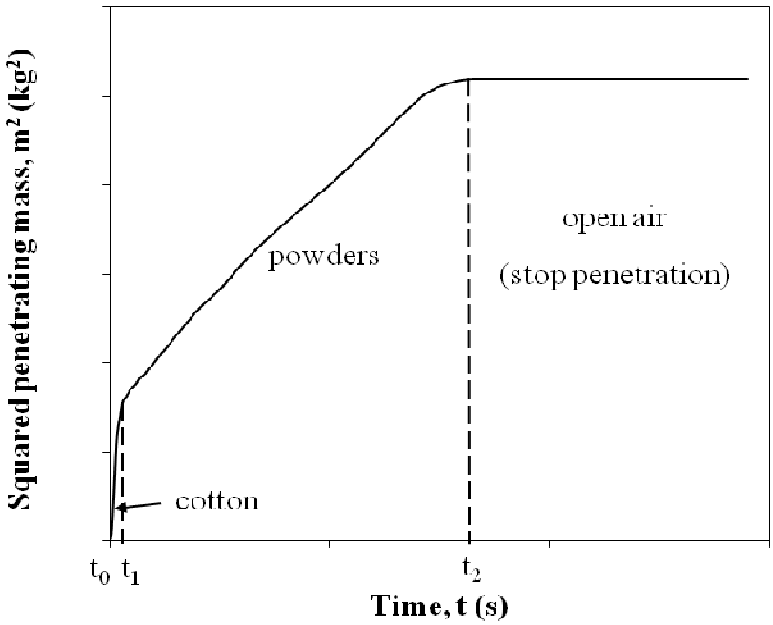

Figure 5.1 A typical profile of penetrating rate, in term of mass square (m^2), of a liquid rising up a packed tube (In this particular case, octane was the penetrating liquid, and the tube was packed, from bottom up, with 0.02 g cotton and 0.2 g nylon 6/6 powders)

The advancing rate profiles of octane and water through the tubes packed with PS, PMMA, nylon 6 and nylon 6/6 are shown in Fig. 5.2A, B, C and D, respectively. For PS and PMMA, water slowly penetrated through only the lower portion of the packed tubes and then stopped because of the relatively high hydrophobicity of these two polymers. The advancing water contact angles characterized by using WCR from these curves, those measured by sessile drops, and those reported in the existing literatures are summarized in Table 5.1. For PS, the advancing water contact angle ($\theta_{A\text{-}w}$) characterized by using WCR was close to that measured by sessile drop as well as to that reported in literature. On the other hand, for PMMA, nylon 6 and nylon 6/6, large differences (i.e. ~ 11^o, 10^o and 12^o, respectively, using tubes packed with powders of 500 – 2000 μm) between the values of $\theta_{A\text{-}w}$ from WCR and those measured by sessile drops were observed. Results from other researchers, as summarized by Chibowski and Perea-Carpio (2002), also indicated that the advancing contact angle estimated by using WCR was overestimated when compared with that measured directly on a smooth surface by the sessile drop method. In addition, Xue et al. (2006) had experimentally obtained a much higher (40 – 45º higher) advancing contact angle of silicone oil on glass using capillary rise and applying Washburn equation as well as a modified equation that takes into account of the hydrostatic effects on liquid rising up the capillary tube. They attributed their results to two possible reasons. One is the contact angle hysteresis and the other is the dynamic contact angle effects. Our experimental results did also show that the deviation of $\theta_{A\text{-}w}$ characterized by using WCR increased when the contact angle hysteresis of polymers increased (Table 5.1). A potential reason could be that a surface having a higher contact angle hysteresis would likely have a greater number of metastable states (Johnson et al., 1977) and a lower energy barrier between adjacent metastable states (Long and Chen, 2006). As a result, the liquid could advance easier from one metastable state to its adjacent higher energy state. These in conjunction with the jumping motion of the air/liquid/solid three phase contact line, caused by overcoming the relative greater energy barriers in the advancing front (as compared to the receding front), would likely lead to the greater advancing contact angle.

According to the values reported in Table 5.1, nylon 6/6 was the most hydrophilic among the four polymers (based on the contact angles from sessile drops) and showed the highest difference in contact angles by WCR and by sessile drop as well as the highest water contact angle hysteresis. Therefore, nylon 6/6 was selected to determine the potential cause(s) of the large deviation of contact angle characterized by using WCR from those measured by sessile drops and the values reported by others.

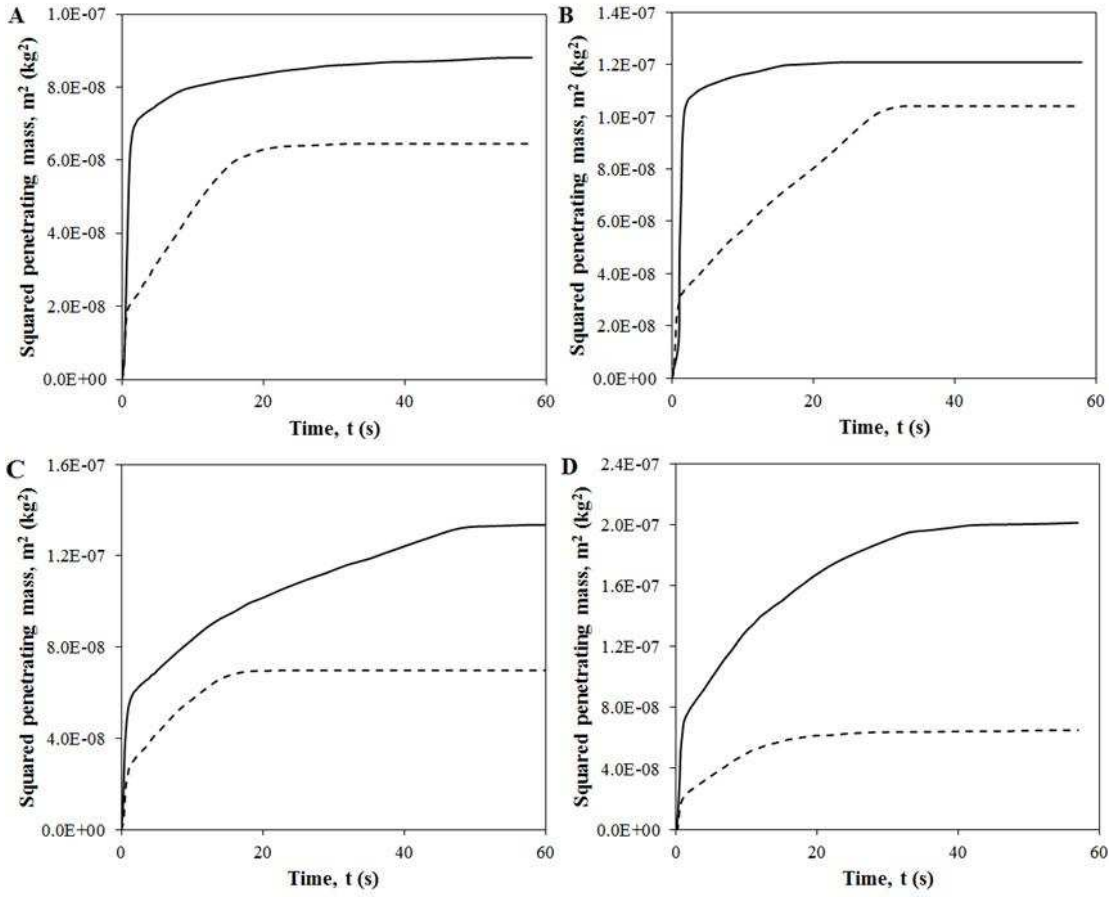

Figure 5.2 Penetrating profiles of octane (dashed line) and water (solid line) through the tubes packed with 500-2000 μm of powders of (a) PS, (b) PMMA, (c) nylon 6 and (d) nylon 6/6

Table 5.1 Water contact angles obtained by WCR using tubes packed with 500-2000 µm powders and those measured by the sessile drop method on thin films of the four polymers. The reported advancing angles in the literatures for these four polymers are also presented

Polymer	Advancing water contact angle, $\theta_{A\text{-}w}$ (^{o})			water contact angle hysteresis (^{o}) by sessile drop
	WCR	Sessile drop	Literature	
PS	88.1 ± 0.2	91.6 ± 2.5	90.0[(Occhiello et al., 1991)]	10.5 ± 2.5
PMMA	87.7 ± 1.4	76.9 ± 2.2	74.0[(Dann, 1970)]	17.2 ± 2.2
Nylon 6	78.4 ± 1.6	68.4 ± 4.4	60.5[(Omenyi et al., 1981)]	23.2 ± 4.1
Nylon 6/6	62.9 ± 1.8	51.2 ± 2.4	65.0[(Dann, 1970)]	23.9 ± 2.6

Note. The error for each was the standard derivation value obtained for at least three different runs. To minimize the potential concerns that polymer thin films prepared by the two different methods (spin-coating vs. melt pressing) could lead to different surface roughness, PS and PMMA films were also prepared by melt-pressing in between two glass slides, and no noticeable difference in $\theta_{A\text{-}w}$ or receding contact angle, hence the contact angle hysteresis, was found for the two different preparation methods.

5.3.2. Effects of powder size/packing on wettability determined by WCR

In a pre-experiment, three alkanes (octane, decane and hexadecane) were examined to determine the complete wetting liquid for the polymers. From the sessile drop method, liquid spreading on the polymer surface was only observed when octane was used. For decane and hexadecane, small contact angles (less than 10^o) were noticed. Also, the advancing rate of octane in the polymer packed tube was higher than the other two (data not shown) due to its low surface tension and low viscosity. Furthermore, octane has a negligible evaporation. Thus octane was chosen as the complete wetting liquid for these polymers.

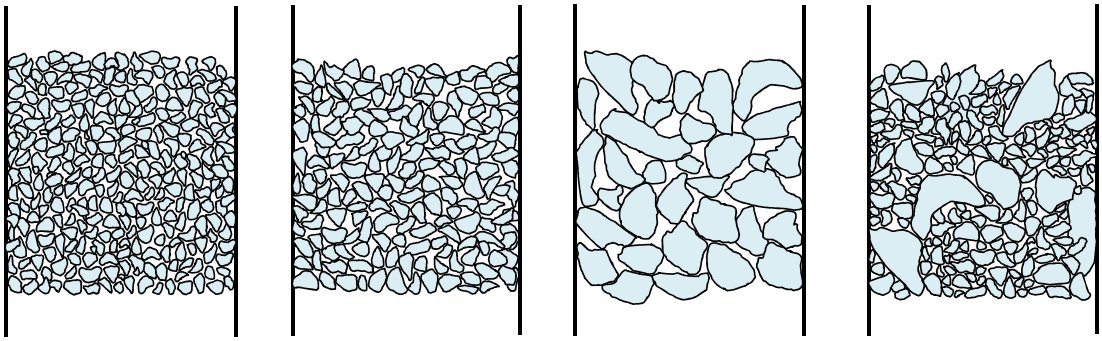

Figure 5.3 Sketches of packing with nylon 6/6 powders of different sizes: (a) 0-250, (b) 250-500, (c) 500-2000, and (d) 0-2000 μm

The effect of material packing on wettability was investigated by using the powders of nylon 6/6 having different sizes (0-250, 250-500, 500-2000 and 0-2000 μm). C values obtained by using the advancing rates of octane in the packed tubes, each packed with the same amount (0.2 g) of powders, are summarized in Table 5.2. Since the powders were grounded from polymer sheets using a coffee grinder, they were highly irregular in shape and having very different lengths in the three dimensions. The potential structures of packing for tubes packed with powders having different sizes are illustrated in Fig. 5.3. The packing structure of powders with the size of 0-250 μm was expected to be relatively uniform, similar packing was also expected for powders with the size of 250-500 μm. In case of 0-2000 μm powders, the filling of big voids with smaller powders could reduce void size. Based on C values, the void sizes of the tube packed with powders of different sizes would likely be: 0-250 μm < 250-500 μm $\leq$ 0-2000 μm < 500-2000 μm. Smaller pore sizes leading to larger C values have been reported by the study of Dang-Vu and Hupka (2005) using packing of glass beads.

Table 5.2 C values of the tubes packed with nylon 6/6 powders of different sizes, liquid penetration rates and advancing contact angles of water and ethanol obtained by using WCR through these tubes

Powder size	C value[1] ($\times 10^{16}$ m^5)	Water		Ethanol	
		Penetrating rate ($\times 10^9$ m^2/s)	Advancing contact angle (^{o})	Penetrating rate ($\times 10^9$ m^2/s)	Advancing contact angle (^{o})
0-250	4.3 ± 0.4	9.3 ± 0.2	74.8 ± 0.4	4.4 ± 0.2	35.7 ± 3.6
250-500	3.8 ± 0.1	9.1 ± 0.1	72.5 ± 0.1	4.1 ± 0.3	30.1 ± 7.5
500-2000	1.5 ± 0.2	5.6 ± 0.3	62.9 ± 1.8	2.2 ± 0.3	1.7 ± 2.7[2]
0-2000	3.1 ± 0.6	7.8 ± 0.5	71.8 ± 1.3	3.6 ± 0.2	21.7 ± 8.3

[1] The value of C reflects the geometrical factor associated with packing, which includes greater voids caused by wall effect when packing larger powders near the wall (Mehta and Hawley, 1969).

[2] The three values of the advancing ethanol contact angle were ~ 0, 0 and 5^o. The error for each was the standard derivation value obtained for at least three different runs.

Water and ethanol advancing rates through the packed nylon 6/6 powders with different sizes are presented in Fig. 5.4A and 5.4B, respectively, and the differences are obviously observed. For the tubes packed with powders of 0-250, 250-500 and 0-2000 µm, both water and ethanol advanced faster (i.e. greater slopes of m^2 *vs.* t curves within the first few seconds) through these packed tubes than that for powders of 500-2000 µm. For the tube packed with powders of 500-2000 µm, the penetration of water ceased ~ 20 seconds later than those packed with 250-500 and 0-2000 µm sized powders (Fig. 5.4A). In the case of the tube packed with the powders of 0-250 µm, the liquid quickly penetrated through the bottom of the packing and then slowed down for the rest. It was noticed that, during packing, the 0-250 µm powders appeared to be harder to settle and could not be packed tightly because of static electricity at a relatively low humidity (< 25% relative humidity in the winter months)

environment during the experimentation time. As a result, the top of the packing could be much looser than the rest of packed regions. As seen in Fig. 5.4A and 5.4B, for tubes packed with powders of 0-250 μm, the penetrations of water and ethanol had abnormal profiles and took much longer (80 and 110 seconds, respectively) to reach the top as compared to those packed with other sized powders.

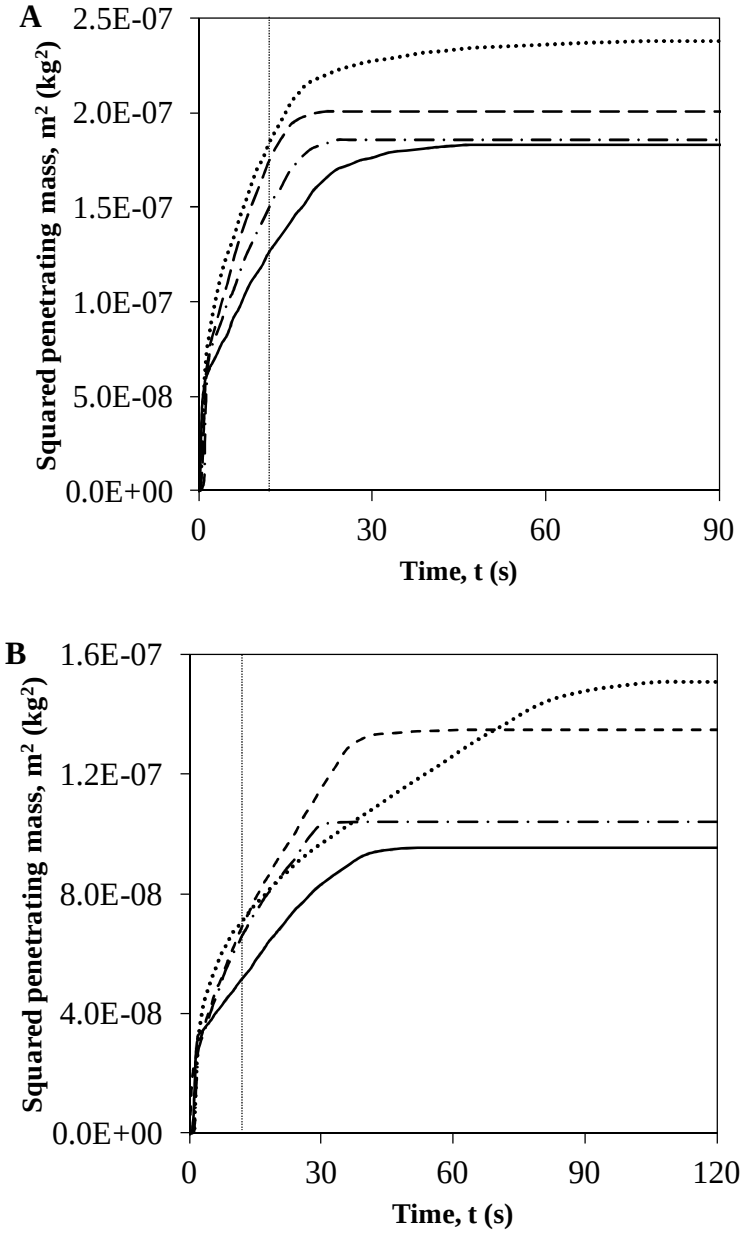

Figure 5.4 Penetrating profiles of (a) water and (b) ethanol up the tubes packed with powders of different sizes of nylon 6/6: (dotted line) 0-250, (dashed line) 250-500, (solid line)500-2000, and (dot-dash line) 0-2000 μm

The water and ethanol advancing rates and advancing contact angles in packed tubes are also summarized in Table 5.2. The results showed that, during the first 10 s, the liquids in general penetrated through the tubes packed with smaller powders faster than those packed with bigger powders. The advancing water contact angles characterized by using WCR for 0-250, 250-500, 500-2000 and 0-2000μm nylon 6/6 powders were ~75, 73, 63 and 72^{o}, respectively, which were about 24, 22, 12 and 21^{o}, respectively, higher than those measured by the sessile drop method. For ethanol, the advancing rate was also the fastest for the 0-250 μm powders and it was the slowest for the powders of 500-2000 μm. While the expected ethanol contact angle on nylon 6/6 was zero, the only value that was closed to zero was obtained using tubes packed with 500-2000 μm powders. For the tube packed with 0-2000μm powders, the advancing rates of both liquids and the contact angles were close to those of the tube packed with 250-500 μm powders because of their similar C values. The sequential photographs in Fig. 5.5 detail water penetrations in various packing by using water stained with red food dye. The initial (≤ 10 s) fast liquid penetration and with an uniform advancing front was observed only in the tube packed with 0-250 μm powders, which likely had small voids and narrow void size distribution at the bottom portion of the packing. The void size and void size distribution of the tube packed with 0-2000 μm powders were also expected to be small and narrow, respectively, because the big voids created by large powders (> 500 μm) were likely being filled with the smaller powders as illustrated in Fig. 5.3D. As a result, the liquid penetrated through the tube packed with 0-2000 μm powders was found to be faster and with a more uniform advancing front than that packed with 500-2000 μm powders. The packing of 500-2000 μm powders likely created large voids, especially near the tube wall due to wall effect (Mehta and Hawley, 1969), and a wider void size distribution, so the liquid penetrated through the packed tube with an un-even penetration rate and a non-uniform advancing front, as shown in Fig. 5.5C. Although the observed liquid advancing front (smooth, uniform) of the tube packed with 0-250 μm sized powders was most similar to the assumed conditions of WCR, the deviation of the water contact angle characterized by WCR was the largest when compared to that measured by sessile drop. On the other hand, the smallest deviation of water contact angle was

found for 500-2000 µm sized powders, for which the liquid penetrated slowest through the packed tube and with an irregular advancing front.

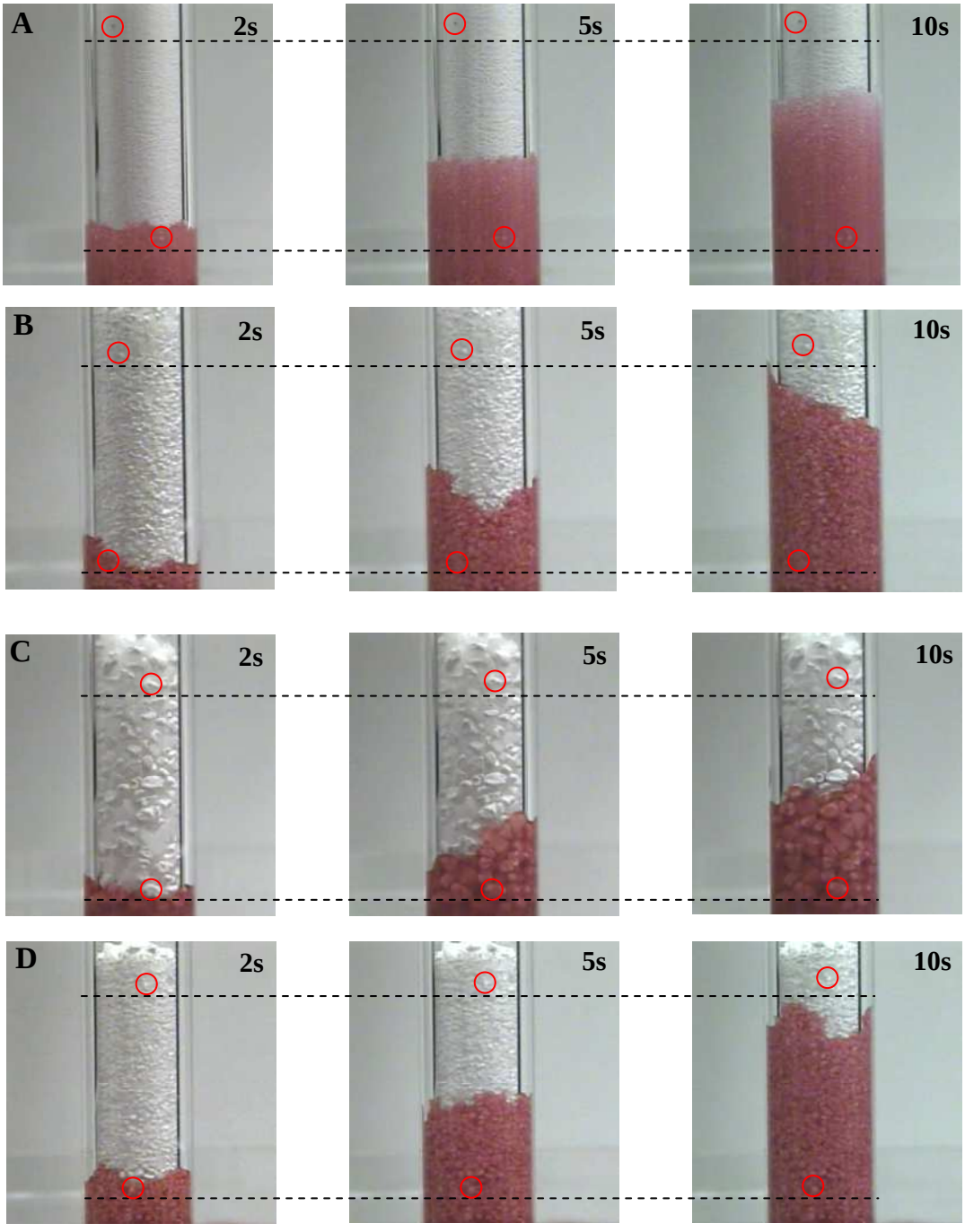

Figure 5.5 Some representing sequential images of the penetration of water, stained with red dye, up the tubes packed with (a) 0-250, (b) 250-500, (c) 500-2000, and (d) 0-2000 µm sized nylon 6/6 powders. The circled powders and the dashed lines are used to guide the eyes to show the powders moving upward as liquid penetrates

5.3.3. Effect of advancing rate on contact angle

The above results indicated that a larger advancing contact angle was resulted when the liquid penetration rate was higher. The advancing contact angle increases with the increase of advancing rate, or the velocity of the air/liquid/solid three phase contact line, has been noted by many others using different contact angle determination methods (Xue et al., 2006 ; Johnson et al., 1977 ; Tretinnikov and Ikada, 1994 ; Dussan, 1979). Xue et al. (2006) applied the capillary rise and obtained a 40 – 45º higher advancing contact angle, as compared to the expected value, of silicone oil on glass. Tretinnikov and Ikada (1994) employed the Wilhelmy plate method by immersing polymer plates at different advancing rates to obtain the advancing water contact angles on polymer films. Their advancing contact angles of water were found to increase when the advancing rates increased. Theories based on fluid mechanics have shown that the macroscopic advancing contact angles increase with the advancing velocity, especially when the velocity is in the range of mm/s to m/s while the capillary number is large (Dussan, 1979 ; Cox, 1998 ; Tavana and Neumann, 2006). In our WCR experiments, the advancing velocity is in mm/s. With such a high advancing velocity, the contact angle obtained is predominately affected by dynamics, and the value would derivate greatly from its static value and even from the value obtained under slow advancing rates (i.e. μm/s or less).

In order to further experimentally verify that a faster liquid advancing rate led to a greater advancing contact angle for the polymers used in this study, a separated contact angle measurement approach using sessile drops on flat polymer thin films was carried out. For the sessile drop method, the advancing contact angles were measured by adding liquid into a liquid drop when the drop was placed on a flat solid surface. As can be seen in Fig. 5.6, the advancing contact angle increased with the increase of advancing rates, with the largest increase for nylon 6/6. The advancing water contact angles of PMMA, nylon 6 and nylon 6/6 were observed to increase about 10, 17 and 25^{o}, respectively, when the advancing rate was increased from 0.1 to 1 mm/s. These results supported the observed advancing contact angle increase with liquid advancing rate (Table 5.2) for more hydrophilic polymers that exhibited high contact angle hysteresis.

On the other hand, there was only a slight effect of the advancing rate on the advancing water contact angle of PS, which was the most hydrophobic amongst the four polymers. Also, 0-250 µm of PS powders packed in glass tubes were used to observe the advancing rate effect on $\theta_{A\text{-}w}$ by WCR. The results indicated that $\theta_{A\text{-}w}$ characterized by using tubes packed with 0-250 µm powders was only 1º higher than that by using tubes packed with 500-2000 µm powders. From Fig. 5.6, the effects of advancing rate on advancing water contact 500-2000 µm powders. From Fig. 5.6, the effects of advancing rate on advancing water contact angles characterized by sessile drops were noticed to increase when the polymers were more hydrophilic and having a higher contact angle hysteresis. The potential reason of the effects of contact angle hysteresis on advancing contact angle was described earlier. With more hydrophilic surfaces, the interactions between water and these surfaces would be stronger. For PMMA, nylon 6 and nylon 6, 6, the enhanced interaction could be resulted from potential hydrogen bonding between water and the ester linkage and amide linkage, respectively. As a result, the time required to reach equilibrium (i.e. for water molecules to spread/cover the surface) could be longer. With a faster advancing rate, the deviation from equilibrium would be greater, leading to a larger advancing contact angle (i.e. further away from the equilibrium contact angle). Also, the surface reorientation could occur for the hydrophilic polymers. With a slower advancing rate (i.e. 0.1 mm/s), the surfaces of the polymer thin film might be able to adjust the functional groups for minimizing the interfacial free energy. For hydrophobic polymers, the weaker interactions between water and these surfaces could make the effects of time on reaching equilibrium and the effects of reorientation of any surface functional groups on the surfaces on wettability less obvious (Tretinnikov and Ikada, 1994).

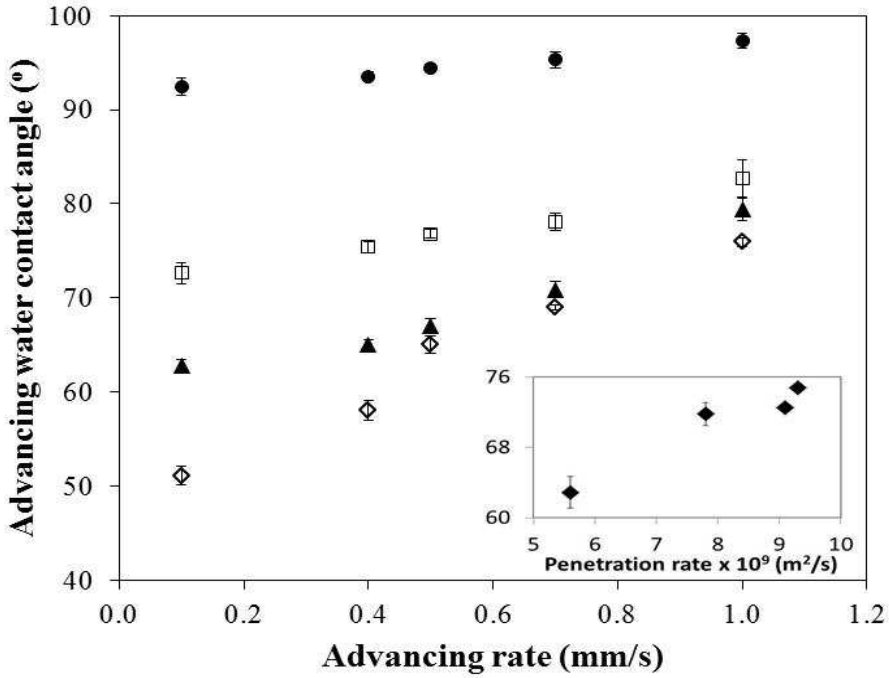

Figure 5.6 The advancing water contact angles on PS (filled circle), PMMA (square), nylon 6 (filled triangle) and nylon 6/6 (trapezoid) measured by the sessile drop method with different water advancing rates. The small insert summarizes the advancing water contact angles obtained on nylon 6/6 powders via WCR under different water penetration rates. The error bars for each were the standard derivations obtained for at least eight data points

5.3.4. Analysis of liquid penetrating profile to obtain suitable contact angle values by WCR

To characterize wettability (contact angle/surface energy) of powders/porous materials, WCR is a simple method to use. However, many details are needed to be considered when analyzing the liquid penetrating profile. From equation (4), the relationship between the squared mass of penetrating liquid and time should be linear, but the experimental penetrating rate profiles, for most cases, were gradually curved, as seen in Figs. 5.1 and 5.2. During the first few seconds when liquid rose in the powders packed section, the penetrating rate profile was found to be linear (with a $R^2 > 0.99$). This portion of the profile was used to estimate the value of C and contact angle in our experiments, while the rest of the profile was mostly

ignored. Whether or not the rest of the profile should be included for estimating the value of C and contact angle, we need to look into how and why the profile deviated from the linear relationship.

A main factor for the penetration rate profile to curve was packing. During the preparation of the packed tube, the bottom of the tube was tapped at least 100 times, intended to provide a uniform packing. However, the resulting packing was looser at the top and tighter at the bottom, thus the geometric factor (i.e. C value) of the packing decreased within one single packed tube from the bottom to the top. If a constant C value was assumed for the entire powder packed section to estimate the value of contact angle, potential errors would result. An alternative approach was to use different C values and liquid penetrating rates at different locations along the packing to obtain contact angles; however, such approach also resulted in some unreasonable values. For example, the contact angles of water were expected to be 50-65^{o} for nylon 6/6, but those obtained from powders having the size of 250-500 µm were 66, 56, 39 and 21^{o} at four different locations from the bottom to the top of the packing. Another example, for 500-2000 µm powders, contact angles of water were 63, 51, 43 and 36^{o} from the bottom to the top of the packing. As mentioned above, in the packed tube, the liquid penetration gradually slowed down because the packing at the top was looser than that at the bottom, therefore, the contact angles should gradually decrease from the bottom to the top of the packing due to the decreased liquid penetration rate. However, for the obtained contact angles to be much lower (30-40º) than the expected value, additional explanations would be required.

One point worth noting of the lower than expected contact angle values obtained from our experiments was a slight upward movement of packed powders as water and ethanol rising up the packed tube, especially for tubes packed with the smallest powders (Fig. 5.4). As shown in Fig. 5.5, upward movements of powder particles (circled) in the upper section of the packing were clearly observed, while the powders closer to the bottom of the packing retained at their locations. The upward lifting of the powders was not observed when octane rose up the packed tube, so the C values at different portions of the packed tube obtained using octane penetration profiles might not necessary be the same as those when water and ethanol rose up the packed tube. One reason for the upward lifting of powders could be the static

electricity presented in the powders due to packing in a low humidity environment; octane is a non-polar liquid while water and ethanol are polar liquids, the potential electric static interaction might repel the very light powders. When the packing was done in a high humidity environment, such upward lifting of the powders was minimized. To minimize the effects of upward lifting of powders on packing geometric factor, when applying WCR, a more reasonable contact angle could be obtained by using only the linear penetration rate profile at the beginning of the penetration process, which appeared to be least affected by the lifting of powders.

The wettability of powders/porous materials can also be measured by using the capillary rise method in a "pseudo" equilibrium state where the penetrating liquid reaches to a certain final height prior to reaching the top of the packed tube. However, such approach was unfeasible in our case, since the equilibrium liquid rise height would be in meters. For example, by assuming the porosity of 500-2000 µm powders packed in a tube to be 0.5, the height estimated was ~ 8 meters, which was impossible to be operated to receive the wettability information.

5.3.5. Contact angles of water on bacterial cellulose-alginate composite sponge

A case study to verify our approach was to determine the contact angle of water on porous BCA sponge. It is complicated that BCA provided an asymmetric structure consisted of nanoporous layer on the surface and interconnected macroporous layer in the interior, therefore; the direct contact angle measurements and thin layer wicking (our preliminary results) could not be used to characterize its wettability. By using WCR, $\theta_{A\text{-}w}$s of BCA were obtained and are summarized in Table 5.3. Reported values of static water contact angles on freeze dried calcium alginate and BC were 52^o (Lin and Ciou, 2010) and 49^o (Tom et al., 2011), respectively, so the expected value should be ~ 50^o. $\theta_{A\text{-}w}$ of BCA characterized by using WCR was found to be 75.8^o. This could be the result of the high contact angle hysteresis (an increased advancing contact angle and a decreased receding contact angle) of the highly heterogeneous BCA, the trapping of air in the nanopores of the BCA as well as the overestimation by WCR because of the high advancing rate. To assess whether or not WCR could still be used to characterize wettability of such complex porous materials,

BCA was treated by UV/O_3 for 15 min (U-BCA) and its wettability was characterized by using WCR. Due to the presence of ionic oxygen, $\theta_{A\text{-}w}$ of U-BCA was expected to be lower, and it was found to be ~ 17^o lower than that of BCA without UV/O_3 treatment (Table 5.3). These results indicated that WCR might be applied to roughly characterize wettability and assess wettability variation due to surface modification of real porous materials.

Table 5.3 Advancing water contact angles characterized by WCR using tubes packed with 500-2000 µm powders of BCA and U-BCA

Material	Treatment	Advancing water contact angle (^{o})
BCA	-	75.8 $\pm$ 2.3
U-BCA	UV/O_3 for 15 min	59.0 $\pm$ 6.8

Note. The error for each was the standard derivation value obtained for at least three different runs.

5.4 Conclusions

Applicability of WCR for assessing wettability of polymer powders and porous materials were examined to determine factors that could lead to the overestimation of advancing contact angle (θ_A). The overestimation by WCR appeared to correlate with the advancing rate of liquid rise up the packed materials, and such correlation is more apparent for a surface that is hydrophilic and having a higher contact angle hysteresis. Nylon 6/6 powders of different sizes were used as model materials, which provided packing containing various sized voids that affected the advancing rate of a liquid rising up the packed tube. When larger powders were packed to have bigger voids, a slower liquid advancing rate resulted, leading to a smaller overestimation of $\theta_{A\text{-}w}$ from the literature value and the value measured using the sessile drop method on a flat film. Also, the powders might not be packed uniformly from the bottom to the top, thus it was more suitable to only utilize the

initial portion of the liquid penetration rate profile where a linear relationship resulted. By applying the conditions that lead to the smallest overestimation on $\theta_{A\text{-}w}$, the advancing water contact angles of BCA and its UV/O_3 modified counterparts were characterized by using WCR. The results indicated that WCR was suitable for characterizing wettability and assessing wettability variations of very heterogeneous porous materials. To ensure the applicability of WCR for advancing contact angle determination, careful attentions should be paid when preparing the packing, following the liquid penetration and analyzing the penetration profile. While attaining a linear portion of penetration rate profile is necessary for applying WCR, a packing that allows a slower liquid penetration is advantageous for the applicability of WCR for powders/porous materials.

CHAPTER VI
EFFECT OF OXYGEN PLASMA ON BACTERIAL CELLULOSE-ALGINATE COMPOSITE SPONGE AS A YEAST CELL CARRIER FOR ETHANOL FERMENTATION

6.1 Introduction

IC systems have been extensively applied in ethanol fermentation because of high cell density, short operational time and low recovery cost (Sree et al., 2000). Alginate gel is one of the most common materials used as a yeast cell carrier. However, the dense structure of the gel is the barrier causing mass transfer limitation of substrates to the immobilized cells (Maryse and Dravko, 1996). Also, fast degradation and low mechanical strength of the gel limit long-term operation in industrial processes. In our previous works, the sponge composed of BC and alginate gel was developed for use as a wound dressing material (Chiaoprakobkij et al., 2001) and a cell carrier for ethanol fermentation .Because BCA had asymmetric structure consisted of nanoporous layer on the outer and interconnected microporous layer in the interior, it was a good support material for immobilization of yeast cells in ethanol fermentation. From a previous report, the increase in hydrophilicity of cell carriers could result in the accelerations of water and nutrients diffusion into the hydrogel (Srivastava and Behari, 2006). To improve hydrophilicity of the BCA, the sponge was treated by oxygen plasma. The chemical structure, morphology, contact angle and uptake abilities of the plasma-treated BCA (P-BCA) were investigated. Ethanol production by batch fermentation using IC in the P-BCA was compared with that using IC in the BCA and SC.

6.2 Material and methods

6.2.1 BCA surface modification by oxygen plasma treatment

BCA was fabricated by crosslinking of alginate chains by calcium salts and freeze drying. BCA in square shape of 2×2 cm^2 with a thickness of 0.2 cm was treated in a plasma chamber (PC-1100, Samco, US) for 15 min each side with the oxygen gas flow rate of 40 SCCM and the pressure of 15 kPa.

6.2.2 Material characterizations

BCA and P-BCA were identified for the chemical structural information by FT-IR Spectrometer (SX-170, Nicolet, US) in the region of 4000-400 cm^{-1}. The surface morphology was examined using SEM (JSM-5410LV, JOEL, Japan). The samples were coated with gold and photographed at an accelerating voltage of 15 kV. The advancing water and ethanol contact angle were assessed by WCR technique, as described in (Kirdponpattara et al., 2013).

Water/ethanol uptake ability was determined by immersing the pre-weighted of dried samples in distilled water/98% of ethanol at room temperature until equilibration. The weight of the swollen samples was measured. All testing was run in 5 times. The water uptake ability was determined by using the following equation:

$$\text{water/ethanol uptake ability} = (W_w - W_d)\rho_m / (W_d \rho_l).$$

where W_w and W_d represent the weight of wet and dry samples, respectively and ρ_l and ρ_m represent the density of material and liquid, respectively, by assuming $\rho_m = \rho_{cellulose} = 1.25$.

6.2.3 Ethanol fermentation

Starter culture was obtained by transferring cells from an agar slant into 150 mL sterilized cultivation medium. Cell culture was cultivated in a refrigerated incubator shaker (Innova 4330, New Brunswick Scientific, US) at 150 rpm, 33°C for 20-24 hours. The cells were concentrated by decantation to obtain stock cell suspension.

To immobilize cells into the materials, stock cell suspension of 10 mL and 2.5 g of the sterilized BCA and P-BCA in square shape of 2×2 cm^2 with a thickness of 0.2 cm were added to 250 mL sterilized culture medium and incubated at 33ºC, 150 rpm for 20-24 hours. For batch ethanol fermentation, cane molasses was used as a substrate for ethanol fermentation. Experiments were initialed by transferring SC culture or IC culture into 250 mL of the medium. Fermentation flasks were then shaken in the incubator at 150 rpm, 33°C for 72 h. The experiments were monitored by removing 2 mL samples every 8 h for sugar and ethanol analyses. Ethanol concentration was analyzed by a gas chromatograph (GC-7 AG, Shimadzu, Japan) equipped with a flame ionization detector.

6.3 Results and discussion

6.3.1 Materials characterizations

After BCA was treated with oxygen plasma, it was immediately analyzed for chemical functional structure using FTIR spectra. FTIR spectra adsorption bands of BCA and P-BCA were compared (Figure not shown). It was noticed that there was no alteration of carbonyl and carboxyl groups in P-BCA when compared with BCA. The spectra bands of BCA and P-BCA were very similar. Generally, during the plasma process, hydrogen atom on polymeric chain is abstracted or polymeric chains are split, and free radicals are created by plasma. Afterward, the free radicals are activated to incorporate with a gas. The incorporation of cellulose and oxygen mechanism (oxidation reaction) was proposed by Calvimontes et al. (2011), and carbonyl and/or carboxyl groups would increase after cellulose was

treated with oxygen plasma (Calvimontes et al., 2011; Malek and Holme, 2003; Carlsson and Strom, 1991). However, in this work, oxygen plasma was unable to create detectable hydrophilic functional groups on the surface of BCA. Due to the complex 3D structure of BCA (the intermolecular interaction between hydroxyl group of cellulose and carboxyl group of alginate (Chiaoprakobkij et al., (2011)), the incorporation of cellulose and oxygen mechanism might not be the same as those of pure cellulose materials.

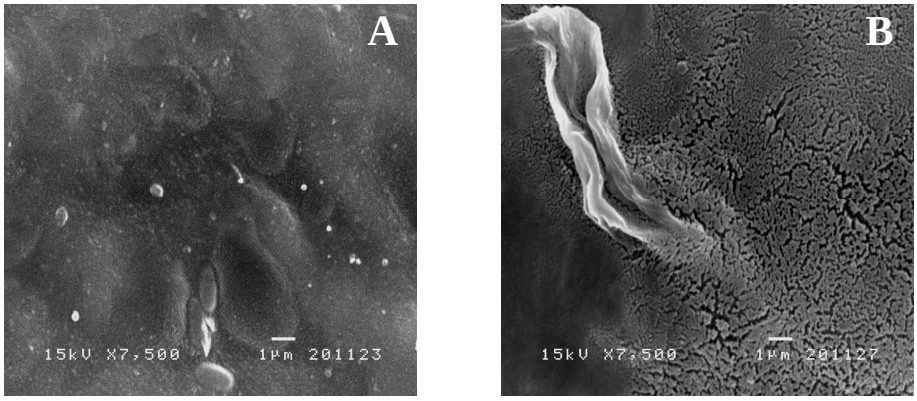

Figure 6.1 SEM images of BCA surface (A) and P-BCA surface (B)

The surface morphologies are shown in Fig. 6.1. Surface area of P-BCA was damaged by oxygen plasma treatment as shown in multiple surface cracks in Fig. 6.1B. The etching effect on material surface has been observed by applying plasma (Malek and Holme, 2003 ; Kurniawan et al., 2012 ; Demura et al., 1992). The surface of P-BCA appeared to be rougher as compared to that of BCA. A rougher surface might enhance cell adsorption. However, due to the nanoporous and relatively denser outer layer of the BCA sponge, the amount of plasmatic oxygen ions reaching the interior surface of the sponge could be limited.

Table 6.1 Advancing water and advancing ethanol contact angles obtained by WCR using tubes packed with 500-2000 µm powders

Material	Advancing contact angle (^{o})	
	Water	Ethanol
BCA	75.8 $\pm$ 2.3	31.2 $\pm$ 3.5
P-BCA	51.7 $\pm$ 1.0	34.5 $\pm$ 7.8

The contact angle was used to identify the improvement of the material hydrophilicity. The advancing water and advancing ethanol contact angles are summarized in Table 6.1. The advancing water contact angle of P-BCA was significantly lower than that of BCA ($\approx 24^o$ difference). But, the advancing ethanol contact angles were similar. These results showed that the hydrophilicity of P-BCA was enhanced by oxygen plasma treatment. According to the results of FT-IR and SEM, a cause of the improvement of P-BCA hydrophilicity is likely the increase of surface roughness. Zemljic et al. (2009) claimed that the major effect on the increase hydrophilicity of the material treated with plasma was the formation of new functional groups but might also be the morphology change and/or cleaning process.

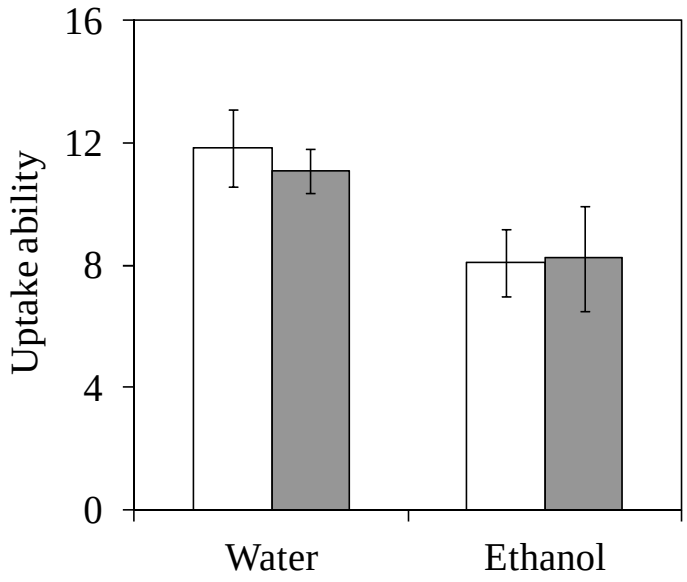

Figure 6.2 Uptake ability of BCA (white) and P-BCA (gray)

BCA and P-BCA were immersed in water/ethanol to determine the uptake abilities and the results are presented in Fig. 6.2. There was no significant difference in water/ethanol uptake abilities between treated and untreated BCA, which could probably be the result of little to, no formation of hydrophilic functional group in the interior of the BCA sponge with oxygen plasma treatment.

6.3.2 Ethanol fermentation.

Ethanol production using IC in P-BCA was compared with those of IC in BCA and suspended cells, as shown in Fig. 6.3. Ethanol concentrations obtained from IC in P-BCA were almost equivalent to those in BCA. The ethanol fermentation by IC in both BCA and P-BCA carriers showed comparable productivity to that of the SC system. The main reason for no substrate limitation in the IC systems was that the inter-connected macro porous structure in the interior of the BCA facilitated the transmission of substances and products between the carrier and the medium. The etching of plasma on BCA surface did not show significant effect on ethanol production.

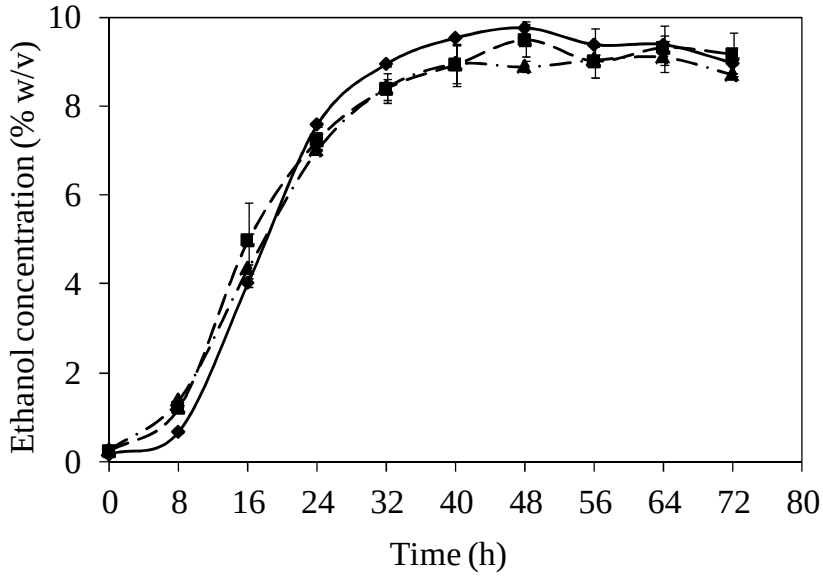

Figure 6.3 Profiles of ethanol concentration of batch fermentations using SC (solid line) and ICs in BCA (dashed line) and P-BCA (dot-dash line)

6.4 Conclusion

The hydrophilicity of BCA sponge was improved by oxygen plasma treatment. It was shown that the water contact angle was decreased because of increasing surface roughness by etching effect. No formation of new hydrophilic functional groups on P-BCA was detected. There was no significant difference in water/ethanol uptake abilities between treated and untreated BCA. Consequently, there was no significant difference in ethanol production obtained from the systems of IC in P-BCA and BCA. Oxygen ions might not be able to incorporate with the 3D chemical structure of BCA due to its complex chemical and physical structure.

CHAPTER VII
FABRICATION OF BACTERIAL CELLULOSE-ALGINATE COMPOSITE POROUS STRUCTURE FOR SCAFFOLD DEVELOPMENT

7.1 Introduction

In order to replace damaged or lost tissue by transplanting cultured cells in vivo, the fabrication of potential three-dimensional (3-D) scaffolds for all growth and proliferation has been focused. The desired 3-D scaffolds including highly interconnected porous structure, large surface area, high porosity, and suitable pore size allow the achievement of the high density of seeded cells and the adequate nutrient and oxygen transmission in the system (El-Ayoubi et al., 2008 ; Hou et al., 2003). Also, guiding cellular migration and natural extracellular matrix mimics (ECM) are obtained (Mano et al., 2007 ; Chen and Ma, 2004 ; Wislet-Gendebien, 2011). In addition, biocompatibility and biodegradability of 3-D scaffold are required (Ma and Choi, 2001 ; Onuki et al., 2008).

In our previous study (Chiaoprakobkij et al., 2011), BC and alginate, which are biocompatible and non-toxic materials, were blended to gain their beneficial properties. Bacterial cellulose-alginate composite sponge (O-BCA) has been successfully fabricated and tested in vitro study with human keratinocytes (HaCat) and gingival fibroblasts (GF) (Chiaoprakobkij et al., 2011). The results demonstrated that O-BCA supported the proliferations of the cells. Because of its structure consisted of the dense layers on the outer, BCA might prevent bacterial invasion and avoid wound dehydration, and the interconnected porous in the interior, which might help removing of wound exudates. It was would concluded that O-BCA has good potential to be applied as a wound dressing and as a mucosal flap in oral tissue regeneration. However, O-BCA structure might limit its applications such as 3-D scaffold implanted in vivo.

Various techniques have been applied to fabricate 3-D porous scaffold for obtaining the desired structures, such as electrospinning (Shalumon et al., 2009 ; Zhou et al., 2009), gas foaming (Lim et al., 2008 ; Yoon et al., 2003), and salt leaching (Lee et al., 2005 ; Flaibani and Elvassore, 2012). Lyophilization or freeze drying is one of simple and non-toxic techniques which can provide porous structure by using ice crystal as porogen. Many researchers have successfully fabricated materials such as gelatin (Wu et al., 2010), collagen (Davidenko et al., 2012), keratin (Hamasaki et al., 2008) chitosan (Yang et al., 2010) and alginate (Zhao et al., 2012) via freeze drying approach.

For O-BCA fabrication, the mixture of BC and alginate was firstly cross-linked with $CaCl_2$ solution. The interface between the mixture and the $CaCl_2$ solution was rapidly cross-linked which resulted in the dense structure. After freeze drying step, nanoporous thin layer on the outer surface of O-BCA was obtained.

In the present study, BCA was conversely fabricated from the previous work (Chiaoprakobkij et al., 2011) to achieve a three-dimensional sponge with open and interconnected porous structure. Firstly, ice crystals in the frozen BCA mixture were sublimated by freeze drying step to generate open and interconnected porous structure throughout the sponge. Subsequently, cross-linking step was carried out to maintain the open porous structure, avoid dissolving alginate in water and enhance the stability of the sponge. After that, the sponge was freeze dried again. The fabricated sponge was characterized its properties to compare with those of O-BCA. Pure BC and pure alginate were also prepared by following the above mentioned steps. The sponges were further evaluated for their cytoxicity by testing with L929 mouse fibroblasts.

7.2 Material and methods

7.2.1 Materials

BC, which was synthesized by *Accetobactor xylinum* AGR 60, was provided by Institute of Food and Research and Product Development, Kasetsart University, Bangkok. BC was removed bacterial cells by treating with 1% w/v NaOH and then was neutralized with 1% w/v acetic acid. The cleaned BC was rinsed with DI water until pH was 7. The BC was immersed in deionized (DI) water and was kept in a refrigerator at 4 °C before use. Sodium alginate was purchased from Acros Organic, US. Calcium chloride was supplied from Ajax Finechem Pty. Ltd., Australia.

7.2.2 Fabrication of sponges

The preparation steps of O-BCA were thoroughly described in (Chiaoprakobkij et al., 2011). To fabricate N-BCA, blended BC was mixed with 1.5 % by wt. sodium alginate solution in a weight ratio of 100/0, 70/30 and 0/100, as named BCB, N-BCA and AL, respectively. The homogeneous slurry mixture was poured into a tray and then was frozen in a freezer at -40°C for 24 h. After that, the frozen mixture was lyophilized under vacuum pressure (<100 mTorr) for 48 h to obtain the sponge with open porous structure. After that, the lyophilized sponge was cross-linked with a 0.12 M $CaCl_2$ solution for 24 h and was rinsed thrice with DI water to remove any excess Ca^{2+} except BCB (from previous study (Chiaoprakobkij et al., 2011), there was no effect of $CaCl_2$ on BC cross-linking). Eventually, the sponge was lyophilized again under the same condition. For the fabrication of another sponge (BCF), the stored BC was lyophilized. The details of the sponge are summarized in Table 7.1.

Table 7.1 The detail of the compositions and the methods of fabrication of the sponge

Name	Composition	Fabrication
BCF	Pure BC	Freeze drying
BCB	Pure BC	Blending and freeze drying
AL	Pure alginate	Freeze drying and cross-linking
N-BCA	70/30 (BC/alginate)	Blending, freeze drying and cross-linking
O-BCA	70/30 (BC/alginate)	Blending, cross-linking and freeze drying

7.2.3 Sponge characterization

7.2.3.1 Scanning Electron Microscope (SEM)

To examine the morphology of the sponge, SEM was performed. The sponge was rapidly cut a sharp blade and then was sputtered with gold and photographed. The coated specimen was examined its structure by using a JOEL JSM-5410LV microscope (Tokyo, Japan).

7.2.3.2 Mechanical properties measurement

The mechanical strength of the sponge was measured by a Universal Testing Machine-H 10 KM (Hounsfield, USA). The test conditions followed the standard procedure ASTM D882. The samples were cut into strip-shaped specimens of 10 mm in width and 5 cm in length (with 50 mm between the grips). The stretch rate was 2 mm/min. The tensile strength was averaged over five specimens.

7.2.3.3 Water uptake ability

The pre-weighed dry sponge was immersed in DI water at room temperature until equilibration occurred. After that, the swollen sponge was weighted again. This procedure was repeated until there was no further weight change. All tests were run five times, and the water uptake ability was determined using the following equation:

$$\text{Water uptake ability} = (W_w - W_d)/W_d$$

where W_w and W_d represent the weight of wet and dry samples, respectively.

7.2.3.4 Structure stability

The dry sponge was immersed in DI water and phosphate buffer saline (PBS) to observe the change of the sponge shapes every 24 h for 7 days. The swollen sponge was removed from the solution to photograph.

7.2.4 Cytotoxicity assay

7.2.4.1 Cell culture and seeding

Mouse fibroblast L929 cell was used to examine the indirect toxicity of the sponges. The cells were cultured in Dulbecco's modified eagle medium (DMEM) supplemented with 10% fetal bovine serum (FBS), 1% L-glutamine, 100 units/mL penicillin, 2 mg/L lactabumin and 100 µg/mL streptomycin in a humidified incubator in an atmosphere of 5% CO_2 at 37°C.

For sterilizing the sponges, the sponges were immersed in 70% w/v ethanol solution for 1 day. After that, the sponges were placed in 24-well plate, were rinsed twice with PBS and then were rinsed twice with serum-free culture

medium (SFM). Finally, the sponges were incubated at 37◦C in serum-free culture medium (SFM) for 24 h. The weight of sponge per volume of medium ratio was 10 mg/ml. The extraction medium from the sponge incubation was used to culture L929 mouse fibroblast cells. SFM was used as control. The cells were cultured in 24-well plates at concentrations of 5×10^4 cells in 500 µl culture medium per well, and the cells were allowed to attach to the plates for 16 h in a humidified atmosphere of 5% CO_2 and 95% air at 37°C. Then, the cell-culture medium was replaced with 500 µl of the 100% (v/v) extraction medium, the 50% (v/v) extraction medium or the control medium. The number of living cells was finally quantified using MTT assay.

7.2.4.2 MTT assay

To quantify the cells, 3-(4,5-dimethythiazolyl-2)-2,5-diphenyltetrazolium bromide (MTT) was used. MTT solution (0.5 mg/mL in DMEM without phenol red) of 350 µL was added to each well and incubated at 37°C for 30 minutes. After that, the MTT solution was removed and 900 µL of dimethylsulfoxide and 100 µL of glycine buffer (pH 10.5) were added. The spectrophotometer (Genesis 10 UV scanning, Rochester, NY) was used to measure the optical densities at 570 nm.

7.3. Results and discussion

7.3.1 Characterizations of sponges

7.3.1.1 Morphology of sponge

The cross-sectional and surface morphologies of the sponges were investigated by using SEM, as shown in Fig. 7.1. The structure of BCF (Fig. 7.1A and 7.1B), the lyophilized BC without blending, was consisted of the thick and

dense layer on the outer and the interconnected nano-porous structure in the interior. It might be because of its high water holding capacity and the initially rapid freeze-drying rate on the surface causing the structural collapse to become dense layer. Consequently, the thickness of BC hydrogel reduced from ≈ 5 mm to < 1mm, after freeze drying step. The similar structure was also observed by Yoshino et al. (2013). On the other hand, the blended and lyophilized BC hydrogel (BCB) showed interconnected porous structure throughout the sponge, as seen in Fig. 7.1C and 7.1D, For AL structure (Fig. 7.1E and 7.1F), the elongated pores were formed. However, in the preliminary result, alginate sponge, which fabricated by cross-linking and then freeze drying, could not form the porous structure (figure not shown). The dense layer hydrogel on the outer surface, the sodium alginate gel was rapidly cross-linked with calcium ions, and then the $CaCl_2$ solution slowly penetrated and cross-linked alginate gels throughout the interior parts. Therefore, the interior of hydrogel was not as dense and rigid as the interface. After the hydrogel was freeze dried, the heterogeneous structure, which consisted of thin layer on the outer and small hollow flakes in the interior, was obtained.

To develop the open porous structure (N-BCA), the mixture of BCA was firstly freeze dried and then cross-linked. It was found the BCA sponge with open interconnected porous structure was synthesized throughout the N-BCA sponge (Fig. 7.1E and 7.1F). In contrast, the heterogeneous structure of O-BCA consisted of a top skin layer and sponge-like porous layer (Fig. 7.1G and 7.1H), as above mentioned. The results demonstrated that the alternative procedure to fabricate the open and interconnected porous structure throughout the sponge was the freeze drying followed by cross-linking process.

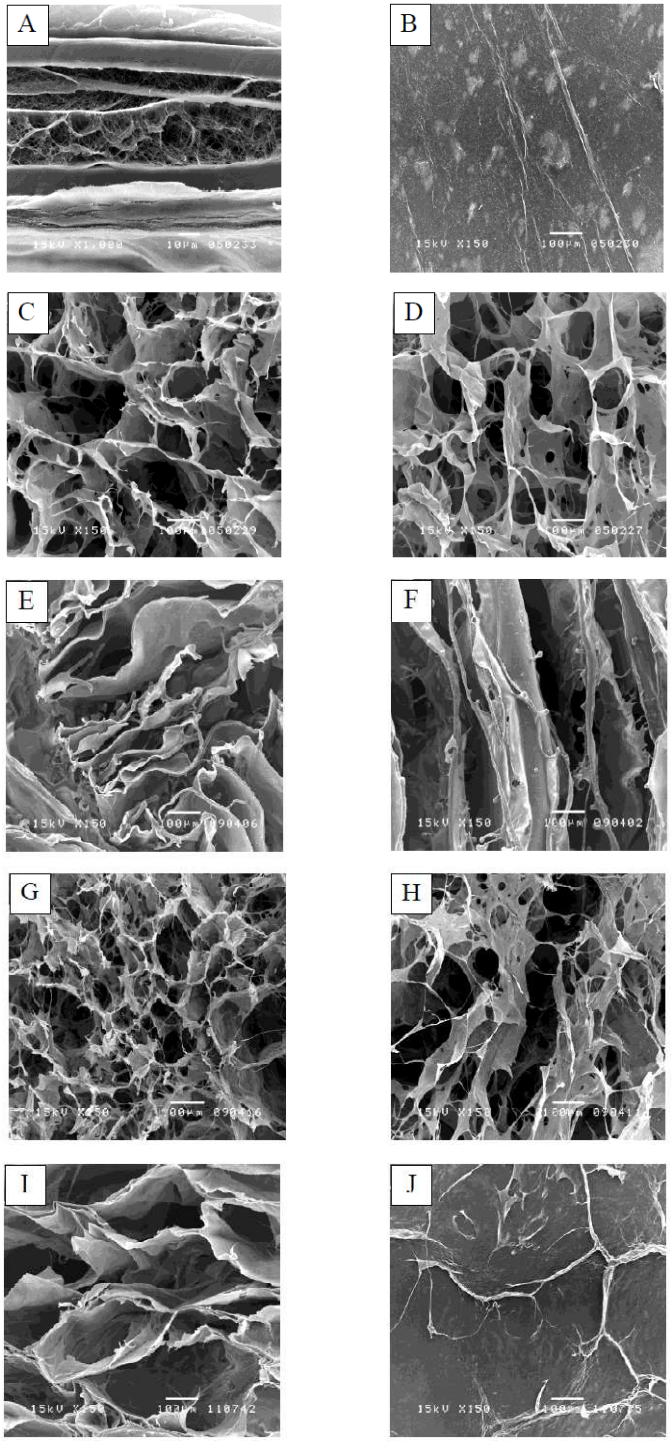

Figure 7.1 SEM images of cross-sectional area of BCF (A), BCB (C), AL (E), N-BCA (G) and O-BCA (I) and surface area of BCF (B), BCB (D), AL (F), N-BCA (H) and O-BCA (J)

7.3.1.2 Mechanical strength

The tensile strength and elongation at break are summarized in Table 7.2. BCF showed the highest value of tensile strength because of the nano-fibril network structure of BC and hydrogen bond between fibrils (Scionti, 2010). On the other hand, BCB was fabricated from homogenized BC fibrils so the structure of BCB was much weaker than that of BCF. But the elongation at break of BCF and BCB were similar. It might be because of the interconnected porous structure of BCB. Therefore, BCB was flexible as much as BCF. For the comparison of AL and N-BCA, AL showed a bit of higher tensile strength when compared with that of N-BCA. The open porous structure of N-BCA was firstly developed by freeze drying step and then the cross-linking of sodium alginate with calcium ions was formed. The homogenized BC might obstruct the cross-linking between alginate and $CaCl_2$ solution. Consequently, the cross-linked structure of N-BCA was looser than that of AL. It was optically observed that the size of AL sponges shrunk down approximately 0.4 times of its original size, after the cross-linking step. But no size reduction was observed in N-BCA. For the results of the elongation at break, the elongation of N-BCA was higher than that of AL.

For the comparison of N-BCA and O-BCA, it was found that the structure of O-BCA was stronger than that of N-BCA. Chiaoprakobkij et al. (2011) claimed that the intermolecular interaction occurred between the hydroxyl group of BC and the carboxyl group of alginate in O-BCA structure.

Table 7.2 Mechanical properties of the sponges

Material	Tensile strength (MPa)	Elongation (%)
BCF	49.07±18.16	8.50±1.97
BCB	1.21±0.14	8.61±0.55
AL	0.87±0.17	2.96±0.41
N-BCA	0.56±0.04	4.61±0.46
O-BCA	12.16±2.57	5.97±0.81

7.3.1.3 Water uptake ability

Swelling is one of the important factors for selecting the suitable sponge which permits more cell invasion into the sponge and abundant nutrient supply (Mohan and Nair, 2005). The water uptake abilities are presented in Fig. 7.2. It was found that the water uptake ability related with the structure of the sponge. Because of the dense and thick skin structure on the outer part and low porosity of BCF, the water uptake ability of BCF was only ≈7 times of its dry weight. On the other side, BCB could uptake water approximately 61 times of its dry weight. BCB rapidly swelled after the immersion of water because of the highly porous and flexible structure, and the high hydrophilicity of BC. Although the structure of N-BCA was similar to that of BCB (≈47 times of its dry weight), the water uptake ability of N-BCA was relatively lower than that of BCB ≈13 times. It might be because of the alginate composition in N-BCA. In the same way, AL sponge absorbed water only ≈15 times of its dry weight. For O-BCA, it was found that the water uptake ability of O-BCA was much lower than those of BCB and N-BCA. According to the structure of O-BCA, the dense layer on the outer might limited the swelling ability of O-BCA.

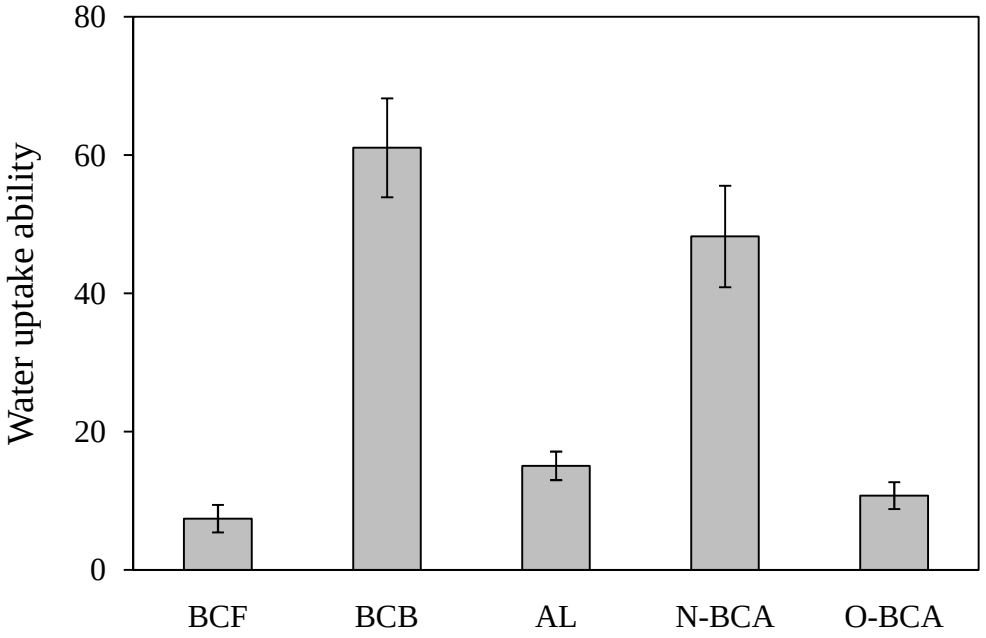

Figure 7.2 Water uptake ability of BCF, BCB, AL, N-BCA and O-BCA

7.3.1.4 Structural stability

The stability of the structural sponge was investigated by immersing in DI water and PBS, respectively. Firstly, the sponges immersed in DI water were described. The structural stability of BCB was very poor. After one day, the BCB structure was not firm and also was easily broken during the transferring. Because there was no a strong linking network, BCB structure collapsed easily. On the third day, the unstable of O-BCA structure was found. For BCF, AL and N-BCA, only swelling of these sponges was observed. After the immersion in DI water for 7 days, these sponges were still firm.

By immersing the sponges in PBS, there was no change in BCF. For BCB, the structure behaved like it was immersed in DI water. On the other hand, AL, N-BCA and O-BCA, which consisted of Na-alginate, were fabricated by cross-linking with $CaCl_2$ (exchanging the salt ion of Na^+ to Ca^{2+}). PBS solution contained a lot of salt ions, which could exchange with Ca^{2+} in the structure of the sponge. Therefore, the structures of AL, N-BCA and O-BCA were weaker and then

collapsed easily in PBS solution. Consequently, after 3 h, PBS solutions immersing AL, N-BCA and O-BCA became turbid which exhibited that some components containing in these sponges might dissolve in the solution. The degree of turbidity of the PBS solutions with different immersed sponges would likely be: AL > O-BCA > N-BCA. From 0-12 h, the PBS solution gradually became more turbid and then it was constant by optical observation. In case of AL, the AL sponge swelled and got bigger than its original size (≈0.4 times) which showed that after AL was immersed in PBS solution, the AL sponge swelled to normal size of AL sponge before cross-linking step. It could be summarized that large amounts of Ca^{2+} in AL structure were exchanged with salt ions in PBS solution which resulted in the weak, unstable and un-firm structure of AL. Consequently, AL structure collapsed and disintegrated within one day. In the similar way, the structure of O-BCA was unstable and some part was disintegrated after the first day. Since the intermolecular interaction between BC and alginate was destroyed. By exchanging between Ca^{2+} and other ions in PBS solution, the structure of O-BCA easily collapsed. On the other hand, the N-BCA structure was still firm and stable. Since N-BCA was firstly formed quite strong network structure by freeze drying and then the stability was enhanced by cross-linking step. Therefore, the structure of N-BCA was more stable than AL and O-BCA.

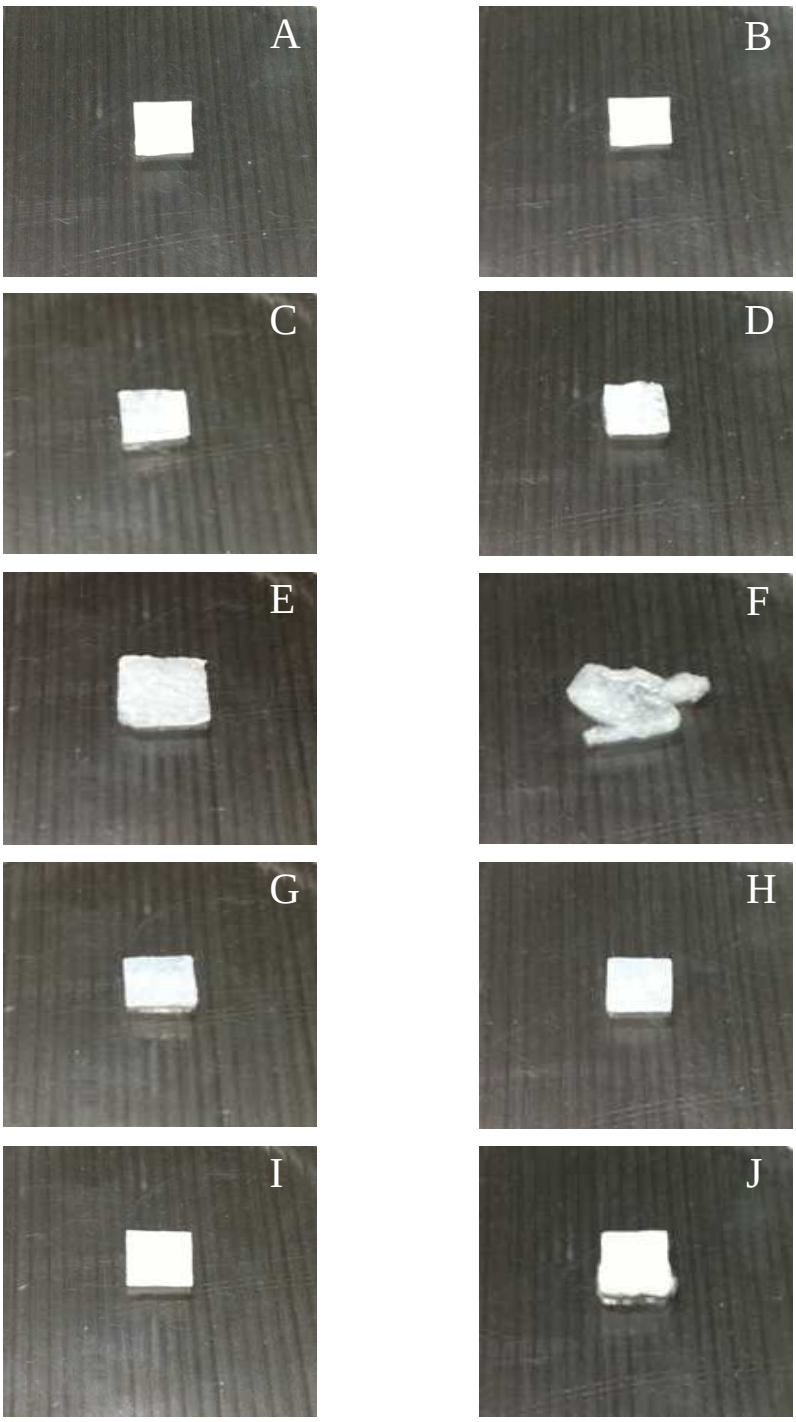

Figure 7.3 Photos of the immersion in PBS for 3 h of BCF (A), BCB (C), AL (E), N-BCA (G) and O-BCA (I) and the immersion in PBS for 24 h BCF (B), BCB (D), AL (F), N-BCA (H) and O-BCA (J)

7.3.2 Cytotoxicity

The toxicity of the sponges was tested against the fibroblast mouse L929 cell. As seen in Fig. 7.3, BCF, BCB and O-BCA had no toxicity against L929 cells with no statistically significant difference ($P > 0.05$). On the other hand, the results of 50% the volume of medium of AL and N-BCA exhibited that the extractions of AL and N-BCA promoted the cell growth and the relative cell number of AL and N-BCA were higher than that of the control plate approximately 33 and 65%, respectively. However, for the volume of medium of 100%, the relative cell number of AL and N-BCA decreased. The results demonstrated that the small amount of the AL and N-BCA extractions could promote the cell growth

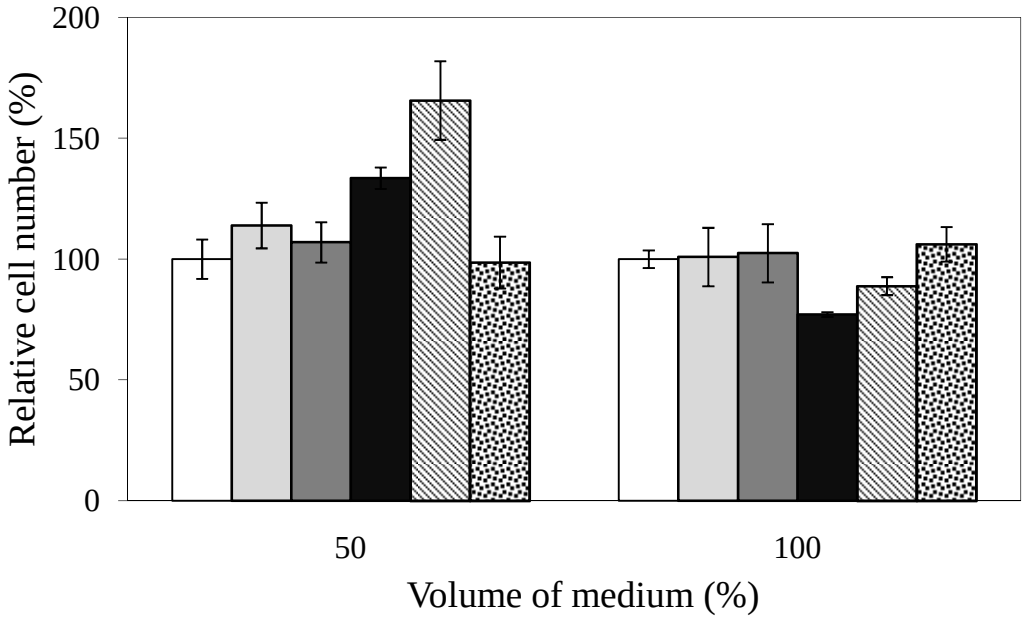

Figure 7.4 Toxicity test against L929 mouse fibroblast cell at the extraction medium volumes of 50% and 100% on the polystyrene control plate (white bar), BCF (light gray bar), BCB (gray bar), AL (black bar), N-BCA (diagonal striped bar) and O-BCA (dot striped bar)

7.4. Conclusions

The development of BCA fabrication to obtain the highly open and interconnected porous structure throughout the sponge was studied. The mixture of BC and alginate was firstly freeze dried to achieve the open and interconnected porous structure and then was cross-linked to avoid in water and also to enhance stability of the sponge. N-BCA showed the lowest mechanical strength when compared with others. However, in the wet state (immersing in DI water), the structure of N-BCA was more stable than that of BCB. Also, N-BCA presented the firm and stable structure in PBS solution for at least one week. Moreover, the water uptake ability of N-BCA was significantly higher than those of AL and O-BCA about 3.2 and 4.5 times, respectively. For the cytotoxicity result, no toxicity was observed in all sponges. The small amount of AL and N-BCA extractions could promote L929 cell growth. All results demonstrated that the N-BCA sponge fabrication by freeze drying followed by cross-linking has high potential for tissue engineering applications.

CHAPTER VIII
CONCLUSIONS AND RECOMMENDATIONS

8.1 Conclusions

To gain the beneficial properties of both BC and alginate, a sponge and a scaffold of BCA were fabricated, characterized and applied in ethanol fermentation and tissue engineering. BC supplemented in alginate hydrogel enhanced mass transfer of substrates and products. Consequently, the increasing of the ethanol production was observed. To improve the efficiency of ethanol fermentation system, BCA hydrogel was freeze dried to obtain BCA sponge which consisted of thin layer on the outer and interconnected porous structure in the interior. In batch and repeated batch fermentation, the IC system in BCA sponge presented higher ethanol productivity and more stability when compared with IC system in AL and SC system. It meant that there was no significant mass transfer limitation in the structure of BCA sponge. The high efficiency and high stability of BCA sponge were observed by the approximately constant of ethanol concentration at 92 g/L during 30 days.

The hydrophilicity of BCA sponge was modified by treating with oxygen plasma. The WCR method was used to assess the hydrophilicity of BCA sponge (water contact angle) of BCA sponge. To evaluate contact angle of powders/porous material using the WCR method, powder size, packing and contact angle hysteresis needed to be paid attention. After the treatment, the advancing water contact angle of BCA sponge decreased. However, there was no difference of ethanol productions between the IC system in un-modified BCA and that in modified BCA sponge.

For tissue engineering application, a new fabrication method was used to create open and interconnected porous structure throughout N-BCA sponge. The characterizations results demonstrated that N-BCA sponge might probably applied as a scaffold for tissue engineering.

8.2 Recommendations for future studies

For ethanol fermentation application, the continuous fermentation in IC system in BCA sponge should be carried out by operating with a packed bed reactor to observe the optimal condition and the scaling up possibilities. Due to the structure BCA sponge which facilitated the transmission of substrates and products between the carrier and the medium, something interesting may obtain from the continuous fermentation experiment.

In order to achieve an accurate advancing contact angle, the simulation may help deduce the overestimate value obtained from WCR analysis. It may be necessary to study more on material properties such as density, porosity and surface energy.

There are many techniques used to improve hydrophilic properties of materials. In the case of oxygen plasma treatment, the interior of BCA sponge, which played an important role on the no substrate limitation in the IC system, was not affected by oxygen plasma treatment. Therefore, the further research is needed to focus on the technique which can also treat the interior of BCA sponge such as grafting alginate powders with hydrophilic monomer or polymer.

N-BCA sponge should further test with a suitable cell to examine the cell attachment and proliferation. Moreover, the studies of effect of BC/alginate ratio and alginate concentration on BCA sponge fabrication may present different structures, chemical and mechanical properties, which may be suitable for other cells.

Due to the advantages, easy fabrication and interesting results of BCA sponge, the sponge may be applied in a lot of works such as food packaging, drug delivery, membrane filtration, etc.

REFERENCES

Bai, F.W., Anderson, W.A., and Moo-Young, M. Ethanol fermentation technologies from sugar and starch feedstocks. Biotechnology Advances 26 (2008) : 89-105.

Bangrak, P., Limtong, S., and Phisalaphong, M. Continuous ethanol production using immobilized yeast cells entrapped in loofa-reinforced alginate carriers. Brazilian Journal of Microbiology 42 (2011) : 676-684.

Brown, R.M. Jr. The biosynthesis of cellulose. Journal of Macromolecular Science Pure and Applied Chemistry 10 (1996): 1345-1373.

Calvimontes, A., Mauersberfer, P., Nitschke, M., Dutschk, V., and Simon, F. Effects of oxygen plasma on cellulose surface. Cellulose 18 (2011) : 803-809.

Carlsson, C.M.G., and Strom, G. Reduction and oxidation of cellulose surfaces by means of cold-plasma. Langmuir 7 (1991) : 2492-2497.

Caykara, T., and Demirci, S. Preparation and characterization of blend films of poly(vinyl alcohol) and sodium alginate. Journal of Macromolecular Science Part A 43 (2006) : 1113-1121.

Caykara, T., Demirci, S., Eroglu, M., and Guven, O. Poly(ethylene oxide) and its blends with sodium alginate. Polymer 46 (2005) : 10750-10757.

Chandel, A.K., Narasu, M.L., Chandrasekhar, G., Manikyam, A., and Rao, L.V. Use of *Saccharum spontaneum* (wild sugarcane) as biomaterial for cell immobilization and modulated ethanol production by thermotolerant *Saccharomyces cerevisiae* VS_3. Bioresource Technology 100 (2009) : 2404-2410.

Chen, V.J., and Ma, P.X. Nano-fibrous poly(L-lactic acid) scaffolds with interconnected spherical macropores. Biomaterials 25 (2004) : 2065-2073.

Cheng, K., Catchmark, J. M., and A. Demirci.Effect of different additives on bacterial cellulose production by *Acetobacter xylylinum* and analysis of material property. Journal of Biological Engineering 3 (2009) : 1033-1045.

Chibowski, E., and Perea-Carpio, R. Problems of contact angle and solid surface free energy determination. Advances in Colloid and Interface Science 98 (2002) : 245-264.

Chiaoprakobkij, N., Sanchavanakit, N., Subbalekha, K., Pavasant, P., and Phisalaphong, M. Characterization and biocompatibility of bacterial cellulose/alginate composite sponge with human keratinocytes and gingival fibroblasts. Carbohydrate Polymers 85 (2011) : 548-553.

Costanzo, P.M., Wu, W., Giese, R.F., and van Oss, C. J. Comparison between direct contact angle measurements and thin layer wicking on synthetic monosized cuboid hematite particle. Langmuir 11 (1995) : 1827-1830.

Cox, R.G. Inertial and viscous effects on dynamic contact angles. Journal of Fluid Mechanics 357 (1998) : 249-278.

Dang-Vu, T., and Hupka, J. Characterization of porous materials by capillary rise method. Physicochemical Problems of Mineral Processing 39 (2005) : 47-65.

Dann, J.R. Forces involved in the adhesive process: II. Nondispersion forces at solid-liquid interfaces. Journal of Colloid and Interface Science 32 (1970) : 321-331.

Dar, A., Shachar, M. Leor, J., and Cohen, S. Optimization of cardiac cell seeding and distribution in 3D porous alginate scaffolds. Biotechnology and Bioengineering 80 (2002) : 305-312.

Davidenko, N., et al. Biomimetic collagen scaffolds with anisotropic pore architecture. Acta Biomaterialia 8 (2012) : 667-676.

Demura, M., Takekawa, T., Asakusa, T., and Nishikwan, A. Characterization of low-temperatureplasma treated silk fibroin fabrics by ESCA and the use of the fabrics as an enzyme-immobilization support. Biomaterials 13 (1992) : 276-280.

Dubey, V., Pandey, L.K., and Saxena, C. Perpaporation separation of ethanol/water azeotrope using a novel chitosan-impregnated bacterial cellulose membrane and chitosan-poly(vinyl alcohol) blends. Membrane Science 251 (2005) : 131-136.

Dussan V, E .B. On the spreading of liquids on solid surfaces: Static and dynamic contact lines. Annual Review of Fluid Mechanics 11 (1979) : 371- 400.

Eiselt, P., Yeh, J., Latvala, R.K., Shea, L.D., and Mooney, D.J. Porous carriers for biomedical applications based on alginate hydrogels. Biomaterials 21 (2000) : 1921-1927.

El-Ayoubi, R., Eliopoulos, N., Diraddo, R., Galipeau, J., and Yousefi, A.M. Design and fabrication of 3D porous scaffolds to facilitate cell-based gene therepy. Tissue Engineering Part A 14 (2008) : 1037-1048.

Flaibani, M., and Elvassore, N. Gas anti-solvent precipitation assisted salt leaching for generation of micro- and nano-porous wall in bio-polymeric 3D scaffolds. Materials Science and Engineering C 32 (2012) : 1632-1639.

Fujii, N., Sakurai, A., Onjoh, K., and Sakakibara, M. Influence of Surface characteristics of cellulose carriers on ethanol production by immobilized yeast cells. Process Biochemistry 34 (1999) : 147-152.

Ghorbani, F., Younesi, H., Sari, A.E., and Najafpour, G. Cane molasses fermentation for continuous ethanol production in an immobilized cells reactor by *Saccharomyces cerevisiae*. Renewable Energy 36 (2011) : 503-509.

Goksungug, Y., and Zorlu, N. Production of ethanol from beet molasses by Ca-alginate immobilized yeast cells in a packed-bed bioreactor. Turkish Journal of Biology 25 (2001) : 265-275.

Guzun, A.S., Stroescu, M., Tache, F., Zaharescu, T., and Grosu, E. Effect of electron beam irradiation on bacterial cellulose membranes used as transdermal drug delivery systems. Nuclear Instruments and Methods in Physics Research B 265 (2007) : 434-438.

Hamasaki, S., Tachibana, A., Tada, D., Yamauchi, K., and Tanabe, T. Fabrication of highly porous keratin sponges by freeze-drying in the presence of calcium alginate beads. Materials Science and Engineering C 28 (2008) : 1250-1254.

Hou, Q., Grijpma, D.W., and Feijen, J. Preparation of interconnected highly porous polymeric structures by a replication and freeze-drying process. Journal of Biomedical Materials Research Part B: Applied Biomaterials 67 (2003) : 732-740.

Idris, A., and Suzana, W. Effect of sodium slginate concentration, bead diameter, initial pH and temperature on lactic acid production from pineapple waste

using immobilized *Lactobacillus delbrueckii*. Process Biochemistry 41 (2006) : 1117-1123.

Inal, M., and Yigitoglu, M. Production of bioethanol by immobilized *Saccharomyces cerevisiae*. Journal of Chemical Technology and Biotechnology 86 (2011) : 1548-1554.

Jackson, P.V., Hunt, J.A., Doherty, P.J., Cannon, A., and Gilson, P. J. Hydrophilicity of 3-D biomaterials: the Washburn equation. Journal of Materials Science: Materials in Medicine 15 (2004) : 507-511.

Johnson Jr., R.E., Dettre, R.H., and Brandreth, D.A. Dynamic contact angles and contact-angle hysteresis. Journal of Colloid and Interface Science 2 (1977) : 205-212.

Jonas, R., and Farah, L.F. Production and application of microbial cellulose. Polymer degradation and Stability 59 (1998) : 101-106.

Kanjanamosit, N., Muangnapoh, C., and Phisalaphong, M. Biosynthesis and characterization of bacterial cellulose/alginate film. Journal of Applied Polymer Science 115 (2010) : 1581-1588.

Kim, J.O., et al. Development of polyvinyl alcohol-sodium alginate gel-matrix-based wound dressing system containing nitrofurazone. Pharmaceutics 359 (2008) : 79-86.

Kirdponpattara, S., Phisalaphong, M., and Newby, B.Z. Applicability of Washburn capillary rise for determining contact angles of powders/porous materials. Journal of Colloid and Interface Science 397 (2013) : 169-176.

Krajewska, B. Application of chitin-and chitosan-based material for enzyme immobilizations: A review. Enzyme and Microbial Technology 35 (2004) : 126-139.

Kurniawan, H., Lai, J.T., and Wang, M.J. Biofunctionalized bacterial cellulose membranes by cold plasmas. Cellulose 19 (2012) : 1975-1988.

Leach, G., Oliveira, G., and Morais, R. Production of a carotenoid-rich product by alginate entrapment and fluid-bed drying of *Dunaliella salina*. Science of Food and Agricuture 76 (1998) : 298-302.

Lee, S.B., Kim, Y.H., Chong, M.S., Hong, S.H., and Lee, Y.M. Study of gelatin-containing artificial skin V: Fabrication of gelatin scaffolds using a salt-leaching metod. Biomaterials 26 (2005) : 1961-1968.

Lee, T.H., Ahn, J.C., and Ryu, D.D.Y. Performance of an immobilized yeast reactor system for ethanol production. Enzyme Microbial Technology 5 (1983) : 41-45.

Li, J., Wan, Y., Li, L., Liang, H., and Wang, J. Preparation and characterization of 2,3-dialdehyde bacterial cellulose for potential biodegradable tissue engineering scaffolds. Materials Science and Engineering: C 29 (2009) : 1635-1642.

Li, Z., Ramay, H. R., Hauch, K. D., Xiao, D., and Zhang, M. Chitosan-alginate hybrid scaffolds for bone tissue engineering. Biomaterials 26 (2005) : 3919-3928.

Lim, Y.-M., Gwon, H.-J., Shin, J., Jeun, J.P., and Nho, Y.C. Preparation of porous poly(ε-carprolactone) scaffolds by gas foaming process and in vitro/in vivo degradation behavior using γ-ray irradiation. Journal of Industrial and Engineering Chemistry 14 (2008) : 436-441.

Lin, H.-Y., and Ciou, S.-Y. Modifications of alginate-based scaffolds and characterizations of their pentoxifylline release properties. Carbohydrate Polymers 80 (2010) : 574-580.

Long, J., and Chen, P. On the role of energy barriers in determining contact angle hysteresis. Advances in Colloid and Interface Science 127 (2006) : 55-66.

Lui, C.Z., Wang, F., and Yang, F.O. Ethanol fermentation in a magnetically fluidized bed reactor with immobilized *Saccharomyces cerevisiae* in magnetic paticles. Bioresource Technology 100 (2009) : 878-882.

Luo, H., Xiong, G. Huang, Y., He, F., Wang, Y., and Wan Y. Preparation and characterization of COL/BC composite for potential tissue engineering scaffolds. Materials Chemistry and Physics 110 (2008) : 193-196.

Ma, P.X., and Choi, J.-W. Biodegradable polymer scaffolds with well-defined interconnected spherical pore network. Tissue Engineering 7 (2001) : 23-33.

Malek, R.M.A., and Holme, I. The effect of plasma treatment on some properties of cotton. Iranian Polymer Journal 12 (2003) : 271-280.

Mano, J.F., et al. Natural origin biodegradable systes in tissue engineering and regenerative medicin: Present status and some moving trends. Journal of The Royal Society Interface 4 (2007) : 999-1030.

Maryse, G., and Dravko, D. Wood blocks as a carrier for *Saccharomyces cerevisiae* used in the production of ethanol and fructose. Chemical Engineering Journal 61 (1996) : 233-240.

McHugh, D.J. Production and utilization of products from seaweeds. Rome: Campbell, 1987.

Mehta, D., and Hawley, M. Wall effect in packed column. Industrial and Engineering Chemistry Process Design and development 8 (1969) : 280-282.

Melzoch, K., Rychtera, M., and Habova, V. Effect of immobilization upon the properties and behavior of *Saccharomyces cerevisiae* cells. Biotechnology 32 (1994) : 59-65.

Millon, L.E., Guhados, G., and Wan, W. Anisotropic polyvinyl alcohol-bacterial cellulose nanocomposite for biomedical applications. Biomedical Materials Research 86 (2008) : 444-452.

Mohan, N., and Nair, P.D. Novel porous, polysaccharide scaffolds for tissue engineering applications. Trends in Biomaterials and Artificial Organs 18 (2005) : 219-224.

Mongkolkajit, J., Pullsirisombat, J., Limtong, S., and Phisalaphong, M. Alumina-doped alginate gel as a cell carrier for ethanol production in a packed bed bioreactor. Biotechnology Bioprocess Engineering 16 (2011) : 505-512.

Moon, S., Ryu, B.Y., Choi, J., Jo, B., and Farris, R.J. The morphology and mechanical properties of sodium alginate based electrospun poly(ethylene oxide) nanofibers. Polymer Engineering and Science 49 (2009) : 52-59.

Najafpour, G., Younesi, H., and Ismail, K.S.K. Ethanol fermentation in an immobilized cell reactor using *Saccharomyces cerevisie*. Bioresource technology 92 (2004) : 251-260.

Nikolic, S., Mojovic, L., Penjin, D., Rakin, M., and Vukasinovic. Production of bioethanol from corn meal hydrolyzates by free and immobilized cells of *Saccharomyces cerevisiae* var. *ellipsoideus*. Biomass and Bioenergy 34 (2010) : 1449-1456.

Nguyen, D.N., Ton, N.M.N., and Le, V.V.M. Optimization of *Saccharomyces cerevisiae* immobilization in bacterial cellulose by adsorption-incubation method. International Food Research 16 (2009) : 59-64.

Occhiello, E., Morra, M., Garbassi, F., Johnson, D., and Humphrey, P. SSIMS studies of hydrophobic recovery: Oxygen plasma treated PS. Applied Surface Science 47 (1991) : 235-242.

Omenyi, S.N., Neumann, A.W., and van Oss, C.J. Attraction and repulsion of solid particles by solidification fronts I. Thermodynamic effect. Journal of Applied Physics 52 (1981) : 789-795.

Onuki, Y., Bhardwaj, U., Pharm, M., Papadimitrakopoulos, F., and Burgess, D.J. A review of the biocompatibility of implantable devices: Current challenges to overcome foreign body response. Journal of Diabetes Science and Technology 2 (2008) : 1003-1015.

Pandey, L.K., Saxena, C., and Dubey, V. Studies on pervaporative characteristics of bacterial cellulose membrane. Separation and Purification Technology 42 (2005) : 213-218.

Phisalaphong, M., Budiraharjo, R., Bangrak, P., Mongkolkajit, J., and Limtong, S. Alginate-loofa as carrier matrix for ethanol production. Bioscience and Bioengineering 104 (2007) : 214-217.

Phisalaphong, M., Suwanmajo, T., and Tammarate, P. Synthesis and characterization of bacterial cellulose/alginate blend membranes. Journal of Applied Polymer Science 107 (2008) : 3419-3424.

Rambo, C.R., Recouvreux, D.O.S. Carminatti, C.A., and Pitlovanciv, A.K. Template assisted synthesis of porous nanofibrous cellulose membranes for tissue engineering. Materials Science and Engineering: C 28 (2008) : 549-554.

Rattanapan, A., Limtong, S., and Phisalaphong, M. Ethanol production by repeated batch and continuous fermentation of black strap molasses using immobilized yeast cells on thin-shell silk cocoons. Applied Energy 88 (2011) : 4400-4404.

Recouvreux D.O.S., Rambo, C.R., Berti, F.V, Carminatti, C.A., Antonio, R.V., and Porto, L.M. Novel three-dimensional cocoon-like hydrogels for soft tissue regeneration. Materials Science and Engineering: C 31 (2011) : 151-157.

Rezaee, A., Solimani, S., and Forozandemogadam, M. Role of plasmid in production of *Acetobacter Xylinum* biofilms. American Journal of Biochemistry and Biotechnology 1 (2005) : 121-124.

Sakurai, A., Nishida, Y., Saito, H., and Sakakibara, M. Ethanol production by repeated batch culture using yeast cells immobilized within porous cellulose carriers. Journal of Bioscience and Bioengineering 90 (2000) : 526-529.

Sang, L., Luo, D., Xu, S. Wang, X., and Li, X. Fabrication and evaluation of biomimetic scaffolds by using collagen-alginate fibrillar gels for potential. Materials Science and Engineering: C 31 (2011) : 262-271.

Schoelkopf, J., Gane, P. A. C., Ridgway, C. J., and Matthews, G. P. Practical observation of deviation from Lucas-Washburn scaling in porous media. Colloids and Surfaces A: Physicochemical and Engineering Aspects 206 (2002) : 445-454.

Scionti, G. Mechanical Properties of bacterial cellulose implants. Master's Thesis, Department of Chemical and Biological Engineering, Faculty of engineering, Chalmers University of Technology, 2010.

Seki, M., Furusaki, S., and Shigematsa, K. Cell-growth and reaction characteristics of immobilized *Zymomonas mobilis*. Annual N.Y. Academic Science 163 (1990) : 290-302.

Shao, X., and Hunter, C.J. Developing an alginate/chitosan hybrid fiber scaffold for annulus fibrosus cells. Biomedical Materials Research 28 (2007) : 701-710.

Shachar, M. Gang, O.T., Dvir, T. Leor, J., and Cohen, S. The effect of immobilized RGD peptide in alginate scaffolds on cardiac tissue engineering. Acta Biomaterialia 7 (2011) : 152-162.

Shalumon, K.T., et al. Electrospinning of carboxymethyl chitin/poly(vinyl alcohol) nanofibrous scaffolds for tissue engineering applications. Carbohydrate Polymers 77 (2009) : 863-869.

Shang, J., Flury, M., Harsh, J.B., and Zollars, R.L. Comparison of different methods to measure contact angle of soil colloids. Journal of Colloid and Interface Science 328 (2008) : 299-307.

Shapiro, L., and Cohen, S. Novel alginate sponges for cell culture and transplantation. Biomaterials 18 (1997) : 583-590.

Siebold, A., Walliser, A., Nardin, M., Oppliger, M., and Schultz, J. Cappillary rise for thermodymic characterization of solid particle surface. Journal of Colloid and Interface Science 186 (1997) : 60-70.

Solak, E.K. Asman, G., and Sanli, O. Sorption, diffusion, and pervaporation characteristics of dimethylformamide/water mixtures using sodium alginate/polyvinyl pyrrolidone blend membranes. Vacuum 82 (2008) : 579-587.

Sree, N.K., Sridhar, M., Suresh, K., Banat, I.M., and Rao, L.V. High alcohol production by repeated batch fermentation using an immobilized osmotolerant *Saccharomyces cerevisiae*. Journal of Industrial Microbiology and Biotechnology 24 (2000) : 222-226.

Sriamornsak, P., and Sungthongjeen, S. Modification of theophylline release with alginate gel formed in hard capsules. PharmSciTech 51 (2007) : 1-8.

Srivastava A., and Behari, K. Synthesis and characterization of graft copolymer (Guaran-g-N-Vinyl-2-Pyrrolidone) and investigation of metal ion sorption and swelling behavior. Journal of Applied Polymer Science 100 (2006) : 2480-2489.

Stevens, M.M., Qanadilo, H.F., Langer, R., and Shastri, V.P. A rapid-curing alginate gel system: utility in periosteum-derived cartilage tissue engineering. Biomaterials 25 (2004) : 887-894.

Subrahmanyam, T.V., Prestidge, C.A., and Ralston, J. Contact angle and surface analysis studies of sphalerite particles. Minerals Engineering 9 (1996) : 727-741.

Sun, J., Wang, L., Tan, Y.F., Xiao, Y.M., Fan, H.S., and Zhang, X.D. Improvement of bioactivity of collagen/alginate scaffolds by hydroxyapatite for tissue engineering cartilage. Key Engineering Materials 21 (2008) : 445-448.

Svensson, A., et al. Bacterial cellulose as a potential scaffold for tissue engineering of cartilage. Biomaterials 26 (2005) : 419-431.

Szot, C.S., Buchanan, C.F., Gatenholm, P., Rylander, N.M., and Freeman, J.W. Investigation of cancer cell behavior on nanofibrous scaffolds. Materials Science and Engineering C 31 (2011) : 37-42.

Tarun, K., and Gobi, N. Calcium alginate/PVA blended nano fibre matrix of wound dressing. Indian Journal of Fibre and Textile 37 (2012) : 127-132.

Tavana, H., and Neumann, A.W. On the question of rate-dependence of contact angles. Colloids and Surfaces A: Physicochemical and Engineering Aspects 282-283 (2006) : 256-262.

Tischer, W., and Wedekind, F. Biocatalysis-From Discovery to Application. Germany: Springer, 1999.

Tome, L.C., et al. Preparation and characterization of bacterial cellulose membranes with tailored surface and barrier properties. Cellulose 17 (2011) : 1203-1211.

Tretinnikov, O. N., and Ikada, Y. Dynamic wetting and contact angle hysteresis of polymer surfaces studied with the modified Wilhelmy balance method. Langmuir 10 (1994) : 1606-1614.

Troger, J., Lunkwitz, K., Grundke, K., and Burger, W. Determination of the surface tension of microporous membranes using wetting kinetics measurements. Colloids and Surfaces A: Physicochemical and Engineering Aspects 134 (1998) : 299-304.

Vasconcelos, J. N., Lopes, C. E., and France, F. P. Continuous ethanol production using yeast immobilized on sugarcane stalks. Brazilian Journal of Chemical Engineering 21 (2004) : 357-365.

Verbelen, P.J., Schutter, D.P., Delvaux, F., Verstrepen, K.J., and Delvaux, F. R. Immobilized yeast cell systems for continuous fermentation applications. Biotechnology Letters 28 (2006) : 1515-1525.

Wang, H.Y., and Hettwer, D.J. Cell immobilization in *k*-carrageenan with tricalcium phosphate. Biotechnology and Bioengineering 24 (1982) : 1827-1838.

Wang, L., Shelton, R.M., Cooper, P.R., Lawson, M., Triffitt, J.T., and Barralet, J.E. Evaluation of sodium alginate for bone marrow cell tissue engineering. Biomaterials 24 (2003) : 3475-3481.

Wislet-Gendebien, S. Advances in regenerative medicine. Croatia : InTech, 2011.

Wu, S.C., and Lia, Y.K. Application of bacterial cellulose pellets in enzyme immobilization. Melecular Catalysis B: Enzymatic 54 (2008) : 103-108.

Wu, X., et al. Preparation of aligned porous gelatin scaffolds by unidirectional freeze-drying method. Acta Biomaterialia 6 (2010) : 1167-1177.

Xue, H.T., Fang, Z.N., Yang, Y., Huang, J.P., and Zhou, L.W. Contact angle determined by spontaneous dynamic capillary rises with hydrostatic effects: Experiment and theory. Chemical Physics Letters 432 (2006) : 326-330.

Yang, B., et al. Preparation and characterization of a novel chitosan scaffold. Carbohydrate Polymers 80 (2010) : 860-865.

Yang, G. Zhang, L. Peng, T., and Zhong, W. Effects of Ca^{2+} bridge cross-linking on structure and pervaporation of cellulose/alginate blend membranes. Menbrane Science 175 (2000) : 53-60.

Yoon, J.J., Kim, J.H., and Park, T.G. Dexamethasone-releasing biodegradable polymer scaffolds fabricated by gas-foaming/salt-leaching method.

Yoshino, A., et al. Applicability of bacterial cellulose as an alternative to paper points in endodontic treatment. Acta Biomaterialia 9 (2013) : 6116-6122.

Yu, J., Yue, G., Zhong, J., Zhang, X., and Tan, T. Immobilization of *Saccharomyces cerevisiae* to modified bagasse for ethanol production. Renewable Energy 35 (2010) : 1130-1134.

Yu, J., Zhang, X., and Tan, T. An novel immobilization method of *Saccharomyces cerevisiae* to sorghum bagasse for ethanol production. Journal of Biotechnology 129 (2007) : 415-420.

Zaborowska, M., Bodin, A., Backdahl, H., Popp, J., Goldstein, A., and Gatenholm, P. Microporous bacterial cellulose as a potential scaffold for bone regeneration. Acta Biomaterialia 6 (2010) : 2540-2547.

Zemljic, L.F., Persin, Z., and Stenius, P. Improvement of chitosan adsorption onto cellulose fabrics by plasma treatment. Biomacromolecules 10 (2009) : 1181-1187.

Zhang, S., and Luo, J. Preparation and properties of bacterial cellulose/alginate blend bio-fibers. Journal of Engineered Fibers and Fibrics 6 (2011) : 69-72.

Zhao, Y., et al. Synthesis and characterization of disulfide-crosslinked alginate hydrogel scaffolds. Materials Science and Engineering C 32 (2012) : 2153-2162.

Zhaoxin, L., and Fujimura, T. Ethanol fermentation in an immobilized cell reactor using *Saccharomyces cerevisiae*. Journal of Agricultural and Food Chemistry 48 (2000) : 5929-5932.

Zhou, J., Cao, C., and Ma, X. A novel three-dimensional tubular scaffold prepared from silk fibroin by electrospinning. International Journal of Biological Macromolecules 45 (2009) : 504-501.

Zimmermann, K., LeBlanc, J., Sheets, K,. Fox, R., and Gatenholm, P. Biomimetic design of a bacterial cellulose/hydroxyapatite nanocomposite for bone healing applications. Materials Science and Engineering: C 31 (2011) : 43-49.

Zmora, S., Glicklis, R., and Cohen, S. Tailoring the pore architecture in 3-D alginate scaffolds by controlling the freezing regime during fabrication. Biomaterials 23 (2002) : 4087-4094.

APPENDICES

Appendix A

A-1 Agar slants preparation

In this study, Potato Dextrose Agar (PDA) was used as medium for stock cultures. For sterilization, TOMY SS-325 autoclave was used. The preparation steps of PDA agar slants in details are:

1. Mix 7.8 g PDA powder with 200 ml de-ionized (DI) water in 500 ml glass beaker.
2. Stir the solution with magnetic stirrer and heat it up until it is boiling.
3. Boil the solution for 1 minute or until all powder is dissolved as indicated by the formation of clear yellowish agar solution.
4. Transfer 4 ml agar solution into 16 x 150 mm screw cap culture tube by using 10 ml pipette.
5. Sterilize all agar containing tubes at 121ºC for 15 minutes in autoclave. (Set the tube's cap to be rather loose before autoclaving to facilitate gas expansion inside the tube during sterilization.)
6. After sterilization, tighten the tube's cap and let the tubes to cool down before positioning them in slanted position to obtain agar slant inside the tubes.
7. Precautions:
    a) PDA agar powder is hygroscopic. Minimize exposure time of the powder to the ambient air to avoid excess water absorption.
    b) Sterilization is carried out at high temperature. Wear heat resistant gloves as protection when handling hot materials.
    c) When slanting the agar, provide enough space between tube neck and agar to minimize the risk of contamination from outside the tube.

A-2 Stock cultures preparation

Stock cultures were prepared by aseptic inoculation of the flocculating yeast *S. cerevisiae* M30 on the PDA agar slants. The procedures are as follows:

1. Sterilize all equipments and agar slants with ultraviolet (UV) light with air flow for about 1 hour in the ISSCO VS-124 laminar flow hood.
2. After the UV lamp is turned off, clean all apparatus and the hood's compartment with alcohol 70% v/v solution to ensure asepticity.
3. Open the caps of source culture and fresh agar tubes then heat up the tubes' neck with an alcohol burner.
4. Heat up the inoculation loop thoroughly until it reds up.
5. Cool down the loop by contacting with fresh medium.
6. Transfer the yeast cells from source culture to fresh agar slant. Inoculate the cells on fresh agar by zigzag movement.
7. Heat the tube neck again before securing the cap.
8. Repeat step 4-8 again for other fresh medium until sufficient amounts of stock cultures is obtained.
9. Leave the stock cultures to grow at room temperature for 20-24 hours before use.
10. Precautions:
    a) Be cautious with the UV light as it is harmful for human eyes and skin.
    b) Wear protective gloves during inoculation for safety and aseptic reasons.

A-3 Medium preparation

Palm sugar was designated for cell cultivation. The main component of the medium in earlier experiments (until fermentation 3) was palm sugar which was used as carbon and energy source for the yeast. Palm sugar was dissolved to obtain sugar concentration of about 100 g/l for cell cultivation. The resulting sugar solution had a brown color originated from the palm sugar. The color intensity increases with increasing sugar concentration. The amount of palm sugar required to achieve the

target level of sugar was estimated from previous trial with 3,5-dinitrosalicylic acid (DNS) method (Section A-7).

For 1 liter of sugar solution, nutrients consisted of 0.1 g KH_2PO_4, 0.035 g $MgSO_4.7H_2O$, and 0.5 g $(NH_4)_2SO_4$ were added. The compositions were referred to the one which were used by ethanol producing industries. The pH value of the medium was adjusted to 5 with 0.1 M NaOH and HCl solution. The detailed procedures for medium preparation from palm sugar are listed in the following paragraph.

1. Mix palm sugar and nutrients. Add palm sugar until the desired sugar concentration (100 g/L for cell cultivation) is achieved.
2. Adjust the pH of the solution to 5 by adding NaOH or HCl solution.
3. Pour appropriate volume of medium (100 ml and 250 ml for inoculums development and ethanol fermentation respectively) through a sieve or screen into 500 ml Erlenmeyer flask.
4. Close each flask with cotton plug and wrap with aluminum foil before sterilization.
5. Sterilize the mediums with autoclave for 20 min at 121°C.
6. Precautions and notes:

   a) Avoid wetting the flasks' neck when pouring the solution as the heated solution may act as adhesive so that the plug is difficult to be removed after sterilization.

   b) The pH of the solution may be quite altered after sterilization.

   c) Some precipitates may be formed after sterilization from the sugar solution.

In the fermentation, molasses was used for fermentation medium. For 1 liter of the medium 0.5 g $(NH_4)_2SO_4$ was added as the sole supplement. Before sterilization, centrifugation of diluted molasses mash was necessary to prevent excess mud formation. The mud was created from suspended materials contained in molasses. Palm sugar was still used in inoculums development stage prior to ethanol fermentation. The quantity of molasses needed to reach the intended sugar level was also estimated by DNS trial. The procedures for preparing molasses based fermentation medium are follows:

1. Dilute the molasses mash to intended sugar level with DI water.
2. Centrifuge the solution with Kubota 7820 centrifuge at 2000 rpm for 15 minutes.
3. Mix the diluted sugar solution with appropriate amount of $(NH_4)_2SO_4$
4. Adjust the pH of to 5 with NaOH or HCl solution.
5. Fill 500 ml Erlenmeyer flask with 250 ml medium.
6. Close each flask with cotton plug before sterilization.
7. Autoclave the medium for 15 minutes at 121°C.
8. Precautions and notes are same with palm sugar based medium preparation.

A-4 Cell cultivation and harvesting

Cell cultivation was initiated with the transfer of cells from stock culture tube aseptically to Erlenmeyer flask containing fresh medium by using Gilson Pipetman auto pipette. Thus, sterile pipette tips should be prepared in advance by autoclaving or dry heat in hot air oven. Active yeast cells with generation time (age) 20-24 hours were used for cultivation purpose. After inoculation, cell cultivation was carried out in Innova 4330 Refrigerated Incubator Shaker for 20-24 hours at 150 rpm. After some time, the growing yeast cells could be noticed as brown colored suspended solids inside the sugar solution. The cells were then harvested and concentrated by medium draining. The complete steps are as follows:

1. Sterilize equipments and the laminar flow hood with UV and by wiping with alcohol 70% v/v solution.
2. Heat up the neck of stock culture tube and medium flask after removing the tube cap and cotton plug.
3. Heat up the inoculation loop evenly and then slightly deep it into the fresh medium in the Erlenmeyer flask to cool it down before touching the yeast cells.
4. Scratch the yeast culture on the tube to detach the cells from the surface of the agar using the loop.

5. Transfer the cell at the loop into the Erlenmeyer flask and then close the flask using cotton plug.
6. Repeat steps 3-5 for the other flasks.
7. Put all flasks in the incubator shaker and then operate the shaker at 150 rpm 33°C for a day before harvesting the cells.
8. Let the cells to settle for a while after incubation and then carefully take out 130 ml of the medium from each flask by using 10 ml of auto pipette.
9. Combine the concentrated cells suspension from several flasks by pouring it into one flask.
10. Further draining can be done to concentrate cells by the same method until the desired volume of concentrated cells suspension is obtained.
11. Precautions and notes:
    a) Except the stock culture and the fresh medium, all equipments should be cleaned and sterilized using UV light and alcohol to ensure asepticity.
    b) Clean the outer surface of the tubes and flasks using alcohol before use.
    c) Keep the tube neck and flask opening hot by regular heating after removal of the cap or plug to prevent contamination originated from ambient air.

A-5 Cell immobilization

BCA and palm sugar medium were sterilized with autoclave for 15 minutes at 121 ^{o}C prior to usage. Preparation of cells immobilized in BCA carrier were listed in the following paragraph.

1. Mix 10 ml of concentrated cell suspension with 250 ml of palm sugar medium.
2. Add BCA in the mixture.
3. incubated suspension mixture for 20-24 hours.
4. Precautions and notes:
    a) All procedures are conducted aseptically in laminar flow hood.
    b) All equipments are cleaned and sterilized before use.

A-6 Ethanol fermentation

A-6.1 Batch fermentation

The molasses which has 240 g/l of initial sugar concentration was added by 0.5 g/l of ammonium sulfate as the nutrient. The volume of medium was adjusted to 250 ml in 500 ml Erlenmeyer flask in order to promote anaerobic condition which was favorable ethanol fermentation by yeast. Batch fermentation in shake flasks was performed in Innova 4330 Refrigerated Incubator Shaker (New Brunswick Scientific, USA) at 150 rpm, 33°C.

A-7 Sugar analysis

Sugar (sucrose) concentration was determined using a modified DNS reagent method. All disaccharides in the samples and standard sucrose solutions were first hydrolyzed to their monomers by using acid solution at elevated temperature. The acid residue was then neutralized using a basic solution and the resulting precipitates were settled by centrifugation. After centrifugation, the supernatant was reacted with DNS reagent at high temperature resulting in the formation of brown colored solution. The solution was then diluted before being analyzed by using spectrophotometer. The absorbance of the sample was compared with standard sucrose solutions to obtain the corresponding sucrose concentration. Complete step by step procedures are provided in the following sections.

A-7.1 NaOH and HCl solution preparation

NaOH 20% w/v was prepared by dissolving 200 g of NaOH pellets in 100 mL of water. The reaction is highly exothermic so that the preparation should be done in water bath in order to avoid excess heat generation. Weighing time of NaOH pellets should be minimized because of the hygroscopic nature of NaOH. Solution of

37% w/v HCl was obtained by diluting concentrated HCl solution with DI water. Beware of the acid vapor and wear protective gloves when preparing the solutions. Commercially available HCl 37% can be also be used directly.

A-7.2 DNS reagent preparation

DNS powder is toxic and easy to airborne so that it should be handled with caution. This powder should be added slowly in the mixing process because it is not easy to dissolve. After preparation, the resulting yellow colored reagent is best used in fresh condition so that it is not suggested to keep unused for long time (more than 1 month). The reagent is usually kept in brown bottle to protect it from degradation originated from light for example sun light. The complete preparation steps are:

1. Dissolve 1.633 g NaOH 98% w/w in 20 ml of water. Mix the solution with magnetic stirrer.
2. Under stirring, slowly add 1 g of 3,5-dinitrosalicylic acid powder into the solution.
3. Dilute by adding 50 ml of water. Stir until it is homogeneous.
4. Add 30 g Na-K tartrate & mix it thoroughly.
5. Adjust the volume to 100 ml.
6. Keep the reagent for 3 days before use.

A-7.3 Standard sucrose solution preparation

Standard sucrose solutions were prepared first by making the source solution which was the solution with the highest sucrose concentration as the upper limit. The source solution was then diluted with water so that a set of standard solution with increasing sucrose concentration (for instance 0, 6.25, 12.5, 18.75, and 25% w/v) was obtained. The detailed procedures are as follows:

1. Dry 3.0 g sucrose at 100-105°C in hot air oven for 2 hours.
2. Put the dried sucrose in desiccator for cooling.
3. Dissolve 2.5 g of the sucrose in 10 ml of water to obtain the source solution.

4. Prepare each 2 ml standard solution in small labeled bottle by serial dilution of suitable amount of source solution and diluting it with water as shown in detail in Table A-7. Use auto pipette for the transfer purpose.

Table A-7.3 Standard sucrose solution preparation

Sucrose concentration (% w/v)	**Source solution (ml)**	**Water (ml)**
0	0	2.0
6.25	0.5	1.5
12.50	1.0	1.0
18.75	1.5	0.5
25.00	2.0	0

A-7.4 Sample treatment I

In the first treatment, sample was hydrolyzed using HCl 37% in boiled water bath. After the hydrolysis reaction was stopped, NaOH was added into the solution. The sample was then centrifuged for removing suspended solids. Procedures of the first treatment are:

1. Mix 0.2 ml of sample with 0.8 ml DI water in screw cap tube.
2. Blend the sample with 0.5 ml HCl 37%.
3. Put the tubes in boiling water bath for 10 minutes.
4. Stop the reaction by placing the tubes in ice bath.
5. Add 0.5 ml NaOH 20% w/v and then mix with vortex mixer.
6. Add 10 ml DI water and then mix with vortex mixer.
7. Centrifuge the sample at 2000 rpm for 20 minutes.
8. Precautions and notes:
    a) Use vortex mixer for mixing the fluid in the tubes.
    b) Be cautious when handling the hot apparatus.
    c) The level of boiled water and ice bath must be sufficiently higher than the liquid level in the tubes to ensure good heating and cooling of the sample.

A-7.5 Sample treatment II

In treatment II, supernatant obtained from treatment I was reacted with DNS reagent in boiled water bath. The solution's color transformed from yellow to reddish brown in the course of reaction. The color intensity represents the corresponding sugar concentration. Solution with higher sugar content will have darker color. After the reaction was ended, the solution was diluted with sufficient amount of water until its absorbance spectrum obtained by spectrophotometer was well distributed along the range of concentration being considered (the absorbance measured was not more 0.7). Shimadzu UV-2450 UV-Visible spectrophotometer was used for absorbance measurement. Sample containing only water (0% sugar) which had been treated in the same manner as the other samples was used as blank. At every absorbance measurement, fresh standard solution should be used. Complete procedures are described in the following paragraph.

1. Mix 0.2 ml of supernatant obtained from treatment I with 1.0 ml DNS reagent in screw cap tube.
2. Boil the solution for 10 minutes using water bath.
3. Put the tubes in ice bath to stop the reaction.
4. Add 10 ml DI water and then mix with vortex mixer.
5. Measure the absorbance at 520 nm. Use sample with 0% sugar as blank.
6. Obtain the standard curve by plotting absorbance versus sucrose concentration of standard sucrose solution.
7. Use the standard curve to gain sugar concentration of the samples.

A-8 Determination of cell concentration

Cell concentration was determined by separation of cell from its carrier or medium followed by measurement by spectrophotometer. The cell concentration was obtained by comparing the absorbance of sample with its corresponding standard curve. The standard curve was made by measuring a set of samples of known cell concentration (with dry weight basis).

A-8.1 Dry weight of cell

Dry weight of cell was determined by separating the cells from their suspending liquid medium by centrifugation. The cells were then dried and their weight was measured as the representative of their concentration in the initial suspension. The procedures are:

1. Centrifuge the cell containing medium at 2000 rpm for 15 minutes.
2. Remove the supernatant (discarded or to be used for other analysis).
3. Add HCl 0.1 N to the cell pellet and mix with vortex mixer.
4. Centrifuge the suspension at 2000 rpm for 15 minutes.
5. Discard the supernatant.
6. Disperse the cell pellet with DI water.
7. Repeat step 4-6.
8. Transfer the cell suspension to a pre-weighted aluminum dish.
9. Dry the cell in hot air oven at 100°C for 2 hours.
10. Measure the weight of the cells.
11. Precautions and notes:
    a) The cells cake is fragile. Pour out all of the supernatant in one cycle instead of several cycles.
    b) Dry and measure the weight of aluminum dishes before use.
    c) The dry weight of the cells is obtained as the difference between the weight of the aluminum dish which contains cells and the weight of empty dish.

A-8.2 Free cell concentration

A set of cell suspension with known cell concentration was used as standard. This solution was analyzed at the same time with samples of fermentation and used to generate standard curve of cell concentration. The complete procedures are:

1. Dilute sample with DI water in 16 x 100 mm rimless tube.
2. Centrifuge the cell suspension at 2000 rpm for 15 minutes.
3. Remove the supernatant.
4. Add HCl 0.1 N and mix with vortex mixer.

5. Centrifuge the suspension at 2000 rpm for 15 minutes.
6. Discard the supernatant.
7. Disperse the cell pellet with DI water.
8. Repeat step 5-8.
9. Measure the absorbance of sample at 660 nm.
10. Precautions and notes:
    a) Dilute the sample with DI water before optical density measurement if the cell concentration is too high (its absorbance value is too high).
    b) Mix every sample with vortex mixer before spectrophotometry to ensure homogeneity of the sample.

A-8.3 Immobilized cell concentration

Before the cell concentration could be measured, a measured amount of carrier should be dissolved to obtain cell suspension. The dissolution of BCA was carried out using water. The thin shell silk cocoon was removed from the suspension after the gel was dissolved. The cells suspension was then treated with the same procedures as for free cells suspension in order to obtain its corresponding immobilized cell concentration. The complete procedures are as follows:

1. Cut the BCA carrier in to the small size.
2. Dissolve appropriate amount of BCA carrier with 10 ml water in 25 ml beaker.
3. Stir BCA carrier in the beaker with magnetic stirrer for 30 minutes.
4. Remove the BCA carrier from the suspension and continue with same procedures as step 2-9 of Section A-8.2.

Appendix B

Table B-1 Data of Figure 3.1

Time	SC		AL		BCA hydrogel	
	Run 1	Run 2	Run 1	Run 2	Run 1	Run 2
0	0.52	0.59	0.02	0.32	0.26	0.48
8	6.98	8.31	2.20	2.22	3.02	2.47
16	25.21	25.88	25.95	21.14	27.67	25.07
24	54.88	49.61	48.41	44.10	48.78	48.98
32	72.92	70.10	68.02	70.34	73.81	63.92
40	85.10	92.32	82.25	80.58	71.54	72.22
48	93.14	100.09	75.18	73.51	75.33	74.23
56	92.64	98.42	68.91	70.75	79.95	76.76
64	94.00	94.99	65.93	81.37	78.70	70.17
72	89.97	90.63	74.15	79.81	71.69	75.82

Table B-2 Data of Figure 3.2

Time	SC		AL		BCA hydrogel	
	Run 1	Run 2	Run 1	Run 2	Run 1	Run 2
0	230.37	269.64	204.12	203.49	196.56	207.48
8	216.51	219.87	173.04	175.98	165.06	170.31
16	168.21	169.26	108.57	103.74	113.40	112.35
24	86.10	95.67	63.42	68.88	67.20	67.83
32	62.16	66.36	39.06	43.68	40.95	42.00
40	47.46	51.66	35.91	36.12	33.60	34.23
48	43.89	46.41	35.49	35.49	33.81	33.81
56	40.74	43.05	34.23	33.18	31.92	31.50
64	41.16	43.26	33.39	33.60	30.03	32.55
72	40.32	40.95	36.75	30.03	27.09	28.56

Table B-3 Data of Figure 4.2 (A)

Batch	Time	SC		AL		BCA sponge	
		Run 1	Run 2	Run 1	Run 2	Run 1	Run 2
1	0	0.55	13.11	0.25	0.25	4.26	10.13
	12	10.55	11.34	14.04	15.00	18.63	22.56
	24	56.48	47.27	54.18	54.43	54.35	59.47
	36	76.62	70.25	62.99	61.03	73.07	79.74
	48	85.31	82.04	63.46	65.40	83.71	84.83
2	0	20.54	19.79	17.73	21.59	7.84	17.31
	12	26.21	32.28	37.69	38.06	39.97	33.92
	24	53.07	60.22	52.18	50.37	68.19	66.49
	36	73.15	75.57	63.92	70.49	83.00	78.23
	48	79.15	81.57	61.68	69.49	87.25	81.89
3	0	10.21	10.54	18.85	21.23	7.34	13.16
	12	28.20	27.98	21.52	22.73	19.45	27.12
	24	45.31	49.38	32.11	35.38	39.60	47.55
	36	61.73	63.01	54.34	54.46	58.82	68.92
	48	76.04	76.33	64.99	68.47	6.045	80.58
4	0	20.53	17.57	7.01	17.73	16.47	11.97
	12	31.66	69.29	42.84	47.84	40.73	38.30
	24	55.94	93.56	61.23	60.25	67.82	64.80
	36	79.26	93.98	71.98	72.13	81.62	86.59
	48	79.84	93.71	76.82	74.59	91.26	88.43
5	0	23.65	22.39	11.08	16.43	21.39	11.65
	12	8.80	8.37	14.53	18.95	24.38	27.98
	24	7.39	6.48	17.05	26.68	52.37	59.84
	36	6.51	6.71	26.12	37.59	77.12	82.00
	48	6.76	6.42	53.67	55.56	85.88	85.19

Table B-4 Data of Figure 4.2 (B)

Batch	Time	SC		AL		BCA sponge	
		Run 1	Run 2	Run 1	Run 2	Run 1	Run 2
1	0	225.02	214.19	190.12	199.75	225.02	216.59
	12	180.50	176.89	132.36	132.36	161.24	146.80
	24	82.31	82.79	50.42	48.13	79.30	76.29
	36	40.43	39.47	27.68	28.16	45.85	39.71
	48	37.66	35.14	27.56	27.92	35.86	29.84
2	0	217.12	214.31	1182.90	210.29	214.80	223.39
	12	129.96	108.18	60.389	135.84	122.74	120.33
	24	58.84	48.37	32.49	63.57	67.38	69.91
	36	37.06	39.59	31.77	32.01	43.56	44.40
	48	36.58	34.17	31.41	31.05	36.22	37.78
3	0	210.56	212.98	198.54	215.73	211.81	216.59
	12	126.35	216.58	175.68	170.07	163.24	148.01
	24	77.25	76.12	137.18	109.36	105.27	95.18
	36	45.97	46.93	80.38	69.62	6.678	56.07
	48	37.30	37.00	52.95	41.35	40.21	44.40
4	0	213.36	207.28	216.59	204.56	211.78	210.58
	12	114.31	119.58	80.26	110.43	112.80	115.64
	24	50.94	48.26	40.55	41.15	61.13	38.63
	36	39.51	37.54	35.02	30.92	41.63	40.43
	48	36.26	34.78	31.17	33.69	36.34	34.78
5	0	206.97	221.41	219.00	205.76	221.41	220.20
	12	213.84	212.98	196.14	184.10	146.80	138.38
	24	207.27	209.17	176.89	157.63	83.03	71.84
	36	216.55	214.39	132.36	119.01	49.58	43.32
	48	214.30	214.19	76.41	70.75	39.95	37.90

Table B-5 Data of Figure 4.3

Batch	BCA sponge	
	Run 1	Run 2
1	88.93	88.77
2	93.10	86.13
3	92.74	96.15
4	86.25	89.90
5	92.34	92.89
6	86.76	87.76
7	97.33	94.36
8	90.08	92.26
9	94.07	96.37
10	90.47	90.65
11	96.30	94.79
12	91.32	93.85
13	96.48	93.77
14	90.39	92.40
15	93.91	93.62

Table B-6 Data of Table 4.1

System		Ethanol concentration (g/L)		Sugar concentration (g/L)		Cell concentration			
		Run 1	Run 2	Run 1	Run 2	Free cell		Immobilized cell	
						Run 1	Run 2	Run 1	Run 2
SC		85.74	90.02	35.78	35.97	4.67	4.53	-	-
AL		66.27	70.43	23.55	21.69	1.52	1.61	3.50	3.78
BCA	50/50	90.75	90.67	22.62	25.03	1.41	1.49	3.60	3.38
	60/40	94.19	89.74	31.82	28.11	1.93	1.74	4.74	5.06
	70/30	90.65	88.90	25.64	22.45	1.93	1.91	5.00	5.36

Table B-7 Data of Table 4.2

BCA (60/40)		Ethanol concentration (g/L)		Sugar concentration (g/L)		Cell concentration (g/L)			
		Run 1	Run 2	Run 1	Run 2	Free cell		Immobilized cell	
						Run 1	Run 2	Run 1	Run 2
Alginate concentration (% by wt.)	1.5	91.16	95.65	31.16	31.29	2.60	2.93	4.24	6.41
	2	92.92	94.68	32.07	31.29	2.53	2.46	4.38	5.27
	2.5	93.54	93.66	32.98	32.98	2.90	2.59	5.48	5.51
	3	98.42	100.78	32.98	32.20	1.82	2.55	13.97	10.39
	4	102.28	97.12	30.70	32.21	2.16	2.57	8.39	7.35
	5	97.45	100.55	33.05	34.16	1.83	1.83	7.03	5.72
	6	98.14	100.06	34.72	35.62	2.70	3.71	4.30	4.95

Table B-8 Data of Table 4.3

Property	Alginate concentration (% by wt.) of BCA (60/40)						
	1.5	2	2.5	3	4	5	6
Tensile strength (MPa)	6.48	3.71	4.21	5.03	5.62	8.21	2.77
	3.91	6.66	6.25	7.57	8.32	9.74	3.17
	5.97	6.12	7.01	9.35	5.07	5.68	6.44
Elongation (%)	9.00	13.68	11.03	10.01	9.68	9.50	11.24
	10.10	8.86	8.14	8.90	9.36	10.19	10.28
	11.84	8.08	12.14	12.62	11.28	10.40	10.56
Water uptake ability	5.65	6.34	7.69	7.87	8.17	8.21	6.28
	6.21	7.08	7.24	8.32	8.46	8.22	6.42
	5.91	7.79	8.39	9.63	7.80	7.36	6.56

Table B-9 Data of Figure 6.3

Time	SC		BCA		P-BCA	
	Run 1	Run 2	Run 1	Run 2	Run 1	Run 2
0	0.95	2.18	2.64	2.01	2.31	2.80
8	6.56	6.83	11.79	12.39	13.50	14.08
16	40.83	39.61	55.77	43.75	44.21	42.66
24	75.50	76.15	70.94	73.75	70.05	70.23
32	89.19	89.69	85.56	82.15	86.54	81.83
40	95.40	95.20	92.73	85.84	92.57	86.45
48	96.35	98.69	97.44	92.16	89.73	87.97
56	91.20	96.31	87.56	92.48	90.65	90.17
64	90.57	96.92	91.09	95.06	93.45	88.60
72	89.33	89.81	88.07	95.11	86.82	87.27

Table B-10 Data of Table 7.2

Material	Tensile strength (MPa)				Elongation (%)			
	Run 1	Run 2	Run 3	Run 4	Run 1	Run 2	Run 3	Run 4
BCF	43.96	73.30	49.32	29.96	10.20	5.70	8.45	7.65
BCB	1.37	1.17	1.03	1.26	9.10	9.00	8.45	7.90
AL	0.70	1.10	0.82	0.87	3.19	3.01	2.36	3.27
N-BCA	0.56	0.61	0.52	0.53	4.17	5.25	4.40	4.60
O-BCA	8.94	11.27	13.81	14.60	5.43	5.55	7.17	6.45

Table B-1.11 Data of Figure 7.2

Material	Water uptake ability (times)					
	Run 1	Run 2	Run 3	Run 4	Run 5	Run 6
BCF	6.50	8.75	5.17	7.50	6.00	10.60
BCB	66.67	68.67	57.75	65.67	50.00	57.67
AL	14.40	13.80	19.50	14.56	13.73	15.60
N-BCA	53.25	55.33	41.75	40.50	42.60	56.00
O-BCA	11.38	13.45	8.83	11.91	10.71	8.25

VITA

Miss Suchata Kirdponpattara was born in Phang-Nga, on January 4, 1986. She finished high school from Princess Chulabhon College, Trang in 2004. She received her Bacheler's Degree in Chemical Engineering from Prince of Songkla University in 2008. She directly continued her graduate study in Doctoral degree at Biochemical Engineering Laboratory, Department of Chemical Engineering, Faculty of Engineering, Chulalongkorn University since June 2008 and received scholarship from Thailand Research fund (TRF) through the Royal Golden Jubilee Ph.D program for five years. During her graduate studies, she spent a period of one year in Department of Chemical and Biomolecular Engineering, The University of Akron, Ohio, United State of America for research aboard.